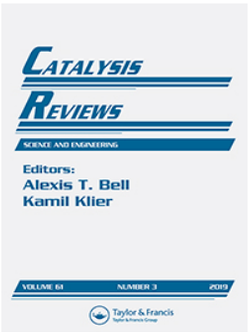

Catalysis Reviews
Science and Engineering

ISSN: 0161-4940 (Print) 1520-5703 (Online) Journal homepage: https://www.tandfonline.com/loi/lctr20

Fluid catalytic cracking technology: current status and recent discoveries on catalyst contamination

Peng Bai, Ubong Jerome Etim, Zifeng Yan, Svetlana Mintova, Zhongdong Zhang, Ziyi Zhong & Xionghou Gao

To cite this article: Peng Bai, Ubong Jerome Etim, Zifeng Yan, Svetlana Mintova, Zhongdong Zhang, Ziyi Zhong & Xionghou Gao (2019) Fluid catalytic cracking technology: current status and recent discoveries on catalyst contamination, Catalysis Reviews, 61:3, 333-405, DOI: 10.1080/01614940.2018.1549011

To link to this article: https://doi.org/10.1080/01614940.2018.1549011

Published online: 13 Dec 2018.

CATALYSIS REVIEWS
2019, VOL. 61, NO. 3, 333–405
https://doi.org/10.1080/01614940.2018.1549011

Taylor & Francis
Taylor & Francis Group

Fluid catalytic cracking technology: current status and recent discoveries on catalyst contamination

Peng Bai[a], Ubong Jerome Etim[a], Zifeng Yan[a], Svetlana Mintova[a,b], Zhongdong Zhang[c], Ziyi Zhong[d], and Xionghou Gao[c]

[a]State Key Laboratory of Heavy Oil Processing, PetroChina Key Laboratory of Catalysis, College of Chemical Engineering, China University of Petroleum (East China), Qingdao, China; [b]Laboratory of Catalysis and Spectrochemistry, ENSICAEN, Normandy University, CNRS, Caen, France; [c]Lanzhou Petrochemical Research Center, PetroChina Petrochemical Institute, CNPC, Lanzhou, China; [d]College of Engineering, Guangdong Technion Israel Institute of Technology (GTIIT), Shantou, China

ABSTRACT

The fluid catalytic cracking (FCC) technology is one of the pillars of the modern petroleum industry which converts the crude oil fractions into many commodity fuels and platform chemicals, such as gasoline. Although the FCC field is quite mature, the research scope is still enormous due to changing FCC feedstock, gradual shifts in market demands and evolved unit operations. In this review, we have described the current status of FCC technology, such as variation in the present day feedstocks and catalysts, and particularly, great attention is paid to the effects of various contaminants of the FCC catalysts of which the latter part has not been sufficiently documented and analyzed in the literature yet. Deposition of various contaminants on cracking catalyst during FCC process, including metals, sulfur, nitrogen and coke originated from feedstocks or generated during FCC reaction constitutes a source of concern to the petroleum refiners from both economic and technological perspectives. It causes not only undesirable effects on the catalysts themselves, but also reduction in catalytic activity and changes in product distribution of the FCC reactions, translating into economic losses. The metal contaminants (vanadium (V), nickel (Ni), iron (Fe) and sodium (Na)) have the most adverse effects that can seriously influence the catalyst structure and performance. Although nitrogen and sulfur are considered less harmful compared to the metal contaminants, it is shown that pore blockage by the coking effect of sulfur and acid sites neutralization by nitrogen are serious problems too. Most recent studies on the deactivation of FCC catalysts at single particle level have provided an in-depth understanding of the deactivation mechanisms. This work will provide the readers with a comprehensive understanding of the current status, related problems and most recent progress made in the FCC technology, and also will deepen insights into the catalyst deactivation mechanisms caused by contaminants and the possible technical approaches to controlling catalyst deactivation problems.

ARTICLE HISTORY
Received 24 April 2018
Accepted 12 November 2018

KEYWORDS
Fluid catalytic cracking catalyst; catalytic activity; contaminants; deactivation

CONTACT Zifeng Yan zfyancat@upc.edu.cn; Xionghou Gao gaoxionghou@petrochina.com.cn

Peng Bai and Ubong Jerome Etim contribute to this work equally.

Color versions of one or more of the figures in the article can be found online at www.tandfonline.com/lctr.

1. Introduction

The fluid catalytic cracking (FCC) is a secondary refining process used primarily for conversion of the high-boiling, high-molecular weight fractions of petroleum to more valuable fuels such as gasoline, diesel, liquefied petroleum gas (LPG), olefinic gases and some other products, and is one of the largest applications of heterogeneous catalysts. In 2014, the global FCC market demand was about 681 kilo tons, and is expected to grow at 3.3% annually until 2020.[1] A global survey showed the existence of about 400–450 FCC units as of 2000[2] and as of the beginning of 2014, over 300 of these units were still in active operation.[3]

Fuel production from the FCC process accounts for about 35–50% of the total gasoline produced worldwide in the petroleum industry.[4–8] However, the process has witnessed uneven utilization in different countries. In China, for instance, FCC is utilized in about 27% of petroleum processing and is responsible for about 80% gasoline production, while it accounts for about one-third of the total gasoline pool in the U.S (Figure 1). In the UK, Germany, France, and Italy, the FCC naphtha and reformer gasoline accounts for 25–30% and 45–50 % of gasoline pool, respectively.[5,9] Besides gasoline production, the FCC technology can be employed in the production of some petrochemicals such as propylene[10] and other olefins.-[11] As a matter of fact, FCC units have become an important source of light olefins.[12–15] In 2000, about 34% of the propylene around the world was from FCC units.[16,17] However, most recent data show a decline to 25–30%, due to increasing exploitation of other processes, such as on-purpose propylene process for its production.[18] The FCC technology, which was introduced over seven decades ago, has been playing a key role in heavy oil upgrading and optimization. The reason for its long lasting lies in the reality of being one of the most important conversion processes in the petroleum

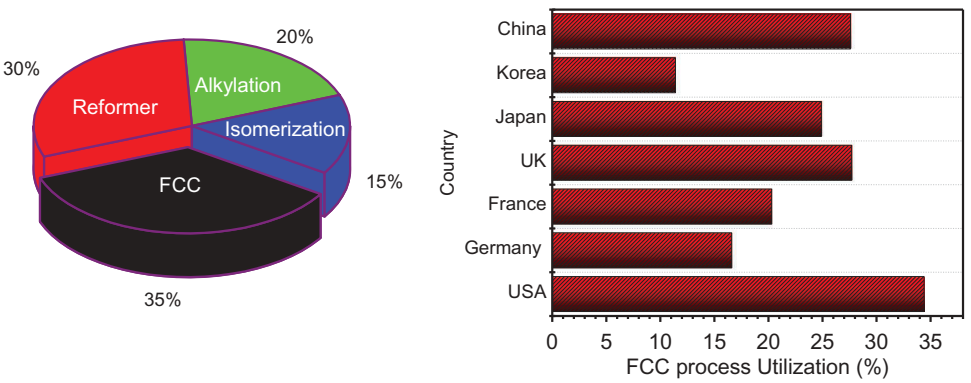

Figure 1. Relevance of FCC in the modern refinery and its utilization in different countries (data adapted from ref..[9].

refinery for transforming heavy fractions of crude oil to more valuable grades.[17,19–25] The high flexibility of operation, the ability to process different types of feedstocks, such as biomass-derived feedstocks, and the switching adaptability to changing product demand offer increasing profitability compared to other petroleum refining conversion processes.[26]

The FCC unit (FCCU) represents the heart of the refinery, and the latest design that is still much used in the refineries around the world consists of two main vessels: a riser (reactor) and a regenerator that are interconnected to permit transferring the spent catalyst from the reactor to the regenerator and the regenerated catalyst back to the reactor in a cyclic manner. The FCC process involves contacting a pre-heated feedstock with hot catalysts coming from the high temperature regenerator at the base of the riser. The high temperature catalytic reaction results in the breakdown of large hydrocarbon molecules to lighter fractions of gasoline and diesel, as well as gaseous fuel (LPG) and coke.[17,20,27] The catalyst spends a short time, usually few seconds in the riser reactor, and is separated from hydrocarbon by stripper in the cyclone. After stripping of residual hydrocarbons with steam, the catalyst is regenerated and the coke deposited on the catalyst is burned off with hot air.[28,29] The regulating flow rate of the spent/regenerated catalyst maintains heat balance of the unit. Generally, the design and operation of the unit is of high relevance to the catalyst properties and feedstock as well.

The modern FCC catalyst comes in the form of fine particles (with typical sizes 60–80 μm) and comprises four major components namely, zeolite Y or its modified type, matrix (silica or alumina or mixture of both), filler (kaolinite) and binder. All components are mixed and spray dried to form microspherical catalyst particles.[30] Additives may be incorporated during preparation for specific purposes, such as ZSM-5 – an olefin enhancer[13,15,31], trap for poisonous metals[32,33], SO_x and NO_x scavenging additives[34] or a CO combustion promoter.[35] Zeolite is the active component, which controls the activity and the product distribution of the FCC catalyst. The matrix performs a supportive role to the zeolite essentially in providing mechanical strength and attrition resistance to the catalyst and for the reduction of the detrimental effects of contaminants.[36–39] Particularly, the active matrix contributes significantly to general performance of FCC catalyst by pre-cracking larger oil molecules to enhance accessibility to the micropores of the zeolite.[37] The filler, generally regarded as an inert part of matrix, serves as a heat sink and transfer medium and provides little or no activity to the catalyst. It also provides mechanical strength and increases apparent bulk density (ABD) of the particle for optimum fluidization properties.[40]

The binder functions primarily as a glue binding zeolite, matrix, and filler together and provides high attrition resistance. In some cases, the binder modifies the coking characteristics and acts as a trap for poison species.[23,41,42]

Before utilization in the real FCC units, the assessment of FCC catalysts not only predicts the unit's performance, but also enables the refiner to make important decisions concerning the unit operation. The activity of the catalyst in its fresh state is an inadequate assessment of its commercial performance, due to deactivation in the commercial FCC units by both hydrothermal effect and metal deposition. Several methods are considered standard to simulate the commercial equilibrium catalyst (E-cat) for testing in laboratory, including Mitchell incipient wetness impregnation (MI) of contaminant metals on fresh catalyst followed by steaming at high temperature[43], cyclic metal deposition (CMD) by repeating cracking reaction and regeneration[44], cyclic propylene steaming (CPS) method by repeating oxidation and reduction of impregnated metals[45,46] and the Engelhard Transfer Method (ETM).[47] The artificially deactivated catalyst can be tested on laboratory units either with fixed bed (MAT reactor type), fixed fluid bed, such as Advanced Cracking Evaluation reactor (ACE)[48,49], the once through or circulating pilot plant[21,50–53] or the CREC Riser Simulator.[54] The summary of the protocols described above is illustrated in Figure 2.

Although the FCC technology is quite mature and the research scope is not changed greatly, it is still facing a number of challenges nowadays from

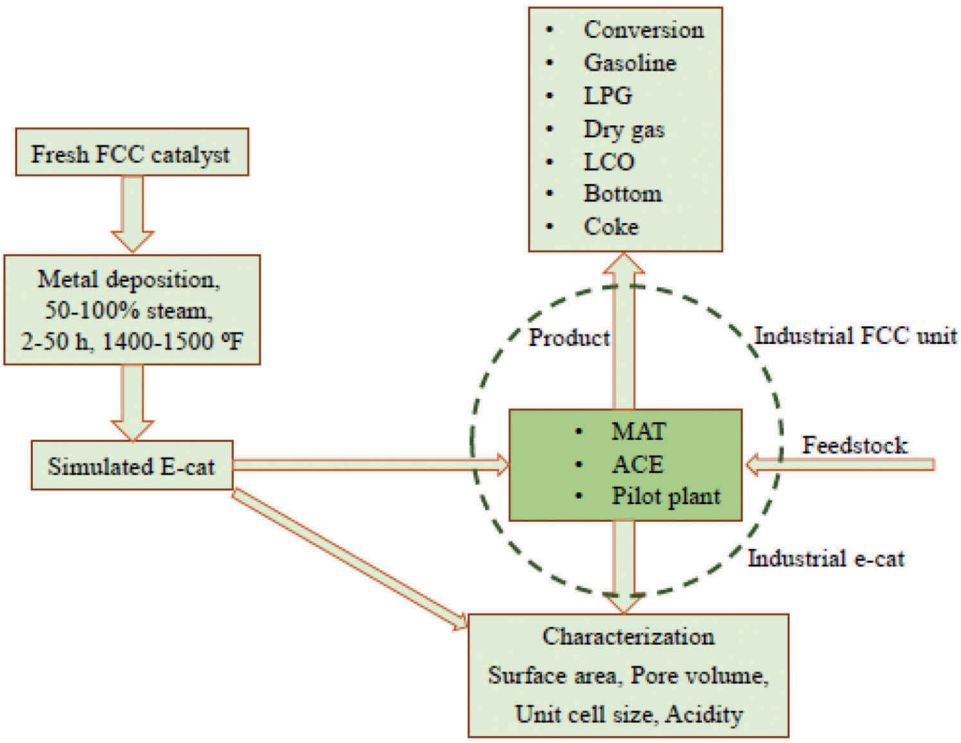

Figure 2. General laboratory procedures for FCC catalyst testing.

the wider diversity of feedstocks which generate demands for new FCC catalysts, reaction conditions, and even production distribution.

It is found that most of the previous reviews in this research area mainly focused on aspects such as assessment of FCC catalyst testing units,[21] deactivation of FCC catalyst,[19] FCC catalyst deactivation methods[55] and the FCC unit itself[56], and little or no attention was paid to the feedstock contaminant effects, which are critical issues in FCC process. Although various researchers have investigated the contaminant effects on FCC catalysts; hitherto, there is still lack of a comprehensive review on the literature results, and many studies were conducted under different reaction conditions, increasing the difficulty to an overall and comprehensive understanding of the effects of the different FCC catalyst contaminants.

In this review, the effects of metal contaminants that deteriorate the performance of FCC catalyst is presented and critically analyzed. In addition, the effects of nitrogen and sulfur compounds that have been considered less of poisons to the catalysts and as serious environmental pollution sources are discussed. Moreover, the mechanisms of FCC catalyst deactivation by different contaminants and the physiochemical properties-performance relationship are summarized. In particular, the recent advances in the deactivation of the FCC catalyst at a single particle level is presented. Putting together, these findings, it is expected that this review will not only serve most of the researchers for a fast and solid grasp of the status in the area, but also act as a good reference for possible improvement in FCC catalyst technology for future applications.

2. Recent developments in FCC technology

Since its inception in the early 1940s, the FCC process technology has witnessed several stages of developments and revolutions. The FCC process is generally improved by combining developments in catalyst, feedstock, process technology, and hardware (reactor design). These advances are continuously improving efficiency, product selectivity, and environmental emissions control. Optimum performance, reliability, and flexibility of the FCC units are essentially desirable for the continued competitiveness of refineries and their ability to meet market demands for refined products. FCC traditionally converts gas oil and heavier oil to mainly gasoline and diesel oils range. However, high demand for transportation fuels globally and emerging markets for other FCC products, such as propylene, an important petrochemicals feedstock, have created a paradigm shift in the operational strategies with huge responses on the feedstock and catalyst selection as well as reactor re-configuration.

2.1. *Changes in FCC feedstock*

2.1.1. *Conventional feedstock*

(1) Crude oil

Conventional FCC feedstocks are high-molecular weight hydrocarbon with various numbers of carbon atoms, mainly composed of paraffin, aromatics, and naphthenes.[20] They boil at high temperatures, usually 343 °C or above and atmospheric pressure. This class of crude oil fraction is generally referred to as "heavy oil". Paraffin are straight or branched chained hydrocarbons in the crude oil which consist of molecules containing between 20 and 40 carbon atoms. Aromatics are compounds that have at least one benzene ring. Naphthenes are saturated cyclic compounds, such as substituted cyclopentanes and cyclohexanes. Heavy oil usually contains 50–60% paraffin, 15–25% aromatics, and 15–25% naphthenes.[5] In addition to hydrocarbons, crude oil fractions for FCC units contain non-negligible amounts of sulfur, nitrogen, carbon residue, and metals such as nickel, iron and vanadium.[19,27,57,58] The overall performance of the FCC process in the production of liquid fuels is strongly affected by the feedstock properties including the feedstock composition and contaminants. For example, the vacuum and atmospheric residue cuts consist of mainly resins and asphaltenes. Resins are fused cyclic compounds with long aliphatic side chains, while asphaltenes are polycyclic aromatic systems with short aliphatic side chains, which are piled up on each other to form asphaltene molecules. Asphaltene is believed to be the most complex, high molecular weight, polar and highly aromatic molecule present in heavy crude oil. Interactions exist between feed contaminants and asphaltene molecule, and the presence of non-metallic elements (sulfur, oxygen, and nitrogen) in asphaltene molecule accounts for its strong coordination with metallic contaminants.[59]

The FCC feedstock has evolved over the period of commercial application, changing from gas oil feeds such as vacuum gas oils (VGOs) in the 1940s, to the present day residues like atmospheric and vacuum residues and hydrotreated feedstocks.[26,60] The residues differ in chemical composition from VGOs and are characterized by high levels of contaminants. Recently, the FCC unit has been tested in the processing of non-conventional petroleum based feedstocks such as vegetable oils and pyrolysis oils.

(2) Tight (shale) Oil

Tight oil also known as shale oil is a light hydrocarbon liquid that is entrapped in petroleum formations (low-permeability shale or sandstone). It is extracted from oil shale by the fracking method and can be employed as an alternative to conventional crude oil as FCC feed.[61,62] The extraction is relatively costlier than conventional crude oil both from financial and

environmental impact points of view.[63] The United States has the largest and most concentrated oil shale resources in the world which constitute 62% of the world's known recoverable shale oil potential.[64] The tight oil has recently emerged as a FCC feedstock and is successfully processed in the North America refineries.[65] Raw shale oil like the conventional petroleum consists of hydrocarbons, usually large quantities of olefinic and aromatic hydrocarbons. It also contains trace amounts of oxygen (0.5–1%), basic nitrogen (1.5–2%), organic sulfur (0.15–1%) and metals.[66] The levels of sulfur and nitrogen, as well as vanadium and nickel are low, but with high levels of iron and calcium although the amount of formed coke is low, and this feed also gives low octane gasoline compared with mid-continent VGO.[65,67] Even though these properties are generally desirable for FCC operation, tight oils give high naphtha and LPG yields that are generally paraffinic, which is problematic to distillation units and gas plants, thus limiting FCC throughput. The low content of Conradson carbon residue and aromatics makes it more difficult to control the coke deposition and correspondingly the unit heat balance.[3] On a laboratory scale, Li et al.[68] have recently reported successful cracking of shale oil on a fixed bed reactor for heavy oil conversion under conventional FCC reaction conditions. The conversion and yield of liquid products increased considerably after pretreatment of the shale oil with HCl and furfural.

2.1.2. *Non-conventional feedstock*

Due to the increasing and stringent governmental policies on the production of cleaner fuels and on environmental emissions around the globe and the depletion of natural reserves of crude oil and the high cost of sweet crude, alternative energy resources become essentially an attractive option for the future. Fuel resources obtained outside the crude oil that can be processed in the FCC units collectively form non-conventional FCC feedstocks.

Non-conventional FCC feedstocks are referred to as alternative feedstocks that have the potentials to be processed in the FCC units to obtain its primary products. Examples of non-conventional feedstocks include biomass-derived feeds, (bio-oils -pyrolysis oil, vegetable oils and animal fats), naphtha feeds, Fischer Tropsch waxes, and alcohols that can be processed (normally blended with gasoil) in the FCC unit.

(1) Bio-oil

Recently, researchers have shown growing interest in renewable fuels, and particularly bio-fuels resources have gained much attention. Biomass-derived feedstocks include bio-oils, vegetable oils and animal fats. Bio-oils are obtained from pyrolysis of biomass. They have high contents of oxygenated compounds in addition to being highly viscous and corrosive.[69] Biomass-derived liquid fuels have the potential to provide a low-cost and sustainable

supply of energy, while meeting the greenhouse gases reduction targets. Vegetable oils are oils exclusively of plant origin. Most vegetables oils are edible and some can be of invaluable medicinal applications. However, in recent years, researchers have considered the exploitation of vegetable oils as a potential renewable energy resource and have experimented processing them in the FCC process. Animal fats are obtained as byproducts from meat processing. They have been less investigated as a potential FCC feedstock as bio-oils and vegetable oils. Biomass-derived feedstocks have been extensively studied as FCC feedstock using conventional FCC reaction conditions, catalysts and test facilities, either as solely pure feed[70–73] or co-fed with gas oil to the FCC unit.[74–76] The results of recent studies employing bio-oils as feedstocks are summarized in Table 1.

While the processing of bio-oils by refiners in the FCC unit has not gained full prominence and implementation, an entirely vegetable oil (100% soybean oil) feed has been tested as a case study for pilot Davison Circulating Riser (DCR) work to understand the impact this type of feed would have on yields and operation.[26] The results obtained showed that at a constant coke basis, the soybean oil produced more light cycle oil (LCO), less gasoline, less C_3s, and less C_4s than the VGO. The gasoline produced by cracking soybean oil was highly aromatic. The heat drop during the reaction in comparison with the heat of cracking a standard VGO resulted in the soybean oil running at a much lower catalyst-to-oil (CTO) ratio than VGO under similar conditions implying that running a 100% bio-feed has implication for riser operation.[26]

Generally, the catalytic cracking performance of pyrolysis and vegetable oils are determined largely by a number of factors. For instance, the cracking of pure pyrolysis oil is a function of operating conditions and catalyst type, whereas co-processing it with a blend of conventional FCC feedstock such as VGO leads to higher conversion than pure VGO.[74,76] High coke formation and irreversible catalyst deactivation fueled by oxygen content in the biomass-derived oil constitute challenges which require further research for upgrading. The higher catalytic cracking conversion of pure vegetable oils than VGO is associated with low thermal stability and high fatty acid contents of the former, which facilitate fast mass transfer in the catalyst pores.[74] Co-processing of vegetable oil with conventional gas oil in the FCC unit improves the conversion than obtained with pure FCC gas oil. The product distribution and selectivity are influenced to an extent by the amount of vegetable oil in the feed, while the yield is determined by properties of the petroleum based feedstock component. For instance, in the co-processing of 10% bio-oil with VGO, similar yields of gasoline, LPG and LCO were obtained in comparison with pure VGO, whereas increasing the amount of bio-oil to 20% significantly deteriorated the product yields.[75]

Vegetable oils product distribution depends largely on the degree of saturation. Gasoline selectivity is favored when vegetable oils are saturated. Compared with VGO, aromatic contents are generally high for biomass-derived oils, and

Table 1. Recent studies on catalytic cracking of biomass-derived oils on conventional FCC test units.

Feedstock Source/type	Catalyst	Feedstock composition (pure/co-processed)	Reactor type	Ref.
Biomass pyrolysis (bio-oil)				
Pine wood	E-cat	Blend with VGO	Fixed bed, riser reactor	[75,77]
Pine sawdust	HZSM-5	Pure/blended with VGO	MAT unit	[78]
Eucalyptus wood	HZSM-5, HY, REUSY	Pure	Fixed bed	[79–81]
Forest residue	E-cat	Pure/blend with long residue	MAT unit	[82]
Canadian white pine	FAU	Pure	In-house designed	[83]
Maple wood	HZSM-5, HY, HMOR, Silicate-1, SiO_2 /Al_2O_3	Pure	Fixed bed	[84]
Swedish pine	HZSM-5	Pure	Plug fixed bed	[80]
Sunflower	E-cat	Blend with VGO	FCC pilot plant	[85]
Vegetable oil				
Rubber seed oil	Zeolites (Y, MCM-41, HZSM-5)	Pure	In-house designed	[86]
Palm oil	E-cat, USY/ZSM-5, HZSM-5/MCM-41	Pure, blend with VGO	MAT unit, FCC pilot plant, FCC riser reactor, fluid bed	[87–90]
Palm oil	Nano zeolite, rare earth Y (REY)	Pure	Fixed bed unit, riser reactor	[91,92]
Rapeseed oil	E-cat	Pure	Micro riser, MAT unit	[71,87]
Rapeseed oil	E-cat, Ecat/ZSM-5	Blend with hydrowax	Microriser reactor	[71]
Rapeseed oil	E-cat, REUSY/ZSM-5	Blend with VGO	FCC pilot plant	[88,93]
Canola oil	E-cat	Blend with VGO	ACE unit	[94]
Soybean oil	E-cat	Pure	MAT unit	[87]
Soybean oil	ZSM-5	Pure	Fixed bed	[95]
Soybean oil	E-cat	Blend with VGO	MAT, FCC pilot plan	[88,89]
Cotton seed oil	E-cat	Pure	Fixed fluidized bed	[96]
Cotton seed oil	E-cat	Pure	Fixed bed	

(*Continued*)

Table 1. (Continued).

Feedstock Source/type	Catalyst	Feedstock composition (pure/co-processed)	Reactor type	Ref.
Ginger oil	Zeolites (MFI, BEA, FAU)	Pure	Fixed bed	[97]
Jatropha Curcas L. seed oil	Mesoporous USY	Pure	Fluid bed	[98]
Waste cooking oil	Nanozeolites (ZSM-5, Y, Beta)	Pure	Fixed bed	[99]
Waste cooking oil	E-cat	Blend with VGO	MAT unit	[89]
Vegetable oil sludge	ZSM-5/MCM-41	Pure	MAT unit	[100]
Palm oil based fatty acids	E-cat, HZSM-5, Al-containing SBA-15	Pure	FCC pilot plant, fixed bed	[101–103]
Canola oil	Zeolites (MFI, BEA, FAU)	Pure	Fixed bed	[104]
Camelina seed oil	ZSM-5-Zn	Pure	Fixed bed	[105]
Waste cooking palm oil	SBA-15, MCM-41/beta	Pure	Fixed bed	[106,107]
Animal fat				
Chicken fat	USY/ZSM-5	Pure, blended with VGO	Fluidized bed	[108]
Grease (inedible fat)	E-cat	Blend with VGO	MAT	[89]

water remains an unavoidable product that must be separated from the desired products. Modification of catalysts and co-feeding the bio-based feedstock with VGO and/or H_2 to the FCC units can augment and significantly enhance selectivity to gasoline and light oil yields.[70] Besides, the adjustment of process conditions, FCC reaction re-configuration and catalyst design seem promising strategies for upgrading to boost production of transportation fuels and olefins.

(2) Naphtha feeds

The increasing demand for ethylene, propylene and other petrochemical feedstocks in large quantities has re-focused attention of the refiners to consider naphtha cracking and to develop FCC-type processes to preferentially crack naphtha range feedstocks to light olefins.[21,26,109–112] Naphtha can be used primarily as a feedstock for the production of propylene using ZSM-5 as additive with the conventional catalyst on the FCC unit and as a feedstock for steam cracking and catalytic reforming. In the near future, the demand growth for naphtha feeds will increase for Asia (China) and the Middle East as a result of the new market demand for propylene as petrochemical feedstock for various commodity chemicals such acrylonitrile and propylene oxide. The cracking of FCC naphtha was tested over a commercial E-cat, and the results indicated that the feedstock required severe operating conditions to crack.[110] The conversion and yield of propylene increased with increasing reaction temperature. Under high operating severities, shortening of residence time is necessary to increase the yield of propylene and to reduce dry gas yield.

(3) Fischer-Tropsch synthesis waxes

The Fischer Tropsch synthesis (FTS) is employed in the production of large quantities of long chain paraffin having wide range of boiling points from renewable energy resources (e.g., biomass). This paraffin can be processed in the FCC unit to high-valued fuels, such as gasoline and diesel. Therefore, FTS paraffinic products have become an attractive feedstock for the FCC units. FTS wax constitutes a future alternative feedstock resource for cleaner fuels, as they are free from impurities such as sulfur and nitrogen. However, selectivity to a particular product is a currently a challenge under the conventional FCC operation but can be realized by adjusting the processing conditions and appropriate catalyst selection. The potential of FTS wax as a FCC feedstock has been demonstrated on a microriser reactor using E-cat by Dupain et al.[72,73] Results revealed that high gasoline yield (up to 70 wt. %), higher than that of most conventional feedstocks and having high MON was obtained, thus making the FTS wax an alternative option to conventional FCC feedstock for the production of motor fuels. Using ZSM-5 and/or combination with zeolite Y-based catalyst, a high selectivity to propene and other olefins have been obtained.[70]

(4) Alcohols and model compounds

Catalytic processes such as methanol to olefins (MTO) can be used to convert methanol into valuable products like ethylene and propylene. Several reactor designs including fixed bed, fluidized bed and riser type reactors have been proposed for MTO.[113–115] Since methanol is much lighter than conventional FCC feedstocks, a modification of the position of feed system is necessary to enable the processing of methanol.[116] Other model compounds such as ketones, glycerol, aldehydes, sorbitol and phenols have been successfully evaluated on the conventional FCC units using zeolite catalyst.[74]

2.2. *Changes in FCC catalyst and reactor*

Conventional FCC (heavy oil) feedstocks contain high levels of contaminants that require feed pretreatments or catalysts with high resistance to contaminants, in addition to excellent hydrothermal stability due to the harsh regenerator conditions. In response, improved technologies have been developed to produce catalysts that can sustain their activities in the presence of various contaminants for longer period and can ensure high conversions possible. Moreover, the need to simultaneously optimizing other products of the FCC process has birthed the selection of new catalysts either as standalone catalyst or co-catalysts with the conventional FCC catalyst. Furthermore, to address the changes in feedstock and new market demands, FCC catalysts formulation and process have been continuously improved.

The FCC catalysts have evolved over the years of commercial applications. The first generation catalysts were based on natural clay that were generally of low activity and selectivity, poor thermal and structural stability, followed by synthetic silica and alumina catalysts that were unstable and difficult to regenerate despite having good activity.[25] Due to the catalyst attrition and sintering problems in the commercial unit, the latter catalysts were formulated as microspherical particles to enhance mechanical strength by Grace Davison in 1948.[117] In 1962, the Y-type zeolite (FAU) based catalyst, having high activity and selectivity to light oil fractions was developed by Mobil Oil Corporation and Union Carbide. Soon after, various modified forms of zeolite Y, for instance, rare earth exchanged Y (REY) and ultra-stable Y (USY) were developed. Rare earth elements stabilize the zeolite framework and increase its thermal and hydrothermal stabilities. USY is a form of zeolite Y in which some of the framework aluminum has been selectively removed to enhance thermal/hydrothermal stability. Later came another important zeolite catalyst named ZSM-5. The ZSM-5 based catalyst is applied mainly as additive to the conventional FCC catalyst to enhance selectivity to light olefins, such as propylene and to increase gasoline octane rating. The zeolites have constantly been improving till date. Improvements in FCC catalyst to

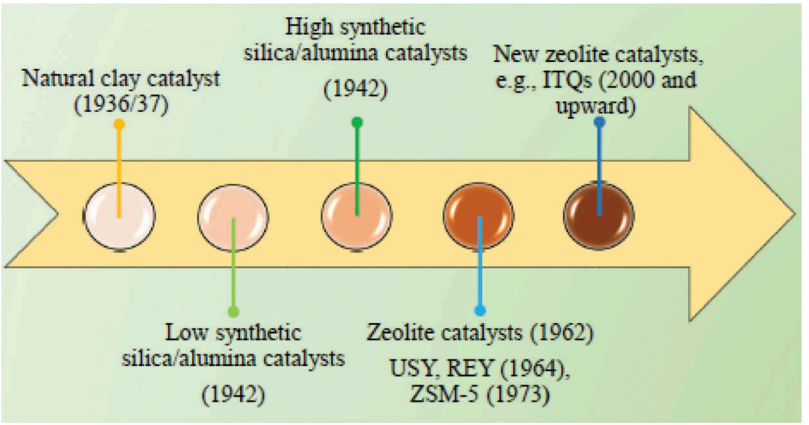

Figure 3. Evolutional trend of FCC catalysts.

enhance its performance is not limited to zeolite, it is common nowadays to find a cracking catalyst that is made of stabilized or modified zeolite Y, matrix and binder, and other catalyst additives. Figure 3 shows the generational evolution of FCC catalysts with time.

Recently, new zeolites have been tested in the FCC process in the place of traditional zeolite Y as FCC catalysts.[3] Zeolites such as ITQ-21 and ZSM-20 have pore structures and openings that resemble Y-type and in some aspects their performance too. ZSM-20 compared to zeolite Y possesses higher thermal stability, but compromised catalytic activity still renders it inferior. Other new zeolites that have been tested as additives in FCC include ITQ-7, ITQ- 13, ITQ-33 and ITQ-39.[118–121] These zeolites have mixed pores systems and most have not shown desired activity or product selectivity for cracking reaction.

The constant improvements in catalyst technology to achieve higher conversion and selectivity toward the desirable products are a clear testament to the radical development that has characterized the FCC process in recent years. For example, the use of stabilized or modified and hierarchical/mesoporous structured zeolites and highly accessible matrix catalysts not only improve performance of the FCC unit, but also provide resistance against feedstock metal contaminants during conversion of heavier feedstocks. Technological advancements and development have also afforded deeper insight into understanding the fundamentals of FCC catalyst contamination and associated challenges to the performance of the FCC process. The catalyst currently employed in the FCC process contains zeolite Y-based active component dispersed in silica-alumina and clay matrices previously described in section 1.

The catalytic cracking generally began with the fixed bed unit (Houdry catalytic cracking unit) in the late 1930s.[25] This unit had two fundamental problems: (i) rapid catalyst deactivation, and (ii) batch catalyst regeneration configuration. Soon was a replacement with a more convenient processing

unit that allowed for continuous circulation of the catalyst from the reactor and with the advantage of operational flexibility as heat transfer was greatly improved. In 1942, the fluidized bed reactor introduced was based on the fluidized characteristic of small particles of silica-alumina catalyst that form mixed fluidized phases in both the reactor and the regenerator when gas oil was passed through during the reaction and air during regeneration for improved.[25] At the time of the zeolite catalyst emergence, the FCC unit designs were modified to accommodate the catalyst change, but most of the basic flow sheets remained the same and only minor changes required in the processing equipment. The recent improvements in the FCC reactors have been reviewed by Chen.[122] The newest riser in use has a technology for minimizing the density and velocity variations and promotes ideal plug flow, in addition to enhancing termination of cracking reaction after a desirable cracking time. The regenerator incorporates a third stage to its conventional two stages, which provides enhanced capacity for achieving low particulate fines and flue gas. Also, improvement in catalyst circulation technology enhances catalyst circulation rate. Recently, catalytic pyrolysis cracking unit has been added to the file, in a quest to produce all petrochemical feedstocks.[123] The Catalytic Pyrolysis Process (CPP) could substitute the fundamental steam cracking process for ethylene production since it offers the utilization of cheaper feedstock and allows to vary ethylene to propylene ratio over a wide range

3. Contaminants in FCC feedstock and catalyst

FCC feedstocks (mainly residues) contain several types of contaminants including different metal-organic compounds. During the operation of the industrial FCC unit, these compounds are fed with the feedstock and once cracked metals are deposited on the cracking catalyst.[124,125] Non-metallic compounds such as organic sulfur and nitrogen compounds also present themselves as feedstock contaminants. The introduction of these contaminant species into the cracking unit has presently become normal due to heavier feedstocks becoming more common and affordable nowadays to the refiners. Consequently, more coke is produced which causes the regenerator to operate at unacceptably high temperatures, changing FCC catalyst activity and selectivity.

3.1. *Non-metal contamination*

3.1.1. *Nitrogen and sulfur compounds*

Organic sulfur and nitrogen compounds are regarded as petroleum feedstock contaminants. The damage by sulfur and nitrogen compounds to FCC catalyst is rather small but they affect the catalyst activity and selectivity.

These types of contaminants can be eliminated from the FCC process in their molecular and/or oxide forms. A significant proportion of the nitrogen is burnt to nitrogen gas, while the other is converted to NO_x species. Most of the non-eliminated sulfur in the FCC feeds is transferred to the FCC gasoline pool. Sulfur in the gasoline contributes to SO_x emissions, and it also reduces the activity of vehicle catalytic converters and accelerates corrosion of engine parts.[126,127] Even as expected that sulfur and nitrogen impurities in the FCC feedstock are oxidized in the regenerator, a better alternative is to remove them by hydrotreating the feedstock before feeding to the FCC unit.

3.1.1.1. ***Nitrogen.*** Although less attention has been paid to the effects of nitrogen compounds on the conversion of hydrocarbons under typical conditions of the commercial catalytic cracking, the damage by nitrogen to the FCC unit is as harmful as some metal poisons, and the effect on the cracking catalyst are comparable to the latter. A typical VGO for FCC process contains approximately 25–30%, whereas vacuum residue contains 70–75% of the nitrogen in crude oil.[19,128] Most of the nitrogen exists as basic nitrogen compounds, which may be aromatic or polyaromatic, branched or not, having predominantly heterocyclic skeleton (pyridine, quinolones, acridine and phenanthridine).[129,130] Others are non-basic compounds including pyrroles, indoles and carbazoles. According to Cheng et al.[34], 50% of feedstock nitrogen ends up in the liquid products, and analysis has shown that nitrogen concentrates in LCO and bottom. About 8% of the feed nitrogen is converted to ammonia and the remaining 42% is found in coke. Most of the nitrogen in coke is converted to molecular nitrogen in the regenerator; about 10–15% of the nitrogen in coke transforms to NO. In commercial FCC regenerators, the fraction of nitrogen released as NO varies from about 3 to 25% depending on the regenerator design and operating conditions.[5,131] Generally, basic nitrogen containing compounds adsorb on the active sites of FCC catalyst and neutralize them. Consequently, activity of the catalyst decreases and the product yields alter. However, the catalyst activity can be restored after regeneration. Regeneration releases both molecular nitrogen and associated oxides (NO_x), which leave the regenerator as one of the flue gases, and the NO_x released contributes to environmental pollution and health problems.[132] The adsorption of nitrogen compounds involves charge transfer and causes blockage of the active sites.

The poisoning effects of nitrogen compounds on cracking catalysts have been widely studied. It has been found that basic nitrogen compounds can reversibly poison the acid sites of the FCC catalyst, resulting in a decrease in acid centers or acting as coke precursor due to their big molecular size and aromatic nature.[133] Li et al.[134] showed that non-basic nitrogen compounds and condensed aromatics in coker gas oil (CGO) could easily adsorb on the cracking catalyst, causing pore blockage and a decrease in conversion and

light oil yields, and could also lead to higher coke yield during cracking under conventional FCC conditions. Caeiro et al.[57] investigated the effects of nitrogen poisoning on the catalytic cracking of gas oil. The catalytic evaluation indicated that basic nitrogen reduced gasoil conversion by 5–10 wt.%, depending on the CTO.[57] Increasing the nitrogen concentration resulted in a decrease in activity and a variation in product distribution. Coke and hydrogen yields increased at the expense of gasoline. The reduced catalytic performance was attributed to the poisoning effect of nitrogen molecules adsorbed on the acid sites where cracking reactions take place. In a related study by Bobkova et al.,[135] the rate constant of n-undecane cracking over zeolite containing E-cats was found to decrease non-linearly as the concentration of nitrogen in the feedstock increased, but yields of the products were independent of the conversion. The poisoning of the catalyst was attributed to the deactivation of the acid sites and to the pore blockage. Basic nitrogen compounds were shown to cause a strong decrease in the conversion of methylcyclohexane over H-MFI zeolite.[136] The decrease in acidity was proportional to the amount of nitrogen retained in the zeolite, and the intrinsic poisoning correlated with the proton affinity of the bases located on the external surface. A study by Ho[137] on the effect of a series of nitrogen compounds on the activity of a cracking catalyst indicated that these compounds exhibited different poisoning tendencies, determined by their physiochemical properties, which include basicity, type of heterocyclic nitrogen (pyridinic or pyrrolic), length and location of alkyl substituents in the heterocyclic rings, number of attached benzene rings, hydrogenation of the nitrogen compounds, and number of nitrogen atoms in the hetero-rings. Fu and Schaffer[133] showed that a correlation exists between the nitrogen gas-phase basicity and its poisoning effect on the cracking catalyst. For instance, the proton affinity that determines the extent of poisoning is dependent on the molecular structure of the particular nitrogen compound. Furthermore, the effects of changing reaction conditions – cracking temperature, zeolite content of the catalyst, and feed properties were explained in terms of the basicity of the nitrogen compounds, which controlled conversion and selectivity of the poisoned catalysts.

The reaction conditions could be controlled to ameliorate the deleterious effects of nitrogen compounds during catalytic cracking. Running the reaction at a high temperature has been shown to alleviate the undesirable effect of basic nitrogen compounds on the cracking of CGO over an equilibrium FCC catalyst. It was found that increasing the reaction temperature (500–580 °C) raised the conversion by 20 wt.%, due to decreasing nitrogen compounds adsorption on the catalyst active sites at higher temperatures.[138] The non-basic nitrogen compounds also interact with the catalyst active site, but to a lesser extent compared to basic nitrogen compounds, resulting in decreases in gasoline and diesel yields. This is explained by the fact that non-basic

Table 2. Effects of sulfur and nitrogen compounds and coke on FCC catalyst.

Contaminant	Effect on FCC catalyst	Ref.
Nitrogen	• Poisons acid sites, reduces activity, increases coke formation, blocks catalyst pores, decreases conversion, decreases reaction rate constant, changes selectivity	[57,68,133–135]
Sulfur	• Decreases conversion, decreases activity, increases coke formation, destroys acid sites	[139–141]
Coke	• Covers active sites, blocks pores, decreases acid sites, reduces surface area and pore volume	[125,142–144]

nitrogen compounds have larger molecular sizes, which make it difficult to access the active sites located in the zeolite.[134] Generally, when present in FCC processing feedstock, nitrogen compounds tend to promote the deactivation of FCC catalyst through various routes as summarized in Table 2. The high coking tendencies of basic nitrogen compounds are attributed to their molecular sizes and aromatic nature, while poisoning of the acid sites is related to their proton affinity.

3.1.1.2. ***Sulfur.*** Sulfur is the most abundant heteroatom in crude oil. The atmospheric residue and vacuum distillate that constitute majority of the FCC feedstocks contain significant amounts of sulfur, generally in the range of 0.5–1.5 wt.%[139], which causes SO_x emission from the regenerator. The amount of SO_x emitted from an FCC regenerator is dependent on the quantity of sulfur in the feed that is converted and coke yield. The sulfur balance of FCC unit showed that about 50–60% of sulfur in the FCC feedstocks ends up in the liquid products, about 35–40% is released as H_2S while a small proportion of 2–5% appears in the coke. Moreover, 2–5% of the sulfur exists in FCC gasoline[145,146], which constitutes as much as 80–90% of the total gasoline sulfur emission originating from FCC gasoline.[34] The species of sulfur in the FCC feedstocks include mercaptans, sulfides, thiophene and its alkyl-derivatives, thiophenols, benzothiophenes, dibenzothiophene and aromatic thiophenes.[34,147] Thiophenes are the dominant sulfur species in FCC gasoline. These species could originate from the cracking of heavy alkylthiophenes or other sulfur containing molecules that are present in the feedstocks. A recombination reaction can also result in the thiophene formation. Olefin-H_2S recombination over equilibrium FCC catalyst was responsible for all the produced thiophenic species in FCC naphtha.[148] However, thiophene or its alkyl derivatives can be saturated to produce tetrahydrothiophenes, which can be easily cracked to produce H_2S and hydrocarbons.[149] Other routes include self-desulphurization, alkylation, polymerization and condensation. Desulfurization occurs through saturation of thiophene to tetrahydrothiophene, which subsequently decomposes to H_2S and hydrocarbons. The mechanism of polymerization and condensation is particularly favored in the presence of contaminant metals in the feedstock, which

reduce thiophenes by converting them to coke.[149,150] The existence of contaminant metals (V and Ni) in a high sulfur feed is of beneficial effects. Myrstad et al.[126] showed that when V and Ni were present in the feed, the level of sulfur in the FCC naphtha was generally reduced.

Sulfur compounds in FCC feedstocks can affect the cracking activity of the catalyst although to a lesser extent as compared with nitrogen. Leflaive et al.[139] investigated the reactivity of thiophene derivatives and their precursors over commercial E-cat under FCC conditions. The results revealed that the conversion of various sulfur containing compounds decreased with time-on-stream over the catalysts. For example, in the transformation of thiophene-based fuels, the conversion was extremely low (< 0.2%), and only trace amounts of gases (C_1, C_2, C_3 and $C^{=}$) were obtained. The main side reaction was the formation of coke on the catalyst, which was up to 2.5 wt.% after 20 h on stream.[139] The addition of H_2S to olefins and diolefins, resulting from cracking of hydrocarbon and thiophene derivatives with long alkyl chains, and cracking over E-cats, produced compounds that were composed of mainly thiophenes with short alkyl chains (1–3 carbon atoms). It was found that thiophene-like poisons on FCC catalyst at individual particle level interacted with the Bronsted acid sites (BASs) of the catalytic materials, forming oligomeric carbocations and coke species.[140] Only zeolite components of the catalysts was responsible for formation of the oligomers, which were influenced by the zeolite pore structure, indicating zeolite controlled the activity. Sulfur compounds were spatially entrapped in the zeolite components of the FCC catalyst.[140] Non-thiophenic sulfur compounds were presented to be responsible for decreasing activity of the cracking catalysts and increasing coke formation. For example, Hernandez-Beltran et al.[141] in their study spiked gas oil with a non-thiophenic sulfur species (hexyl-2-thiol) and cracked over E-cats. The conversions were generally low, and increased sulfur content was detected in gasoline and cycle oils. The hexyl-2-thiol mainly produced H_2S and thiophenic compounds in the gasoline range. The addition of Zn-Al_2O_3 sulfur reduction additive mitigated the harmful effect of the sulfur species on activity of the catalyst by selective adsorption of the sulfur species due to its Lewis acidity properties, and the cracking activity of the catalyst improved drastically. The main effects of sulfur species on FCC catalyst are listed in Table 2.

3.1.2. *Coke*

In catalytic reactions, coke may be defined as any carbonaceous residue on the catalyst which tends to cover the active sites. It could also be referred to as the material that are obtained by the decomposition or condensation of hydrocarbons and retained inside of the catalyst particles after reactions.[151] In addition to the coke formed by cracking reactions on catalyst acid sites, coking can result from thermal reactions and dehydrogenation reactions

promoted by the presence of contaminant metals such as vanadium and nickel and from entrained catalytic products due to partial stripping as these entrained products will be burned in the regenerator and counted as coke.[152] The coke that is formed during catalytic cracking in the FCC unit can be beneficial and harmful. It is advantageous in the sense that the heat provided by coke combustion in the regenerator maintains the heat balance of the reactor.[29,153] The amount of coke on the catalyst is affected by metal contamination, which is dependent as well on the metal type. Metal contaminants play an important role in the enhanced production of carbon dioxide during the regeneration of the spent catalysts.[154] Direct conversion from carbon to carbon dioxide in regenerator is catalyzed by nickel. In this regard, high CO_2/CO ratio during regeneration could be prevented by controlling the nickel content in the feedstock.[154]

In the FCC unit, the amount of coke produced is proportional to the CTO and catalyst properties.[155] Generally, coking results in reversible deactivation of the catalyst in several ways including covering the active sites, limiting access to active sites and blocking the pores[125,142–144,156] and causing surface area reduction.[157] During cracking, the deactivation of the catalyst by coke starts with coverage of the active site (initial coke formation stage) and later pore blockage due to growth of coke layers[144]; in the micro-riser, the initial coke deposition is the main cause of the deactivation of the catalyst.[155] Catalyst deactivation is caused by the formation of coke on both catalyst's external and internal surfaces. Nitrogen adsorption results have shown that during gas oil cracking, coke deposit distributes within the surface and the internal pores of the catalyst. Only 32% of the total coke generated was located on the FCC catalyst surface. The rest was distributed in a 60:40% ratio in the catalyst micropores and mesopores, respectively. Both the acid sites strength and density of the coked catalyst will be unavoidably decreased.[158] The uniform deposition of coke on the micropore walls decreases the pore size and hence, limits molecular diffusion to the active sites. Coke deposition will eventually block the accessibility to catalyst active sites located in the zeolite micropores, affecting both primary and secondary reactions. The extent of pore obstruction by coke correlates well with the loss of specific surface area and pore volume.[125] Furthermore, the effect of coke deactivation of FCC catalyst depends very much on the nature of coke, its structure and morphology.[153]

Different types of coke have been identified (Figure 4). The coke formed during catalytic cracking reactions can be classified as: catalytic coke formed from condensation and dehydrogenation reactions, catalyst-to-oil coke associated with hydrocarbons entrained in the pores, thermal coke formed at high reaction temperatures by free radical mechanism, additive coke (or Conradson coke) formed from heavy molecules presence in the feed and contaminant coke from the dehydrogenation catalyzed by contaminant metals (Ni, Fe and V).[17,19] Thermal coke is less compared to

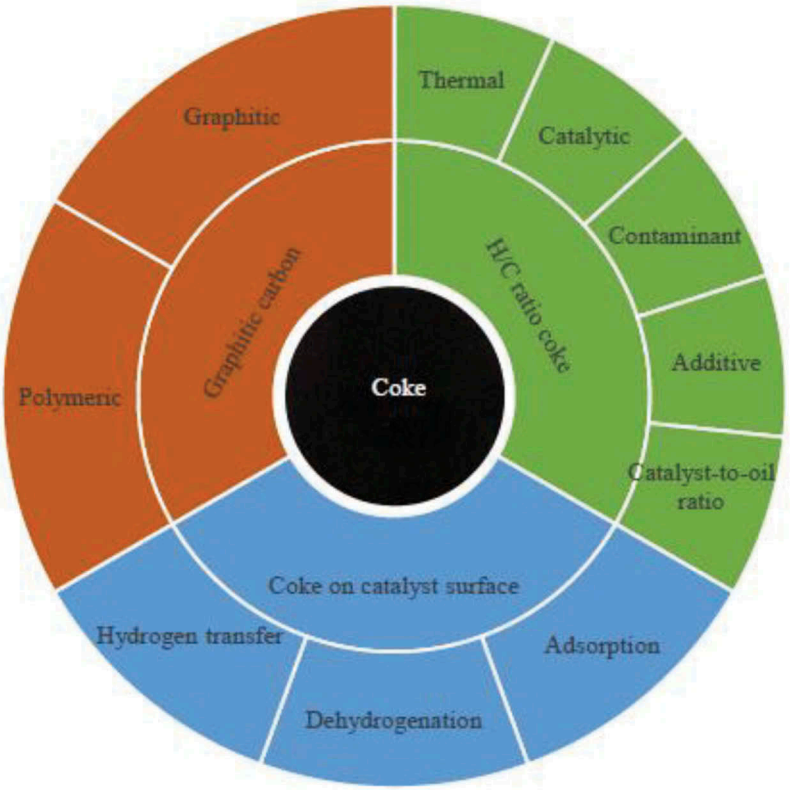

Figure 4. Types of coke formed during FCC reaction.

catalytic coke, due to the low extent of thermal cracking under typical FCC conditions. Recently, Wang et al.[159] studied the coking behavior of CGO over commercial equilibrium FCC catalyst on a MAT unit and identified other types of coke on the surface of FCC catalyst, including adsorption coke (C_{ad}), dehydrogenation coke (C_{dh}) and hydrogen transfer coke (C_{ht}). The C_{ad} coke is derived from nitrogen compounds and adsorbed on acid sites of the catalyst, accounting for 37 wt.% of the total coke under conventional FCC reaction conditions. C_{dh} is produced from dehydrogenation and condensation of polycyclic aromatic hydrocarbons and constitute 43 wt.% of the total coke formed, while the C_{ht} is determined by the extent of secondary reaction inside the catalyst pores. Coke also exists in other forms besides elemental carbon, like graphitic or polymeric carbons having high molecular weights[160,161], and can be grouped structurally into amorphous, aromatic, filamentous or graphitic carbon.[162] The structure of coke obtained from the refinery FCC operations is related to the nature of feedstock, and is mostly aromatic in nature.[152,163,164] Aromatic coke resides on the outside while the inside of the catalyst particles has concentrates of aliphatic coke that is produced during catalytic process.[165]

Hydrotreated feedstocks show much lower coke formation tendencies than the conventional heavy oil under the same operating conditions.[166] By studying the composition of coke and its effects on the acidic properties of USHY zeolite in the m-xylene transformation, Cerqueira et al.[167] found aromatic form of coke having up to four rings were trapped in the zeolite pores. The coke poisoned the protonic (Brönsted acid) sites while the Lewis acid sites were unaffected. The formation of coke was monitored by the decrease in the intensity of IR hydroxyl (acidic) band. The bridging hydroxyls in interaction with extra-framework aluminum species were most affected by coke, whereas no interactions were observed between the non-acidic hydroxyls and the coke molecules.[168] In another report that investigated the influence of coke on the deactivation of FCC catalyst by Wallenstein et al.[14], both coke-free and pre-coked FCC catalysts containing ZSM-5 additive were evaluated by cracking a VGO on a MAT unit at a high temperature in a short contact time. The selectivity of C_6–C_9 olefins was not influenced by pre-coking of the catalyst in the absence of metal, but coking generally lowered activity of the catalyst. Deactivation of the catalyst by coke was similar in the absence of contaminant metals (V and Ni), but when the metals existed, the catalyst without additive deactivated faster than that the one with additive. Although coke is regarded as a contaminant of FCC catalyst due to its effects on the accessibility of catalyst active sites, deactivation by coking is reversible as coke is burnt off in the regenerator. Coke, like the non-metallic contaminants, deactivates the cracking catalysts as summarized in Table 2; but, its deactivation mechanisms are different from those of sulfur and nitrogen compounds.

3.2. *Metal contamination*

Supplying feedstocks to the FCC unit free from metal contaminants is desirable for the petroleum refiners. However, most available feedstocks (heavy fractions) come with certain amounts of metals. The organo-metallic compounds, in the form of porphyrins, decompose in the FCC unit and leave metals on the catalyst. Unlike nitrogen, sulfur, and coke, metals cannot be removed by oxidation, they remain and accumulate on the catalyst after regeneration as poisons, causing irreversible deactivation of FCC catalyst.[19,41,169,170] Depending on the metals level, the conversion drops with the increased production of hydrogen, dry gas, and coke formation at the expense of gasoline and/or fuel oil. As a matter of fact, the presence of metals in FCC feedstock affects the efficiency of catalytic cracking process and increases the cost of running the FCC unit. Various petroleum feedstocks around the world are known to contain at least trace amounts of many metals (V, Ni, Na, Ca, Fe, Zn, Pb, Cu, Cd, Cr, Co, Sb, Te, Hg, Au, and Ag.[19,171–177] Tables 3 and 4 show typical concentrations of metals in petroleum feedstocks and in different types of crude oils around the globe, respectively. It can

Table 3. Typical concentrations of metals in crudes (μg/g).

V	Ni	Fe	Ca	Pb	Zn	Sr	Cr	Co	Al	Ref.
28.2 ± 0.4	17.5 ± 0.2	98.9 ± 1.4		101.1 ± 1.3				0.151 ± 0.005	104	NIST 1084a/1634c
54.6 ± 3.2	28.1 ± 4.5	42 ± 6	156 ± 81	–	4.8 ± 0.7	–	–	–	48 ± 23	[178]
55.6 ± 1.8	28.1 ± 0.7	32.2 ± 0.9	–	0.25 ± 0.03	3.9 ± 0.3	0.61 ± 0.02	0.41 ± 0.04	0.32 ± 0.01	18.5 ± 0.5	[179]
2–180	1–70									[180]
55.1 ± 1.6	28.1 ± 0.7	31.3 ± 1.0	33.2 ± 1.3	3.0 ± 0.1	2.93 ± 0.26	0.40 ± 0.01	0.74 ± 0.03	0.300 ± 0.009	14.6 ± 0.4	[181]
7.1–37.6	6.3–28.6	< 0.5–7.3	< 2.1–7.4							[124]
13.8 ± 1.4	11.2 ± 1.1	2.51 ± 0.24	415 ± 38	0.194 ± 0.020	1.31 ± 0.14	43.1 ± 4.2	0.055 ± 0.005			[172]
53–54.2	27.8–28.6									[182]
8.7–84.1	2.8–25.6	6.7–48.9								[183]
0.3–248.0	< 0.1–83.1									[184]
280–1200	54–107									[185]
18.0–21.9	9.8–13.1			0.206–0.410			0.035–0.062	0.182–0.289		[186]
16 ± 1	2.8 ± 0.1	21.7 ± 0.4								[176]
30 ± 3	12.9 ± 0.7	3.0 ± 0.1								[176]
258	57	10								[187]
200	54	65								[187]
348	89	26								[187]

Table 4. Levels of metals in various crudes around the world[188,189].

Crude oil	V (ppm)	Ni (ppm)	Fe (ppm)
Arabian light	94	22	–
Arabian heavy	171	53	–
Iranian light	188	70	–
Iranian heavy (Gach saran)	404	138	–
Iraq (Kirkuk)	58	< 3	–
Kuwait	59	18	–
Algerian (Hassi Messaoud)	< 5	< 5	–
Libyan (Brega)	24	32	–
Nigerian (Bonny medium)	7	52	–
North sea (Ekofisk)	1.95	5.04	–
South American (Bachequero)	437	75	–
Arabian light (Middle East)	6	10	–
Kuwait (Middle East)	30	8	–
Kern River (Bakersfield)	35	63	28
South Belridge (California)	57	60	35
Hondo (Santa Barbara)	220	68	< 3
Beta (Los Angeles Beach)	135	104	60
Morichal (Venezuela)	282	75	19
Maya (Mexico)	243	46	3
Arabian heavy (Middle East)	55	17	< 3
Boscan (Venezuela)	1180	90	7
Cerro negro (Venezuela)	560	118	–
Wilmington (Los Angeles)	49	60	–
Prudhoe bay (Alaska)	19	9	–

be seen from Table 4 that the levels of metals vary depending on the origin of the crude oil. Generally, crude oils from Africa have lower contents of poison metals than those from the other parts of the world. The principal metal contaminants in crude oil are nickel and vanadium. Crude oils contain from about a few to over 250 ppm nickel[188] and from about 5 to 1500 ppm vanadium.[123,188] Recently, Doyle et al.[124] have determined the levels of V, Ni, Fe, and Ca up to 168.2, 44.6, 26.9, and 11.4 ppm, respectively, in ASTM proficiency fuels. In addition to the metals naturally present in crude oil, petroleum stocks have a tendency to pick up tramp iron from transportation, storage and processing equipment. Most of these tramp irons remain in the FCC unit in the form of large particles and is usually harmless.[190] It is an established fact that the higher the metal level in the feed is, the more enhanced the deactivation/poisoning of the catalyst will be, and consequently, the more often fresh catalyst is added to the regenerator, partially replacing the E-cat withdrawn (and the catalyst fine losses). The different metals found in the petroleum feedstock correspond to different catalyst deactivation behavior. Metals (such as iron, nickel, vanadium, and copper) significantly alter the selectivity and activity of cracking reactions if accumulated on the catalyst.[191] Over the

years, researchers described the extent of poisoning effects of metals by referring to the metals content (so called metals factor) of feedstock in several ways[20,191,192] as given below.

$$\text{Metals factor}(F_m) = \text{ppm Fe} + \text{ppm V} + 10(\text{ppm Ni} + \text{ppm Cu}) \quad (1)$$

$$\text{ppm Ni} + \text{ppm } 0.25\text{V}(\text{Mobil index}) \quad (2)$$

$$\text{ppm Ni} + \text{ppm Cu} + 0.25\text{V}(\text{Davison index}) \quad (3)$$

$$\text{ppm } 1000(14\text{Ni} + 14\text{Cu} + 4\text{V} + \text{Fe}) \text{ (Shell index)} \quad (4)$$

$$\text{ppm } 1000(\text{Ni} + 0.2\text{V} + 0.1\text{Fe}) \text{ (Jersey Nickel equivalent index)} \quad (5)$$

From the relationships given above, a feedstock with a "metals factor" greater than 2.5 is considered to be poisonous to FCC catalyst.[191] For example, Mobil index, the most commonly used metals factor: Ni + 0.25V or 4Ni + V, indicates that nickel is four times as active in hydrogen production as vanadium present in equal concentrations. Since metals induce high coke formation and promote dehydrogenation reactions, these metal indices correlate with metals activity (i.e., hydrogen and coke yields). Generally, the deposition of metal contaminants from crude oil causes an irreversible deactivation of the FCC catalyst. Therefore, it is imperative to understand the associated changes in the physicochemical properties of the cracking catalyst and how these changes affect the catalytic behavior.

4. Influence of feedstock metal contaminants on the properties of FCC catalyst

Studies have shown that the metal contaminants in FCC (petroleum) feedstocks affect the cracking catalyst in various ways including [1] loss of textural properties (surface area and pore volume), [2] loss of crystallinity, [3] structure collapse, [4] dealumination, [5] mesoporosity induction, [6] acid sites destruction, [7] activity loss and [8] selectivity modification.[193–199] These losses or alterations result in degenerative effects of decrease in conversion and valuable product yields.

4.1. *Effect of different metals deposited on FCC catalyst*

Metal contaminants are usually present in the petroleum feedstocks – VGO and atmospheric residue. Under cracking conditions metal contaminants are mobile and the mobility of different contaminant metals can vary significantly. Another important behavior of metals such as vanadium and sodium in the regenerator is their reactions with steam from the coke burning, forming intermediates that accelerate catalyst deactivation. Several

Table 5. State, location and effect of FCC catalyst metal poisons on FCC catalyst.

Metal	State & location of metals	Main effect	Supplementary effect	FCC performance
V	V^{4+}, V^{5+} Zeolite	• Surface area loss, • Acid sites destruction, • Dealumination	• UCS shrinkage, • Large pores	• Severe activity loss
Ni	Ni°, Ni^{2+} Matrix (Alumina)	• Catalyzes dehydrogenation • Increases coke formation	• Poisons acid sites on matrix • Non-selective cracking	• Dehydrogenation reactions • Increases coke formation
Na	Na^{+} zeolite	• De-protonates active sites • Inhibits dealumination	• Causes hydrothermal instability • Neutralizes acid sites • Enlarges zeolite supercage • Loss of micropores • Sintering	• Activity loss
Fe	Fe^{2+}, Fe^{3+} Matrix	• Pore plugging • Destroys surface morphology • Causes fluidization problems	• Poisons acid sites	• Reduces catalyst activity, • Loss of bottom conversion • Increases coke formation, • Increases coke formation
Ca	Ca^{2+} Matrix	• Deprotonation	• Neutralizes acid sites • Causes hydrothermal instability • Collapses pore network	• Increases coke formation

researchers have studied the effects of different contaminant metals on FCC catalysts, which are either the standard commercial catalyst composed of zeolite, matrix and binders or pure zeolites. In the following section, the effects of different metals (Table 5) on both types of catalysts will be discussed.

4.1.1. *Vanadium*

Vanadium is the most significant and common petroleum feedstock metallic impurity. It is widely and abundantly distributed in the earth crust.[200] The vanadium porphyrins or other organic vanadium complexes present in the crude oil are broken down and oxidized in the FCC regenerator, and the released vanadium deposits on the outer surface of the cracking catalyst and migrates to the interior of the catalyst particles.[201,202] Under FCC unit conditions, vanadium may exist as different species, in + 5 or + 4 oxidation states, depending on the environment of the unit or the regeneration mode. The predominant vanadium oxidation state depends largely on how evenly catalyst is distributed in the regenerator and on its operational mode: full or partial combustion.[49] In the full burn mode, vanadium stays for a longer

time in the + 5 state, whereas in the partial burn mode this oxidation state is difficult to reach. Several studies[201,203–206] have identified the different species of vanadium in FCC catalyst. For instance, vanadium in the spent catalyst after regeneration existed as a highly dispersed but isolated oxycationic (VO_x) units, where the value of 'x' is close to 4.[204] Tangstad et al.[206] found in their study by analyzing equilibrium FCC catalysts with electron spin resonance (ESR) and electron spectroscopy for chemical analysis (ESCA) that vanadium also existed in a + 4 (V^{4+}) state, which was converted considerably to a + 3 (V^{3+}) state after treatment with 5% H_2 in N_2 at temperatures between 650 and 750 °C. The reduced catalyst gave higher gasoline and lower coke yields on a MAT unit when processing atmospheric residue, implying that vanadium in lower oxidation states is not or less harmful to the FCC catalysts as a result of its lower mobility and less zeolite destruction. Similarly, vanadium in lower oxidation states has been shown to increase olefin selectivity on the FCC test unit[207] and to improve desulphurization performance.[208] These results combined with a molecular modeling study showed that vanadium with a lower oxidation number could affect the chemical conversion of high molecular weight hydrocarbon molecules.[209] From these results, it is apparent that the effects of vanadium poison are dependent on its oxidation state. V^{3+} is harmless, V^{4+} is less harmful and V^{5+} has amarked destructive influence on zeolites. This is because V^{5+} can form vanadic acid in the presence of steam during regeneration. This acid is volatile under this condition and its mobility causes vanadium distribution throughout the entire catalyst particle, resulting in the destruction of zeolite framework by hydrolysis of the lattice.[210] Upon incorporation into FCC catalysts (USHY and composite catalyst), vanadium was dispersed better in the composite catalyst than in the zeolite.[198] The hydrothermal treatment caused a decrease in vanadium concentration on the surface due to the mobility of vanadium into the interior of the catalysts.[201]

Vanadium significantly alters the physiochemical and catalytic properties of zeolites and FCC catalysts. The textural properties (such as surface areas and pore volumes) of a catalyst before and after deactivation can provide reliable information for predicting its performance. Changes associated with these properties after reaction are generally related to the deactivation of the catalyst. The effects of vanadium on the physiochemical properties of FCC catalyst have been widely studied. Wallenstein et al.[49] used changes in the physiochemical properties of FCC catalysts to evaluate effectiveness of the different methods of introducing contaminant metals to the catalyst. The surface area of the catalyst, and more specifically the surface area of the zeolite decreased with increasing vanadium content. Catalysts metallated by the spray impregnation method showed similar response to vanadium content, but that metallated using Mitchell method showed much weaker response compared to the equilibrium catalyst in terms of the zeolite surface

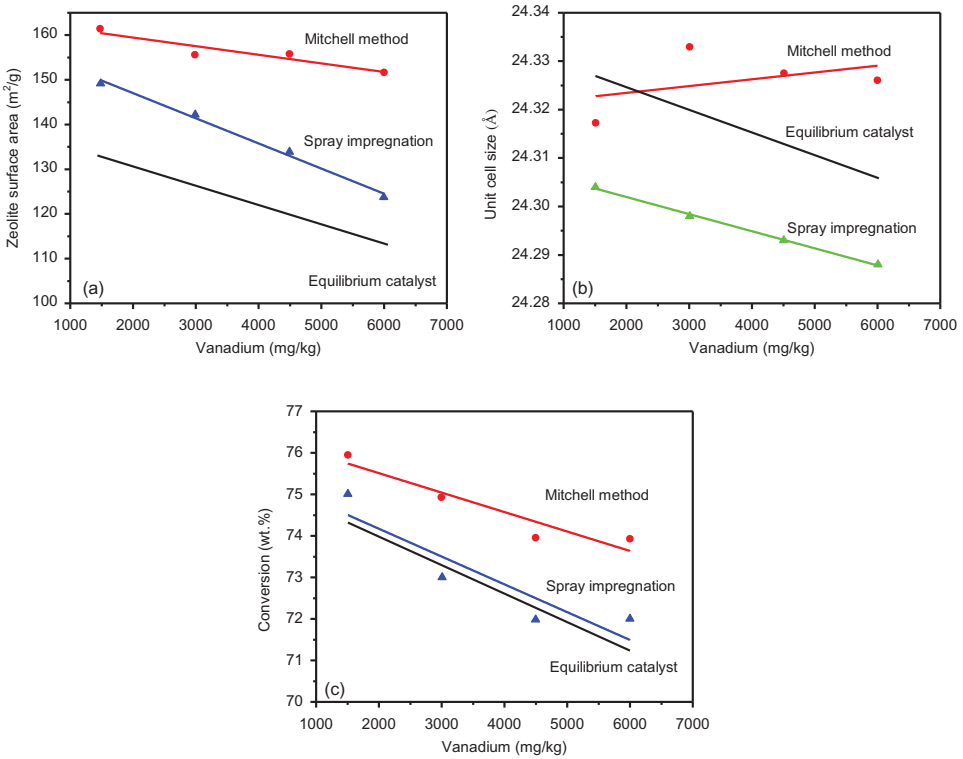

Figure 5. Effect of vanadium on physiochemical properties of FCC catalyst: (a) zeolite surface area, (b) unit cell size and (c) conversion.[49] Redrawn with permission from Elsevier, Copyright 2013.

area (Figure 5a). In a study on nickel and vanadium on zeolites (USHY and REHY) as monitored by measuring the extent of the surface area degradation under hydrothermal conditions.[194] Results indicated that vanadium caused far greater loss of the catalyst surface area in USHY than REHY. The TPR profile of the zeolite containing both nickel and vanadium showed preferential interaction of nickel with the rare earth in REHY, inducing higher vanadium mobility and reducing its ability to passivate vanadium. However, results of this study contradict the observations of Yang et al.[211] in which the presence of nickel in REHY was found to have rather a protective effect on vanadium destruction. A surface area retention of about 62.5% was realized when nickel was incorporated into vanadium-REHY. Generally, surface area measurement of the zeolites after hydrothermal treatment showed this trend of surface area retention: REY-Ni > REY-V-Ni > REY-V. The disagreement with the results of these two authors may be explained by the difference in the contents (3,000 ppm and 10,000 ppm for the former and latter, respectively) of the contaminant metals introduced to the catalyst[194] and the fact that zeolite Y is stable to low than high vanadium contents in them.[193]

Textural characterization results of zeolites after hydrothermal treatment indicated that ZSM-5 zeolite was structurally more stable to vanadium deactivation compared to Y-type at higher vanadium loadings due to the crystalline framework stability as a result of smaller pore opening of the former, and more importantly the lower Al content.[212] The micropore volume of both catalysts (ZSM-5 and Y-zeolite) decreased with vanadium concentration in the catalysts (Figure 6).

Etim et al.[195] have shown that in the presence of steam, vanadium is capable of causing loss of micropores in USY with the evolution of mesopores due to its mobile nature (Figure 7). The formation of non-intracrystalline mesopores, with average pore width greater than 25 nm is caused by accelerated dealumination. The mobility of vanadium was clearly demonstrated by using a vanadium trap, which decreased the mobility of vanadic acid into the zeolite channels, and consequently some micropores were retained. The micropore volume was most unaffected by vanadium in the absence of steam, but the cracking ability of the zeolite decreased and the product distribution in the catalytic reaction modified. In general, unlike coke and nitrogen, vanadium deactivation leads to a permanent deactivation.

Besides textural properties, other features of FCC catalysts are greatly impaired by the deleterious effects of vanadium. Cristiano-Torres et al.[213] reported that in dry atmosphere, vanadium is able to move onto the surface of the catalyst and neutralize strong acid sites. The apparent Brönsted acid sites (BAS) density measured by the isopropylamine decomposition decreased with increasing vanadium loading.[214] It was concluded that acid site neutralization is probably the first step in zeolite destruction under the regenerator conditions

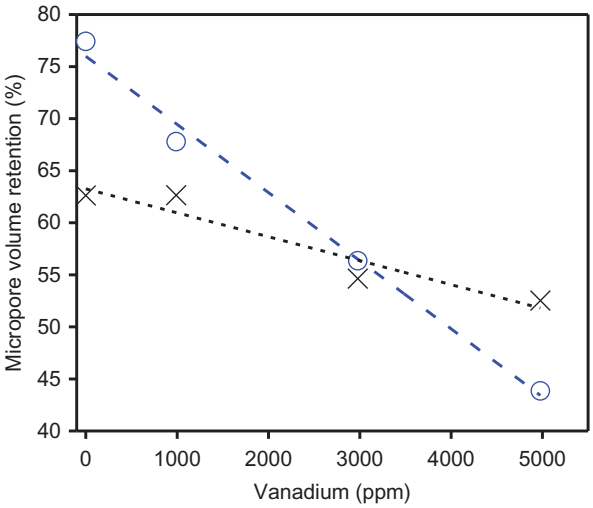

Figure 6. Effect of vanadium on micropore volume of zeolites (x) ZSM-5 (o) Y.[212] Reprinted with permission from Elsevier, Copyright 2008.

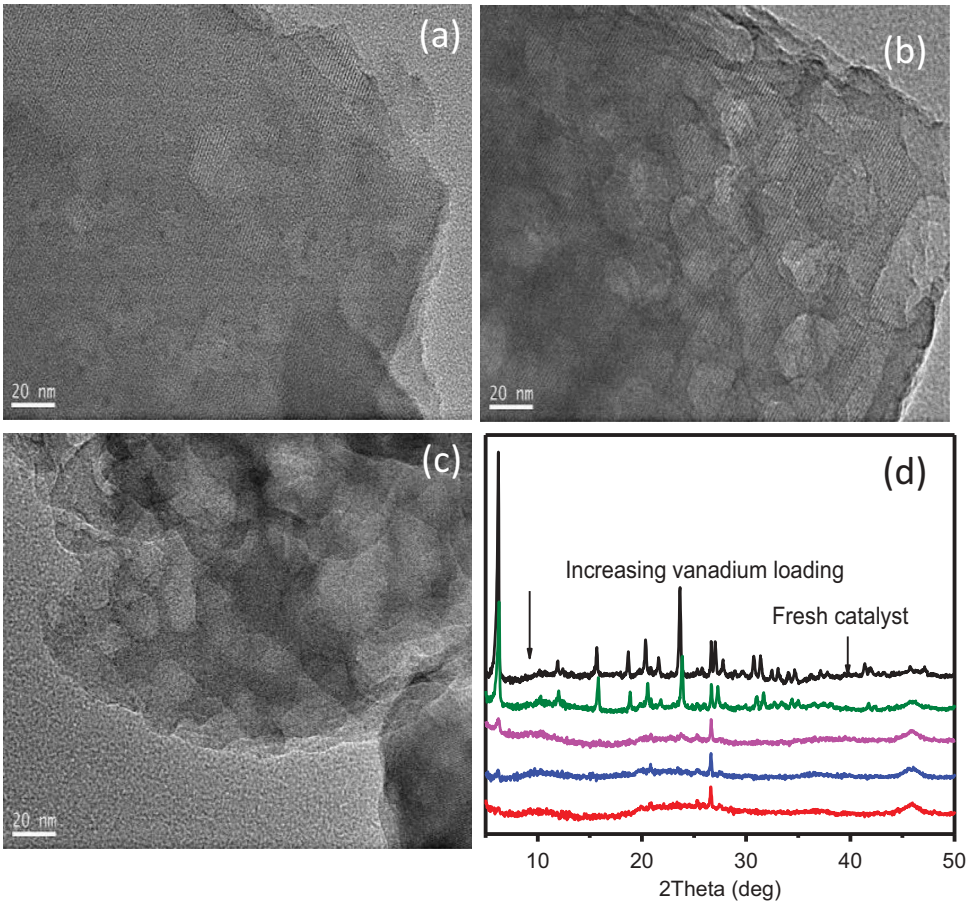

Figure 7. Non intracrystalline mesoporosity formation in USY by vanadium. (a) Parent USY, (b) 0.3 wt.% V/USY, (c) 0.5 wt.% V/USY.[195] Reprinted with permission from Elsevier, Copyright 2016. (d) Zeolite crystal structure destruction by vanadium.

of FCC unit. Pimenta et al.[212] investigated the effects of vanadium contamination on zeolites deactivation over a model cracking reaction using n-hexane as a probe molecule. The decrease in n-hexane conversion suggested that vanadium species poisoned acid sites and also assisted dealumination of the zeolite framework. Another significant effect of vanadium is the shift in the Braggs' angle on the X-ray diffraction (XRD) patterns of vanadium deactivated catalyst which leads to smaller d-spacing and unit cell parameters of the catalyst.[215] Severe deactivation of FCC catalyst by vanadium is also characterized by the decrease in unit cell size (UCS).[49,55] This decrease matches the reduction in the diffraction intensity of the zeolite Y (hkl = 533) peak[49], implying reduced crystallinity (Figure 7d), which is a fallout of excessive dealumination and structure damage. The UCS of a zeolite is a direct reflection of its framework aluminum content. A higher framework aluminum content per unit cell results in a higher UCS because Al-O bond is longer than Si-O bond. As the vanadium

content increases, bond scission takes place with subsequent dealumination, which proceeds via hydrolysis of the framework aluminum atom or through a direct attack of Si-O-Al bonds. Though steaming alone can cause dealumination of a zeolite catalyst, the extent is quite lower than when vanadium exists.

4.1.1.1. ***Vanadium effects on FCC products.*** The effect of metals poisoning on FCC product yields – gasoline, coke and hydrogen was studied by Lappas et al.[216] in an FCC pilot plant at a short contact time (SCT). The results showed that metals (V and Ni) greatly influenced the product yields (Figure 8). At a constant conversion of 65 wt.%, the yields of coke and hydrogen increased by about 80% and 250%, respectively, while the gasoline yield decreased by 7% when 4,000 ppm (Ni + V) existed in the catalyst. The metal contamination effect is proportional to the metal concentration only up to a critical level, beyond which the effect is not severe. In the FCC unit, excessive coke increase is undesirable since the unit operates on a heat balance and thus, it is necessary to limit the coke yield to a narrow range. Similarly, the substantial increase in dry gases has a considerable effect on the performance of the wet gas compressors in the refinery.[216] Besides, increasing vanadium concentration slows down the hydrogen transfer reactions, which increases naphtha octane number and enhances dehydrogenation of paraffin,[217] resulting in higher olefinic products, like higher gasoline RON, and higher LPG olefins.[55]

4.1.1.2. ***Destruction mechanism of FCC catalyst by vanadium.*** Understanding the mechanism by which vanadium deactivates the FCC catalyst is of utmost importance for the improvement in the catalyst design

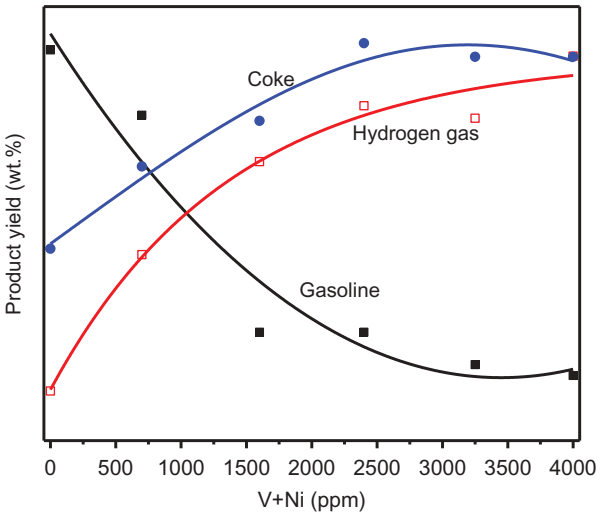

Figure 8. Effect of metals on gasoline, hydrogen and coke yields.[216] Re-drawn with permission from Elsevier, Copyright 2001.

technology, including the design of efficient vanadium scavenger for controlling vanadium deleterious effects.

Different mechanisms for the deactivation of FCC catalyst by vanadium have been proposed. Wormsbecher et al.[196] proposed that vanadium could form a poison precursor, vanadic acid (H_3VO_4), by reacting with steam under the FCC regeneration conditions capable of hydrolyzing the zeolite framework, thereby destroying the catalyst. An equilibrium concentration of H_3VO_4 in the range of 1–10 ppm was determined for vanadium deposited on a cracking catalyst, and this result indicated that vanadic acid is a strong acid, analogous to H_3PO_4 that can attack the Si-O-Al bond removing Al from the lattice and collapsing the structure. Occelli[203] showed that when vanadium-contaminated FCC catalysts were exposed to steam, anionic products $-H_2VO_4^-$ and HVO_4^{2-}, condensation products such as $H_2V_2O_7^{2-}$ and $HV_2O_7^{3-}$ and polyanions such as $H_2V_{10}O_{28}^{4-}$ were formed depending on several factors including contact time, catalyst composition, vanadium loading, and pH of the vanadium precursor solution. The author explained that zeolite destruction was initiated by $H_4V_2O_7$, which can be produced in the stripping section of the FCC unit. In the presence of high temperature steam, oxycations of vanadium (VO_2^+ and VO^{2+}) or hydroxyvanadyl cations and their protonated species could cause scission of Si-O-Al bond in HY, leading to the structure collapse. Under the harsh FCC conditions, vanadium (≥ 1 wt.% or 10,000 ppm) has the capability of converting HY/USY zeolite to mullite and tridymite.[195,197,203]

Pine[218] studied the kinetics of interaction between vanadium and water on USY to avail understanding of the dynamics of zeolite destruction in the FCC unit. Experimental results showed that steam was the main agent for zeolite destruction catalyzed by vanadium. The introduction of REs failed to increase vanadium tolerance, but was found to decrease hydrolysis and improve thermal stability of the zeolite. In another kinetic study of zeolite destruction in the presence of contaminant metals (V and Na), Du et al.[219] found that the formation of NaOH, which was the rate determining step, accelerated the zeolite framework decay in the presence of vanadium. Vanadium and its interaction with REs destroyed the zeolite structure by rupturing the stabilizing bridges in the sodalite cages. In a study that investigated the interaction of vanadium with various silica-aluminas using spectroscopy techniques, Altomare et al.[201] found that vanadium migrated into the particles interior; the presence of magnesium or rare earth oxides decreased mobility of vanadium even under steam-aging conditions. Once FCC catalyst particle interior is reached, vanadium could destroy zeolite even in the absence of steam and stabilizes in the form VO_2^+/VO^{2+} in the zeolite channels near acid sites after heating in oxidizing environment. Extra-framework alumina species competed with the zeolite for vanadium and reduced its migration to the acid sites.[205] In this study, the destruction

FCC catalyst was attributed to the mobility of vanadium caused by the low melting point of V_2O_5 (690 °C), but not to the widely accepted vanadium vapor precursor.

In studies on physically mixed catalyst or catalyst components with vanadium pentoxide powder (V_2O_5) employing Raman spectroscopy, X-ray photoelectron spectroscopy (XPS) and XRD, vanadates of rare earths or aluminum were detected as the major phases present in the deactivated catalysts from the destroyed zeolite phases. Calcined rare earth exchanged Y (CREY) collapsed with the formation of cerium orthovanadate ($CeVO_4$), while HY formed mullite and silicate (tridymite) phases.[220]

Wormsbecher et al.[196] and Occelli[203] have clearly shown that zeolite destruction proceeds via attack of zeolite by vanadic acids, H_3VO_4 and/or $H_4V_2O_7$, respectively. However, Pine[218] demonstrated that vanadium acts as a catalyst for steam destruction of the zeolite. In all cases, these mechanisms require both steam and vanadium for the occurrence of the deleterious effect which infers that vanadium intermediate certainly exists. Sanchez and Hager[221] showed experimental evidence that H_3VO_4 was the acid species formed at high temperature according the reaction below, which validated the proposals of Wormsbercher et al.[196]

$$V_2O_{5(s)} + 3H_2O_{(g)} \rightarrow 2H_3VO_{4(g)} \quad (6)$$

Recent studies[195,205] have also confirmed the fact that H_3VO_4 is the vanadium poison precursor responsible for the destruction of zeolites and FCC catalysts.

Pompe et al.[222] showed that vanadium can destroy REY by attacking the RE component of the zeolite Y, forming a low melting point RE vanadate in which RE ions are incorporated in various proportions depending on the chemical stability. These authors further explained that the vanadate formation required more oxygen than what could be supplied by V_2O_5, and this oxygen has to be therefore taken from the zeolite structure, thereby disrupting the zeolite structure.

4.1.2. *Nickel*

The impact of nickel on the overall utilization of petroleum for fuel production is significant. Nickel accumulates overtime in the FCC unit to unbearable destructive dosages on the cracking catalyst, resulting in several severe effects on cracking reactions. Nickel interferes with many upgrading processes, severely deactivating FCC catalyst and catalyzing undesirable side reactions, such as dehydrogenation and coke formation. In commercial spent catalysts, nickel has been found to exist in different states.[202,223–225] Petti et al.[224] studied the state of nickel in a commercial FCC E-cat by using XPS and observed that nickel existed mainly as $NiAl_2O_4$ or Ni_2SiO_4 with a small portion as NiO. The amount of coke formed was found to correlate

well with the surface Ni concentrations on the catalysts. Busca et al.[223] found that nickel existed as crystalline NiO on the modeled spent catalyst in an amount as low as 1,000 ppmw Ni on the catalyst, while the remaining existed in a highly reduced state (metallic Ni) in alumina matrix. The alumina matrix acts as a trap for this species of nickel, which is unwanted in the FCC riser due to its high dehydrogenation activity, leading to the formation of alumina spinel-like solid solution (Ni_xAl_{3+x}). Stöcker et al.[226] showed the presence of NiO in a FCC equilibrium catalyst, and the reaction of NiO with steam leads to the increased acidity, whereas further reaction with protons lowers the strength of acid sites on the zeolite. Nickel was found to enrich on the external surface of zeolite crystallites and hardly migrated into the interior of the particles in the presence of non-framework aluminum and other cations (Na^+ and La^{3+}).[227] On a commercial FCC catalyst nickel covered the zeolite surface uniformly, and steam aging caused migration of nickel from the zeolite particle into the matrix particles.[228]

The interaction of nickel with FCC catalyst matrix materials was studied employing the temperature-programmed reduction (TPR) technique.[229,230] The extent of reduction of nickel on alumina catalyst increased with an increase in nickel loading and reduction temperature. The reduction of 0.5 and 9.0 wt.% Ni on alumina catalyst at 450 °C reduced total nickel content by 29% and 75%, respectively. For nickel on silica catalysts, a higher nickel reduction was found at a much lower temperature than that on alumina due to the weaker interaction with the silica support.[229] There was also the evidence of correlation between the reducibility of nickel present on the cracking catalyst and their activity for coke formation and dehydrogenation, increasing with easiness of nickel reduction.[230] The extent of dehydrogenation is dependent on nickel concentration, nickel oxidation state, cracking catalyst type and age. A simple mechanism of coke formation by nickel is that the dehydrogenation reaction produces reactive paraffin (unsaturated hydrocarbons), which undergo rapid beta-scission or cyclo-condensations reactions, leading to formation of coke. Although nickel is a dehydrogenation catalyst and negligibly impact cracking catalyst activity, studies have shown that nickel-containing catalysts produced more heavy cycle oil/bottom or decreased bottom conversions[231], indicating a reduced ability to crack heavier feed components. Moreover, the activity of nickel in the regenerator has been shown to be catalytically unfavorable for high CO_2 concentration production; hence, processing high nickel feed can result in a low throughput.[232]

4.1.3. *Iron*

Iron in equilibrium FCC catalyst may come from sources including the feedstock to the FCC unit, the product of corrosion or from storage equipment degradation.[233] Contamination of cracking catalyst by iron has destructive

effects on the performance of the catalyst, obstructing reactants' access to active sites with associated loss of bottom conversions.[234] Unlike vanadium and sodium, iron is least mobile. XPS and SEM-EDS results have shown that surface iron concentration was highly enriched as compared to sodium, indicating that most of the deposited iron remained on the surface of the catalyst particle.[190,233] XPS data also proved that iron on the FCC E-cat existed in the form of Fe^{3+}; however, this oxidation state was not the state in the riser or regenerator. Any reduced form of iron in the E-cat sampled from the FCC unit will be likely oxidized to Fe^{3+} in air.[190] Iron decreases the catalyst activity by two different mechanisms. At low concentrations, deactivation is caused by poisoning of acid sites, while at higher concentrations, deactivation proceeds through the pore blockage.[235] The loss of activity of a cracking catalyst by iron is not only due to the decrease in the accessibility and acid site poisoning, there also a direct ion exchange with catalyst active sites. Iron forms clusters on FCC catalyst particles that could cause catalyst fluidization problems in the FCC unit and catalyzes dehydrogenation reactions, which lead to a higher coke selectivity.[236] These clusters are made up of small crystals of magnetite (iron oxides) that can readily react with hydrogen sulfide in the riser forming iron sulfide, which re-oxidizes in the reactor to magnetite, releasing S and SO_2. This reaction proceeds at a very fast rate with the release of enormous amount of heat that melts the surrounding layer of silica-alumina matrix at the particles surface up to several microns deep. This results in the formation of a dense layer of iron oxide which acts as a barrier at the surface to the diffusion of oil molecules.[190] Figure 9a shows the effect of iron on MAT conversions at different CTOs. It reveals that iron causes a quantifiable decrease in the catalyst activity, which is in good agreement with the decrease in acidity as the iron concentration on the catalyst increases, indicating that the significant reduction in catalyst activity is attributed to the direct poisoning of the catalyst active sites.[235]

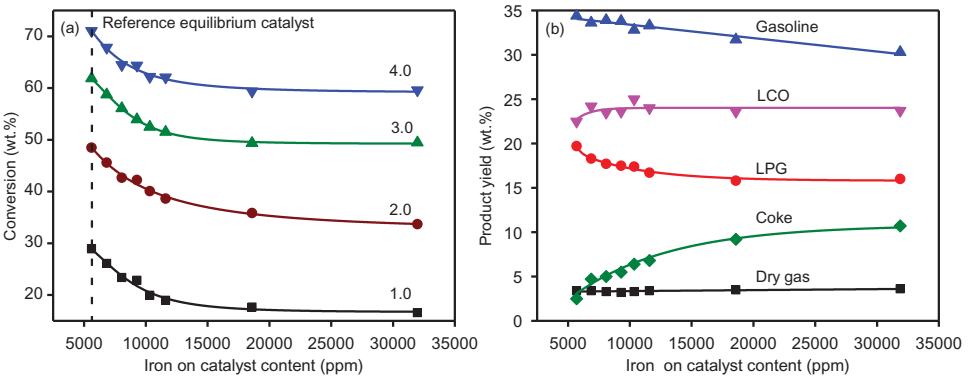

Figure 9. Effect of iron deposition on (a) conversion at different CTOs, (b) product distribution.-[235] Reprinted with permission from Elsevier, Copyright 2014.

Furthermore, it is shown in Figure 9b that iron poisoning of the catalyst decreases the selectivity to LPG, while coke increases in an exponential manner with the rise in the iron content. Increasing coke formation by iron may be caused by high dehydrogenation reactions since they are proportionally related. Also, increase in the iron content on the catalyst causes a monotonous and continuous decrease in gasoline, but an increase in the LCO selectivity.[235] Although this illustration indicates that iron alters the activity and selectivity of the FCC catalyst, the harmful effects on the overall catalytic behavior is approximately a half that of vanadium.[237]

The incipient wetness impregnation technique of introducing metals to the FCC catalyst for laboratory evaluation gives rather a uniform distribution of iron throughout the catalyst surface, which poorly simulates the real FCC situation. To simulate more closely the effect of iron in the real FCC unit, Rainer et al.[234] subjected catalyst to alternating cracking and regeneration cycles with VGO spiked with organic iron. Results indicated that iron formed nodulated structures on the FCC catalyst surface (Figure 10d), destroying the surface morphology. Increasing iron levels promoted catalyst sintering, blocked active sites, and imposed diffusional limitations to access of the

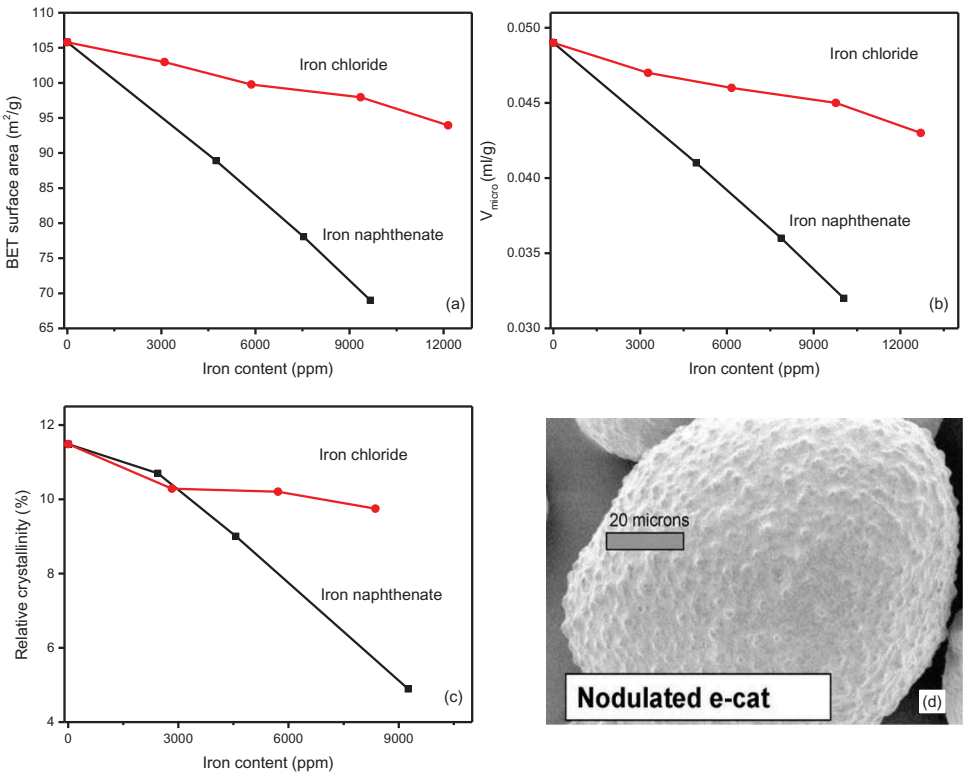

Figure 10. Effect of iron deposition on textural properties, crystallinity and surface structure of FCC catalyst.[238,239] Reprinted with permission from Elsevier, Copyrights 2003 and 2007.

active sites. This behavior was directly reflected by the decrease in AAI. The obstruction of the surface pore structure by the iron-enriched rings protected the interior of the catalyst prepared by using silica-based binders, but caused loss of the activity and bottom conversion. The catalysts containing alumina binder showed high resistance to iron deactivation and maintained high activity and high bottom cracking performance even at high iron loadings.-[190] Iron precursors constitute an important factor for the distribution of iron artificially deposited on the catalyst surface. The poisoning of the cracking catalyst by iron was mainly caused by bigger molecular compounds such as iron naphthenate, which formed iron-enriched nodules on the catalyst surface. Small iron species such as iron chloride had little influence on the catalytic performance due to the uniform distribution of iron. Reduced catalytic performance was also associated with changes in the physiochemical properties, such as variation in crystallinity, surface area and pore volume (Figure 10a-c).[238] The hydrothermal treatment of catalyst contaminated with iron has no significant influences on the textural properties, indicating that iron contamination does not cause additional hydrothermal instability as observed in the case of vanadium.[235]

4.1.4. *Calcium*

Elemental mapping of E-cats has shown calcium deposited as one of the contaminants[240], but its distribution was not as uniform as nickel on alumina and vanadium in zeolite.[241] Calcium contamination causes the deactivation of FCC catalyst by neutralizing acidic sites, similar to sodium, and by lowering the hydrothermal stability, which leads to significant collapse of the zeolite structure.[235] When present together with iron, the resulting large coke formation raised the catalyst temperature in the regenerator, intensifying the destructive actions of calcium. The compromised hydrothermal stability resulted in the decreased accessibility to active sites. As a result, the contamination of FCC catalyst by calcium caused a continuous degradation of surface area as the calcium content on the catalyst increased. Other important parameters that are used to measure the stability of a catalyst, such as crystallinity and acidity also decreased. The degradation of textural properties of FCC catalysts contaminated with calcium is mainly attributed to the collapse of the porous network, differing from the pore blockage mechanism of iron contamination. This effect is suggested to be due to the interaction and ion exchange between USY-H^+ and Ca^{2+}, and is known to lower the hydrothermal stability of FCC catalyst.[235] At low level, most Ca does not exchanged with zeolite. It synergistically combines with Fe to form low eutectic melting points on the E-cat surface resulting in pore blockage.[190] However, at very high calcium concentrations, great losses of catalyst activity become likely (Figure 11a), and the effects on product distribution

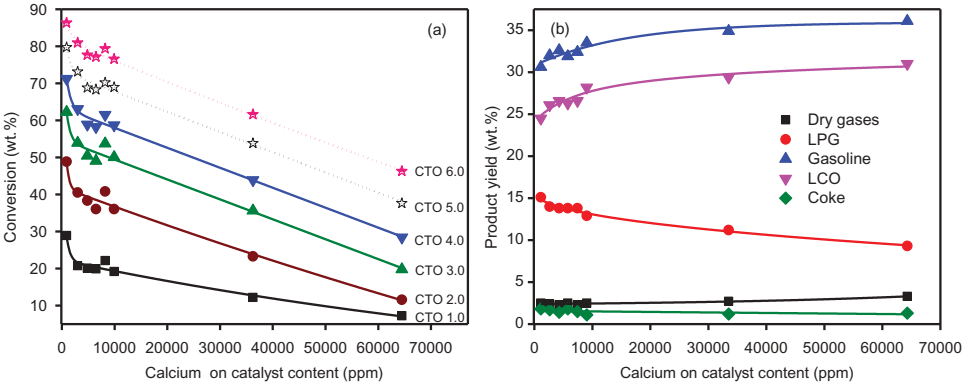

Figure 11. Effect of calcium deposition on (a) conversion at different CTOs, (b) product distribution.[235] Reprinted with permission from Elsevier, Copyright 2014.

are obvious (Figure 11b). A decreasing effect can be observed for LPG and coke selectivity, whereas dry gas, gasoline, and LCO selectivities increased.[235] Similarly, Kumar et al.[242] found that the feed conversion decreased to a marginal extent, while gasoline, LCO, and coke generally increased. On the other hand, both LPG and dry gas decreased. The decrease in the dry gas was attributed to lower mono and bi-molecular reactions, which correlated with acid sites distribution on the FCC catalyst. Unlike vanadium and nickel, calcium shows a very low tendency toward dehydrogenation reactions. However, these two case studies do not seems to portray calcium as problematic in the FCC unit as would be anticipated of a contaminant metal, thus further studies are required on this metal actions under different unit severities for proper elucidation and understanding of dynamics of its undesirable effects on the cracking catalyst.

4.1.5. *Sodium*

Sodium is another metal that presents highly undesirable effects to the cracking catalyst. It originates from several sources including natural content in feedstocks, residual materials from the catalyst preparation or as remains from oil extraction due to faulty desalter.[243] Sodium from these sources deposits on the FCC catalyst and accumulates on zeolite particles. The effects of sodium poisoning of FCC catalyst have been studied by several researchers. In one aspect, the framework destruction of USY is prompted by ion exchange of Na^+ with the protons of the acid sites, resulting in the neutralization of BASs.[214,244,245] The specific surface area of the FCC catalyst decreased with an increase in the amount of deposited sodium (independent of the precursor), and most of the surface area loss was due to the reduction in zeolite surface area.[246,247]

The destruction mechanism of hydrothermally treated zeolite Y by sodium was investigated in detail by Xu et al.[248] It was found that at a low Na^+ concentration, the steam dominates hydrolysis of framework aluminum. At a high Na^+ concentration, the hydrothermal instability is promoted by the metal, leading to the collapse of zeolite structure. Sodium reacts with steam forming surface NaOH, which causes the destruction of zeolite. In the absence of steam, Sandoval-Diaz et al.[244] have shown that at temperatures similar to those prominent in the FCC regenerator, the destruction of the structure of zeolite Y by sodium is not caused by dealumination as in the case of vanadium, which involves the framework aluminum hydrolysis, but by the scission of ≡ Si-O-Si≡ bridges. Dealumination is inhibited because the balancing protons required for this reaction are readily exchanged with Na^+ and are not available for bond rupture. By increasing sodium loading, the activity of n-butane cracking decreased monotonically without affecting the selectivity. This behavior was explained by the inability of sodium to be selectively poisonous to a particular acidic site. Sodium reduces the crystallinity of zeolite which can lead to amorphous materials.[214,244] USY was found to amorphized irreversibly with increasing Na^+ level, accompanied by a remarkable loss of microporosiy, but without significant depletion of framework aluminum.[249] A Combined XRD and Raman scattering experiments revealed that the destruction of zeolite by Na^+ (as NaCl) occurred selectively on the six membered rings of the FAU zeolite. It is revealed in this study that the action of Na^+ over zeolite catalyst is precursor dependent. For example, most Na^+ enters the FCC unit as NaCl, a stable compound of sodium, which is difficult to form NaOH by steaming alone, differing from the claim of Xu et al.[248] that the formation of NaOH was the origin of zeolite collapse. Hagiwara et al.[243] found that sodium, in the absence of steam, created defects (Si-OH) on USY and increased the mean void volume of the supercage. In the presence of steam, zeolite was stable with respect to the crystal structure when a small amount of sodium ions were present. Tangstad et al.[246] showed that the effect of sodium on commercial FCC catalyst was dependent on the source. Sodium emanating from the production of the catalyst affects the catalytic behavior differently from that deposited during operation. The former significantly lowers the gasoline octane number than the latter. These existing arguments render the exact mechanism of sodium actions over zeolites and zeolite catalysts inconclusive. Unlike vanadium, sodium contamination only slightly increased or less reduced the UCS of USY zeolite with increasing sodium loadings after steam-aging. The same trend was observed for the number of framework aluminum atoms, which was ascribed to inhibition of dealumination.[249] An increment in the abundance of framework aluminum atoms results in the expansion of the unit cell due to the longer length of Al-O bond than Si-O bond. Another finding also showed that FCC catalysts containing zeolite Y with increasing sodium content as Na_2O or Na^+ retained a higher

UCS, with a decreased surface area after hydrothermal treatment, collaborating with the above assertion.[248] Correspondingly, the activity and selectivity to the main product decreased.[246,250] A similar dealumination inhibition mechanism by RE holds for sodium for stabilization of the zeolite framework, resulting in the elongation of the coordinating bond between Al and O, which leads to the expansion of UCS of RE-exchanged zeolites. It appears that an interesting study will become of the effect of RE on Na/Y. Generally, sodium inhibits dealumination during steam-ageing and its presence affects product selectivity due to its influence on UCS and Brönsted acid density of zeolite. Sintering of catalysts can also be promoted in the presence of sodium ions.[251] In summary, the ability of sodium to exert undesirable effects on the cracking catalyst originates from its tendency to exchange with the protonic sites in the zeolite, resulting in neutralization of acidic sites and framework instability in the regenerator. Sodium presence even in a low level causes profound loss of catalytic activity and modifies physiochemical properties of the FCC catalyst.

4.2. *Effect of simultaneous deposition of contaminant metals*

Deposition of more than one contaminant metal on FCC catalysts can alleviate or exacerbate the destruction of catalyst activity because of the intrinsic interaction existing between the deposited metals. For example, the coexistence of iron and calcium in FCC catalysts leads to a harmful synergism (Table 6). In combination with iron, calcium exhibited an indirect destructive synergy, increasing the regenerator temperature and at the same time promoting the hydrothermal instability of the catalyst.[235]

Escobar et al.[171] investigated the effects of iron and calcium on the formation of coke on USY. In their experiments, iron and calcium exchanged USY zeolites were impregnated with vanadium and nickel and tested in modeled catalytic reactions to elucidate the roles of metals (Fe and Ca) in coking, acidity and nickel particle formation. Results indicated that

Table 6. Coexistence of metals in FCC catalyst.

Coexistence of metals	Synergy	Interactive effect
V+ Na	• Negative	• Accelerates zeolite dealumination • Destroys zeolite structure
V+ Ni	• Positive/negative	• Lowers coke formation, • Protects zeolite structure • Increases catalyst activity
Ni+ Fe	• Negative	• Decreases dehydrogenation reaction
Fe+ Ca	• Negative	• Increases regeneration temperature, • Causes hydrothermal instability
V+ Ni+ Fe	• Negative	• Increases dehydrogenation reaction • Lowers hydrothermal stability

the bimetallic catalyst (NiVUSY) formed relatively lower coke in comparison with the monometallic (NiUSY and VUSY) ones, and the products had higher olefin-to-paraffin ratios. The amounts of coke on FeUSY and CaUSY were far less than those on NiUSY and VUSY. Generally, coke formation on metal impregnated catalyst would be increased since it is promoted by the active sites of the metals. In a related study, the coke formation by nickel and vanadium coexisting in USY and RE-USY was much lower than that by the individual metals. Rare earths strongly suppressed coke formation on vanadium sites in USY, but promoted it on nickel sites[252], which suggested the coking behavior of bimetals in zeolite Y is controlled by the bimetallic interaction. In another systematic study similar to the bimetallic (Ni and V) USY, Pinto et al.[38] found that the presence of nickel and vanadium in a catalyst formulated of USY significantly decreased the catalyst activity for the cyclohexane transformation. Four catalysts, namely Cat2, NiCat2, VCat2 and NiVCat2 were compared for the investigated metal effects. The cyclohexane activity decreased from 193 for Cat2 to 120, 107 and 113 for NiCat2, VCat2, and NiVCat2, respectively, indicating deactivation of the catalysts by the metals. As a result, coke formation increased due to dehydrogenation reaction, resulting in a higher olefin-to-paraffin ratio. The kind of feedstock appears to influence the interactive effect of metals in a catalyst. Heavy oils such as VGO exhibit positive, while short chain hydrocarbons such as cyclohexane show negative synergetic effects on the catalytic activity.

The oxidation states of the contaminant metals influence the dehydrogenation activity and coke formation of contaminated catalysts in some manner. Tangstad et al.[237] studied the catalytic effects of nickel and iron on the FCC catalyst. The dehydrogenation activity of nickel was observed to be proximate to that of vanadium in an oxidizing environment. Conversely, in a reducing environment, the dehydrogenation activity of nickel was significantly higher at the same temperature. Iron only had a significant dehydrogenation activity after steam aging followed by the reduction in a CO/N_2 environment at 760 °C. The co-impregnation of equal loadings of nickel, iron, and vanadium on the catalyst resulted in a relatively higher dehydrogenation activity than those of single elements. In the reducing environment, the dehydrogenation activity of the co-deposited contaminant metals decreased due to the reduction of the valence state of vanadium from V^{5+} to V^{3+}. The significantly reduced dehydrogenation activity of vanadium in V^{3+} state compensated for the increased dehydrogenation activities of nickel and iron. Besides, the addition of vanadium deteriorated the hydrothermal stability, synergistically deleterious to the zeolite catalyst.

For pure zeolites with a large number of sodium ions, the presence of vanadium causes a synergetic destructive effect. However, for composite FCC catalysts, vanadium had no significant effect coexisting with sodium on the

hydrothermal stability due to the trapping role of the matrix of the catalyst. A mechanism of zeolite destruction by vanadium in the presence of Na^+ has revealed that vanadium (as vanadic acid) acts as a catalyst for the removal of sodium ions from the zeolite in the form of NaOH. Thus, the increase in the concentration of NaOH, being the destructive species, promotes the dissolution of the zeolite crystals.[243,248] The combined pathways can be summarized according to the reactions below.

$$V_2O_5 + 3H_2O \rightarrow 2H_3VO_4 \tag{7}$$

$$3Na - Y + H_3VO_4 \rightarrow Na_3VO_4 + 3H - Y \tag{8}$$

$$Na_3VO_4 + 3H_2O \rightarrow 3NaOH + H_3VO_4 \tag{9}$$

The initial step in this mechanism is the formation of vanadic acid, the poisonous and highly mobile species that is well established to exist in the vanadium poisoned E-cats. This acid then reacts with sodium, which has exchanged with the proton from BASs of H-Y in the form of Na-Y. The second step yields H-Y, regenerating exchanged BASs. The produced sodium vanadate is then converted into NaOH by the action of steam. Under such conditions, the vanadic acid behaves like a catalyst, as it is not consumed. However, this mechanism seems not to be absolutely accurate. Sandoval-Diaz et al.[214] argued that since H-Y is a strong acid and NaOH is a strong base, the reaction should actually occur in the opposite direction. The net reaction would consist of the hydrolysis of a stable salt (Na-Y), which is difficult to occur even in the presence of a catalyst.

$$3Na - Y + 3H_2O \rightarrow 3NaOH + 3H - Y \tag{10}$$

The only ground for this to happen would be through the immediate consumption of the produced NaOH and/or HY to shift the equilibrium forward, but as they are produced on the same BASs, it is much more likely that they are consumed by reacting with each other, which is the opposite reaction. Based on this study, the authors have faulted this mechanism leading to formation of sodium-vanadate, which shows that at the temperature prevalent of the FCC regenerator, vanadium must be present as anion to react with Na^+. However, this sodium is consumed in a previous reaction with the zeolite framework or matrix and is unavailable to react with vanadium oxide.

The effect of simultaneous deposition of nickel and vanadium on a commercial FCC catalyst under hydrothermal conditions was investigated by Tatterson and Mieville.[230] The results indicated that nickel can occupy several sites on the surface of the catalyst. An indirect interaction between vanadium and nickel was found to exist that reduced nickel coking activity during cracking, resulting in the reduced coke formation. Similarly, Etim et al.-[253] showed that when nickel and vanadium are deposited concomitantly onto

FCC catalyst the mutual interaction between the metals can prevent the crystal structure of the catalyst from total collapse. Nickel acts as a vanadium scavenger, consuming part of the vanadium poison precursor (vanadic acid) available for contact with the catalyst, forming nickel vanadate. In this way, the absolute destruction of the catalyst structure was reduced. In another study, Chester[199] showed that nickel and vanadium did not interact synergistically to destroy the catalyst structure. Nickel produced 3 to 4 times as much hydrogen as did an equivalent of vanadium, while the metals were almost equally active for the contaminant coke yield. The lack of the destructive synergism between vanadium and nickel was demonstrated. Although the study did not clearly reveal any harmful synergism for the nickel and vanadium co-impregnated catalyst at low metals level, Jaras[254] observed the activity loss due to the saddling of high metal levels (5000–10 000 ppm).

The extent of the metal effect on FCC catalysts may be dependent on other factors besides the catalyst itself. For example, catalyst formulations with metals traps or passivators, or catalyst containing a high-activity component would be less deactivated than those without these materials. This inherent variation in the FCC catalyst formulation could cause remarkable changes in the metal contaminant effect on product yields, including the undesirable coke formation and dry gas production. Figure 12 shows the responses of four catalysts (W, X, Y and Z, having different resistance to metal poison), to the increasing levels of metal poison. The different slopes of the curves are related to different metal resistance of the catalysts. Catalyst Wwas the most selective with the highest metal resistance and gave the lowest response to metal deactivation. Catalyst X had a high metal resistance at low metal levels, but

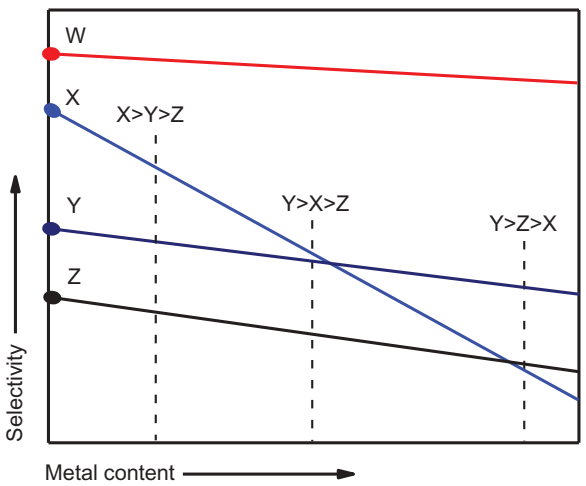

Figure 12. Effect of metal content on the catalyst selectivity. Re-drawn from.[199].

decreased fast with increasing metal contents. On the other hand, catalyst Y was more selective at high metal levels than catalysts X and Z. The interaction between two or more contaminant metals could promote or reduce the destructive ability of a single contaminant. As mentioned above, sodium and vanadium can combine to exacerbate the destruction of zeolite structure. Similarly, iron and calcium coexisting in FCC catalyst can combine to increase the regenerator temperature and deteriorate the hydrothermal stability of catalyst as well. However, the interaction between nickel and vanadium is beneficial to the catalyst structure and coke formation with respect to laboratory scale studies. In fact, nickel reduced the destruction of zeolite Y by vanadium, whereas vanadium can suppress coke formation tendencies of nickel.[211,252,255]

4.3. *Localization and distribution of FCC catalyst contaminants*

Metal contaminants distribute differently when deposited on FCC catalysts. Several studies have revealed the characteristics of metal deposited cracking catalyst from the regenerator and in the laboratory.[234,256] Figure 13 shows the distribution of metal contaminants and their spatial location in the FCC catalyst particle. Electron probe microanalyses (EPMA) have shown that iron deposits on the external surface of FCC E-cat particles, forming iron rings around the particles. Also, Hui et al.[257] using TEM found nodulated structures on the surface, which consist of Fe-bearing nanoparticles imbedded in an amorphous matrix. Increase in the content of iron increases the surface concentration, but not the depth of penetration inside

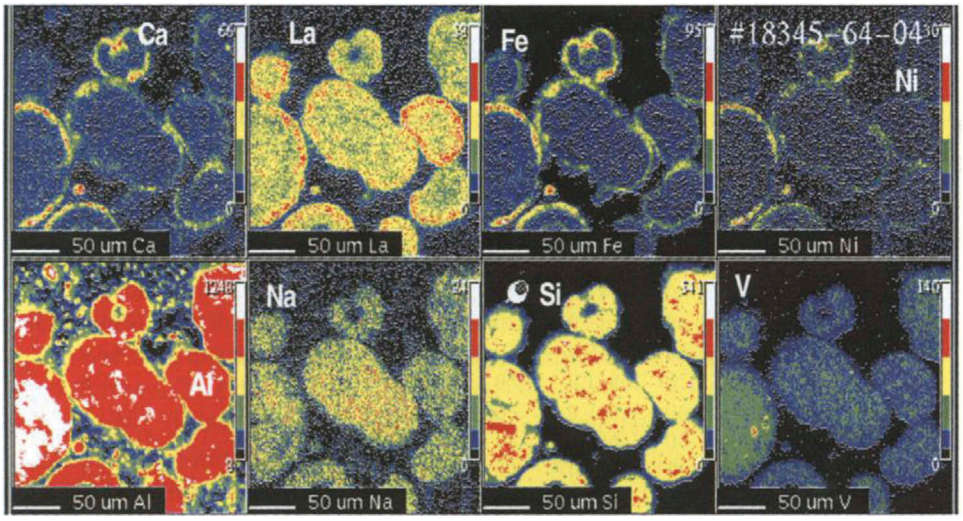

Figure 13. Contaminant metals distribution in a deactivated FCC catalyst (laboratory scale).[190] Reprinted with permission from Elsevier, Copyright 2004.

of the particle.[53,190] In zeolites, nickel is preferentially located on the surface layer of the zeolite crystallite.[227,228] However, for a composite FCC catalyst particle, nickel was detected in a very high concentration in alumina particles[223,224,258], where deposited nickel formed a hard layer difficult to reduce mainly in the form of nickel aluminate spinel – $NiAl_2O_4$[224] and $Ni_xAl_2O_{3+x}$.[223] Psarras et al.[53] observed that the local areas of nickel enrichment in FCC catalyst particle are also those of aluminum enrichment, and they attributed this to the formation of Ni-Al mixed phases such as nickel aluminate. The metal distribution profile of an E-cat from the real FCC unit showed that nickel concentrates mostly on the surface, but its distribution can also be observed in some interior areas of the particles in extreme cases, similar to the deposition profiles of vanadium and sodium.[216] Vanadium first deposits on the surface of the FCC catalyst in the regenerator and later migrates to the interior of the particles. Hence, vanadium could homogeneously distribute throughout the entire catalyst particle due to its mobility.[53,190] Recently, Etim et al.[258], using a chemisorption technique (TPR) suggested the existence of vanadium as $AlVO_4$ in commercial FCC catalyst. Although sodium and calcium can preferentially exchange with the protons sites in the zeolite, electron-microscope imaging revealed that calcium concentrates preferentially on the surface of the FCC catalyst (Figure 13).

4.4. *Control of cracking catalyst contamination*

In spite of the undesirable effects of feedstock contaminants on the performance of the cracking catalyst as discussed above, the processing of heavy oil fractions is ongoing. This is driven by the fact that there are existing technologies for controlling the activities of the contaminants, allowing upgrading and optimization of heavy oil feedstocks. Several strategies for controlling the deleterious effects of the contaminants in the cracking units have been practiced for years. The initial technique was the formulation of the zeolite-based catalyst with matrices, binders and fillers to act as traps for metals and basic nitrogen compounds, in addition to supplying the catalyst mechanical reinforcement.[42,259] Although there was great benefit incorporating the matrix to zeolite catalyst for FCC, the overall performance was generally low in terms of metals trapping. This led to the search for more effective methods to keep the contaminants at bay for improved conversion of heavy feedstocks and residues. The use of contaminant traps that are different from the base catalyst components and can be added to the FCC processing unit boosts the overall performance and increases the unit profit. Introduction of a foreign substance for the purpose of deactivating the catalytic effects of contaminants (metals) may take different forms, including charging to either the

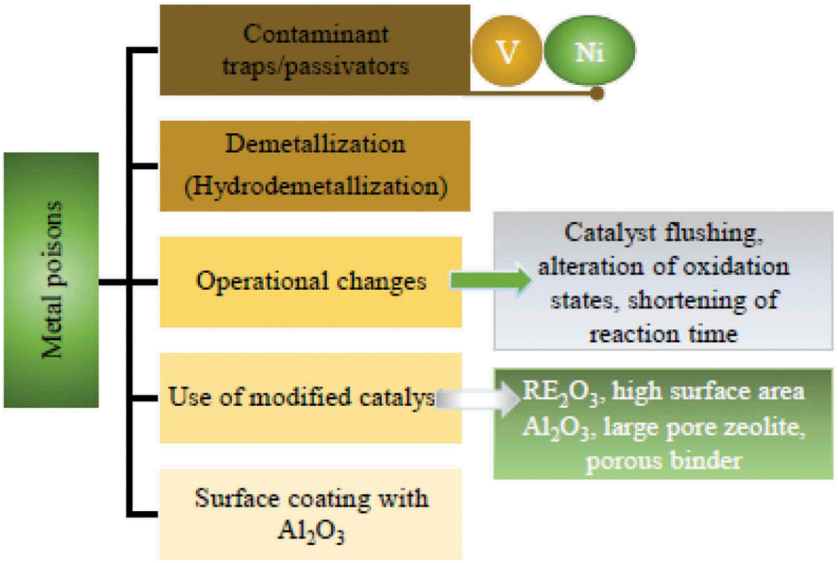

Figure 14. Methods for passivation of metals with destructive effects on FCC catalysts.

feedstock or the catalyst itself or as a co-catalyst to the reactor (Figure 14). Nonetheless, feedstocks can be pretreated to reduce the burden of a particular contaminant, by processes such as demetallization and hydrotreatment.[260] The unit operational changes to alter the oxidation state of the metals also affords a practical method for controlling the harmful effects of metal contaminants.

Demetallization, peculiar to metal contaminants, selectively extracts metals in crude oil from its organic moiety. It is a chemical process that uses different chemicals including inorganic acids (H_2SO_4, HCl, HNO_3, H_3PO_4, etc.) and bases and chloride salts. The acid treatment can successfully remove high loads of metals, but there are exceptions in some cases where the acids reduce to their corresponding oxides, which are detrimental to the FCC unit. For instance, H_2SO_4 and HNO_3, reduce to SO_x and NO_x, respectively, which are dangerous environmental pollutants that contribute to acid rain. Therefore, HCl is the most effectively and widely used demetallization agent. Hydrotreatment is mostly effective for the removal of non-metallic contaminants such as sulfur and nitrogen, and is applicable to metals as well. Hydrotreating consists of the hydrogenolysis of the contaminant heteroatom molecules (containing nitrogen, sulfur, and metals) in the crude oil with hydrogen in the presence of a catalyst. This process is of high importance in the refinery because of its ability to minimize the flue gas emission that contributes to environmental pollution. Hydrotreatment for removal of metals is generally referred to as hydrodemetallization (HDM), whereas those of sulfur and nitrogen are commonly referred to as hydrodesulfurization (HDS) and hydrodenitrogenation (HDN), respectively.

Operational changes involves certain practices that prolong and maintain the activity of the cracking catalyst, such as flushing, alteration of oxidation state of the metals, short contact time (SCT) cracking reactions, etc.; however, the applicability of metal oxidation change and reaction at short contact time will require changes in FCC unit design. The reduction of vanadium to lower oxidation states decreases the active sites thereby reducing dehydrogenation reaction and coke formation, thus maintaining the overall catalyst activity. This can be realized by passing the regenerated catalyst through a reducing atmosphere prior to returning to the cracking zone.[206,261,262] Flushing involves the withdrawal of metal laden catalyst from the circulating inventory, and fresh/low metal equilibrium make-up catalyst introduced to maintain the activity.[232,263]

As previously mentioned, passivating contaminant metals to render their activities harmless under conditions prevalent in FCC units provides a more practical and an effective method for controlling catalyst deactivation. This can be achieved by introducing feed additives into the unit along with the catalysts or the FCC catalyst particle can be formulated with special anti-contaminant agents in the bulk of the catalyst particles during preparation. These additives combine with the metals so that the active component is protected.[7] Passivating agents can be best referred to as "passivators" or "metal traps". A passivator is any additive to the catalytic cracker capable of reducing the deleterious effects of contaminant metals to improve the catalyst activity and/or selectivity toward more desirable products. The two most commonly used passivators are antimony and tin based compounds for passivation of nickel and vanadium, respectively. Antimony-based passivators have been successfully used to passivate nickel at the commercial scale since 1976. They are usually in liquid or semi-liquid form and injected into the feedstock to react with nickel. However, antimony based passivators in solid forms are also available. Other widely used passivators for nickel are based on cerium and bismuth.[264] Incidentally, cerium is also an effective vanadium passivator. Generally antimony based passivators function by reducing gas and contaminant coke caused by nickel catalyzed dehydrogenation reactions through an interaction between the nickel and antimony, forming Ni-Sb alloy that is hard and unreactive on the surface of the catalyst.[231,265,266] Tin and tin-based compounds have been in use since 1982 on industrial scale to effectively mitigate the harmful effects of vanadium.[232] However, in recent days, tin-based passivators, are no longer gaining commercial applications. Vanadium which is mobile under FCC conditions combines with passivating agents to yield vanadate species that is generally inert and thermally stable under FCC unit conditions, preventing the severe catalyst activity decay. While the use of antimony for nickel control has proven a commercial success, significantly decreasing the nickel induced dehydrogenation activity, vanadium contamination management is

still facing serious drawbacks that need further improvements. In this regard, several improvements in the passivation technology have been continuously explored by many researchers. A handful of some technologies are summarized below.

A catalyst containing alumino-sepiolite as binder was shown to maintain a higher conversion/high selectivity due to its ability to trap nitrogen present in the feed.[267] Ammoxidation catalyst as an additive to the FCC unit has been found to reduce NO_x precursors in emissions from the FCC regenerator. This additive consists of mixed metal oxides of Fe, Sb and additional metal such as Mg, Mn, Mo, Ni, Sn, V, or Cu, and can function effectively under both full and partial burn regeneration conditions.[268] The nitrogen control ability is through the conversion of NH_3, HCN or NO_x to N_2 when in contact with the gas phase in the FCC regenerator.

Vanadium could be passivated by interaction with metallic oxides such as REs and alkaline earth, forming stable $REVO_4$ and alkaline earth metal vanadate, respectively, for example, as revealed by a variety of techniques-[193,269,270], hence most passivators are based on rare earths[232,271–273] and alkali earth oxides.[196,274,275] Some other effective vanadium passivators are perovskites such as $CaTiO_3$ and $BaTiO_3$.[276–278] The use of special formulations, including mixed metal oxides[279,280], the oxides, salts and/or the organometallic compounds of the metals Mg, Ca, Sr, Sc, Y, La, Ti, Zr, Hf, Nb, Ta, Mn, Fe, In, Tl, Bi, Te, and the lanthanide series elements[281], phosphorus compounds of bi-valent (Be, Mg, Ca, Sr, Ba, Zn, Cd, and Pb) and tri-valent (Al, Ga, In, As, Sb, Bi, La, Ce, Pr, Nd, Pm, Sm, Eu, and Gd) metals[282] have been demonstrated to effectively deactivate vanadium effects.

Catana et al.[283] proposed a method of catalyst coating for the passivation of vanadium destructive effects, involving the deposition of $[Al_{13}]$ or $[Al_{13}O_4(OH)_{24}(H_2O)_{12}]^{7+}$ complex generally known as keggin ions from aqueous solution. In this way, the surface of the catalyst is coated with a layer of aluminum oxide, which is capable of trapping about 80% of vanadium species. However, this process of vanadium passivation is unlikely to be effective under severe FCC operating conditions.

A process of upgrading feed stream containing residue fractions with high concentration of nickel up to 150 ppm by using a catalyst comprising large pore rare earth FAU zeolite component, pentasil zeolite (MFI type), and pseudoboehemite is described in the U.S. Pat. 2014/0235429.[284]

Modified FCC catalysts with various types of aluminas are known to exhibit improved resistance to the adverse effects of contaminant metals present in the petroleum feedstock. For example, high surface area alumina may serve to trap vanadium and protect the zeolite. However, the alumina is ineffective for nickel passivation as the levels of hydrogen and coke remain high, due to the high dispersion of nickel on the alumina.[284,285] The use of high metal tolerant catalysts, where the inherent catalytic properties are modified, can effectively

manage metal contamination. Recently, modification of the pore structure of the inherent catalyst particle components has shown promise as a control method for metal poisons.[286,287] The improved porous binder increased the conversion and decreased the heavy oil yield by 3.50 and 2.86%, respectively.[287]

5. Understanding of catalyst deactivation at a single FCC particle level using advanced characterizations

In the last few years, attention of researchers in the field of FCC catalysts has been directed to the deactivation of the FCC catalyst at the individual (or single) particle level, and deeper understanding of the deactivation mechanisms has been reached with the use of state-of-the-art characterization tools. Specifically, all stages of the life cycle of a catalyst including deactivation and regeneration have been explored using powerful micro-spectroscopic methods that are able to provide spatial and temporal information similar to those prevalent in the industries. Some studies within the last five years have obtained interesting results, which serve as an extension to the wealth of knowledge in this field and have also provided important insights for further development in FCC catalyst technology.

Through an integrated set-up comprising micro (μ)-XRF, μ-XANES and μ-XRD, with a micrometer spatial resolution in 2D or 3D,[288] it is possible to determine the presence of Ni, V, and the crystalline phases (e.g. zeolite and kaolinite) on FCC catalyst particle after deactivation in the commercial unit. The μ-XRF revealed an egg-shell profile for Ni with a shell thickness in the order of 10–15 μm. Vanadium distributed evenly across the entire FCC catalyst particle which mapped its possible locations. The artificially deactivated catalyst by Mitchell impregnation method gave a false representation of Ni deactivation, indicating inaccurate simulation of the industrial E-cat. The K-edge spectra of Ni and V of the E-cat indicated the presence of Ni^{2+} (8343 eV) and an oxide-type phase, $NiAl_2O_4$ and/or NiO in which Ni^{2+} is six coordinated (8330.5 eV). The bands at 5480.4 eV and 5469.4 eV correspond to a mixture of V^{4+} and V^{5+}. From the μ-XRD-CT patterns, the reflections defining zeolite Y in the E-cat diminished, implying the destruction and dealumination of the zeolite in the catalyst, leading to a decreased Si/Al ratio with associated decreased activity. In addition, the kaolinite component was observed to transform into mullite.

Kalirai et al.[256] investigated industrial E-cats deposited with substantial amounts of poison metals (Fe, Ni, V, and Ca) at an individual particle level by using a micro-XRF Tomography. A 3D imaging with sensitivity at the submicron resolution was achieved with the use of a large-array Maia detector. Results indicated that Fe, Ni, and Ca had significant concentrations co-localized at the external layer, while V penetrated the interior of the FCC catalyst particle. The

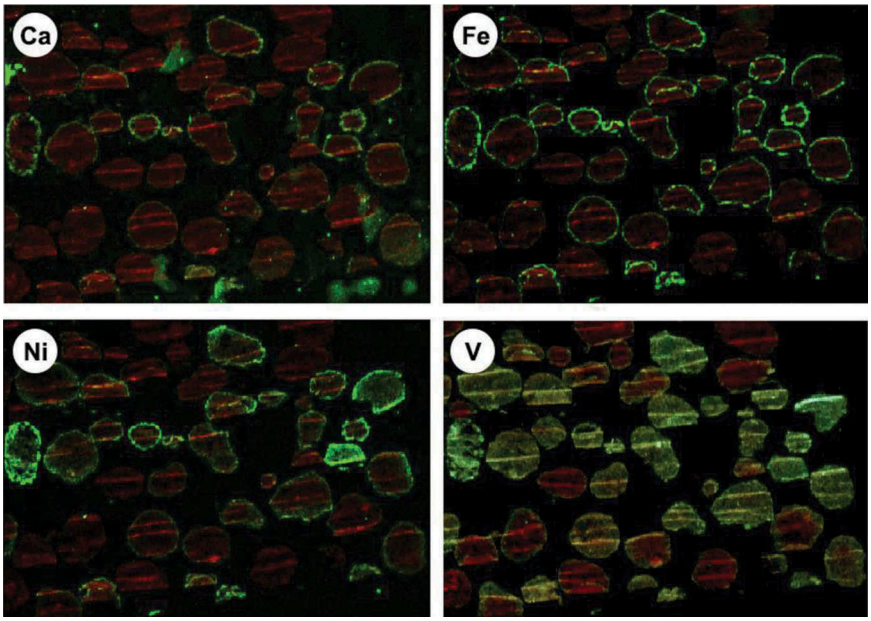

Figure 15. 2D XRF mapping of the poisonous metals, Ca, Fe, Ni and V (green) on Al (red) for 500 nm thin sections of an e-cat particle. Reprinted from.[256] Copyright Wiley Online Library, 2015.

metal deposition profile did not change significantly with age of the catalyst. It was also found that no spatial correlation existed between V and La (a marker for the zeolite domain), suggesting that although V is a known zeolite destroyer of the FCC catalyst, no preferential interaction existed between them. However, V localized near the Al_2O_3 based components of the matrix. The lack of correlation between V and La in this study may seem to still throw wide open the unresolved mechanism of RE-V interaction in REY, needing further research. Figure 15 shows the distribution of poison metals – Fe, Ni, V, and Ca (green) over FCC catalyst particles, which are represented by the florescence channels (Red). It is clearly observed that V exhibited both homogenous distribution and rings of V on the exterior of the catalyst particles, as opposed to the rich ring-like distributions of Fe, Ni, and Ca around the exterior parts with little or no concentrations in the interior of particles. The localization of one metal has an observed effect on the distribution of others. For example, the observed differences in the distribution of mobile V in FCC catalyst particle may results from the effect of the non-moblie Fe.[256] Similarly, when V exhibited uniform distribution over the catalyst particle, the distribution of Fe was not uniform on the surface.[28]

Wise at al.[289] at the nanoscale level studied the chemical state and the deposition profile of Fe in an industrial deactivated FCC catalyst particle. It was found that Fe can penetrate the matrix component of catalyst particles containing zeolite as a result of pre-cracking of iron-containing organic

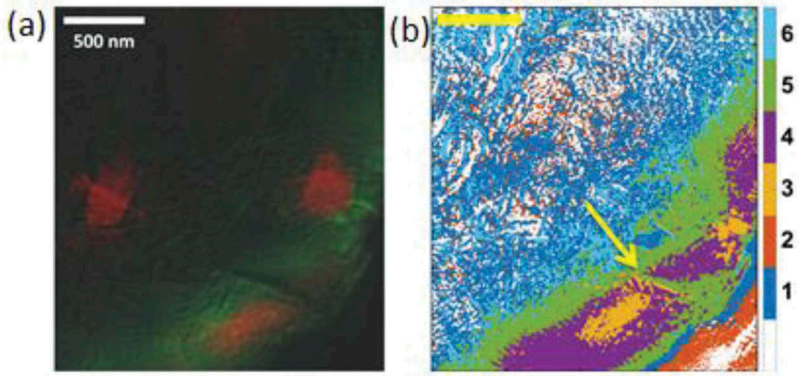

Figure 16. La (red) and Fe (green) distribution map (a) and cluster map (b) generated from principal component analysis and clustering per pixel NEXAFS data. The arrow in (b) highlights the crack visible in the surface layer. Reprinted from.[289] Copyright American Chemical Society, 2016.

molecules. In a further detailed study, the authors found Fe species in the catalyst particle included the "tramp Fe", "fine dust Fe" and "colloidal Fe", from the deposition of inorganic particulate iron, and the accumulation of Fe through pre-cracking of porphyrinic molecular Fe in the matrix. Figure 16 shows a distribution of Fe phases – a more reduced state in the matrix (dark & light blue) and a more oxidized state (from green to purple to yellow) sandwich structure. The results of this study confirmed a previous one[190] that showed the existence of Fe as Fe_2O_3 (Fe^{3+}) and also provided a proof of Fe as FeO (Fe^{2+}) in the matrix. Therefore, the accumulation of Fe on the surface of the catalyst particles is related to the chemical nature of Fe that is deposited.

The distribution of Fe and Ni on the surface of an individual catalyst particle has been studied using X-ray nanotomography.[290] Figure 17 shows an undulating surface of a catalyst particle having a mottled shape caused by deposition of Fe and Ni. The distribution of elements is indicated by the color scale (Fe: red to yellow and Ni: blue to green). The nodulated areas were found to contain high concentrations of Fe, as verified by the high color (yellow) density. The formation of nodules on the surface of the catalyst is a result of interaction between iron and other components of FCC catalyst particles (except zeolite), which lowers the melting point of the Si-rich phase, causing vitrification. In the high temperature FCC unit, vitrification occurs because of the temperature gradient and this causes the collapse of low melting point silica-rich phases around the high melting alumina-phase.[190,290] Deposited metals caused pore clogging. By calculating the permeability through the pores of the particles, the clogging of macropores by Fe and Ni was revealed. The 3D distribution map showed that for a representative sub-volume ($16.6 \times 16.6 \times 10.0\ \mu m^3$), which covers near-surface regions and more central parts, Fe exists in a lower concentration in deeper region of the particle (> ~ 2 μm) as part of the matrix, while Ni was found predominantly at the top of the subvolume (closer to the surface). By analyzing

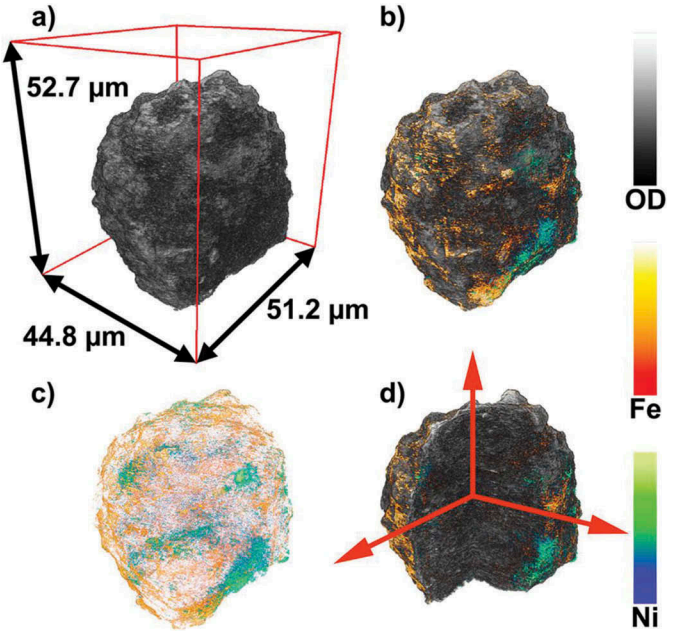

Figure 17. 3D representation of an FCC particle based on TXM mosaic computed tomography: (a) Optical density (OD) as recorded at 7060 eV, and (b–d) Visualization of Fe (orange) and Ni (blue) 3D relative distributions obtained from differences of tomography data. (d) Cut-through of the tomography data showing the inner structure of the particle. Reprinted from.[290] Copyright American Chemical Society, 2015.

the fluid flow through the subvolume, it was found that the flow was restricted in areas of high Ni contents due to the complete blocking of the macropores.[8,290] From the information presented herein, it is apparent that in the lifetime of a FCC catalyst, Ni and Fe accumulated quite early and concentrated in near-surface layers of the particle.[8] The surface deposition profile of Ni and Fe, however, showed a slight but remarkable difference due to the stronger pore narrowing effect by Ni than Fe, particularly at the early stage of the catalyst testing. This could be explained by the temporal fluctuation in the contents of Ni and Fe in the feedstock or the presence of tramp Fe, which preferentially deposits on the outer surface ($< 5\ \mu m$), or because of the higher diffusion ability of the Ni molecules than the Fe complex. As a result, more Ni would be deposited in pore channels.[8]

Not only can these powerful microscopic tools examine the deactivation of a single E-cat particle, but also can reliably dissect a fresh catalyst particle, revealing the most fundamental structural information, e.g., the quantitative size distribution, external shape, and the internal porosity at both micro- and nanometer scales.[28] It has been shown at ensemble level that a large proportion of well over 1200 individual catalyst particles contained internal voids of about 5–8 μm in diameter, which is thought to provide accessibility to large

hydrocarbon molecules, determining catalytic performance, whereas a much smaller sized voids (~ 100 *nm*-12 *μm* in diameter) were observed for the single catalyst particle.[28] Moreover, the local phases of the components present in the catalyst (for e.g. zeolite, TiO_2, La, and clay particles) are clearly discriminated, in addition to the localization of contaminant elements as previously discussed. In a detailed study, the 3D pore structure and inter-particle pores connectivity were elucidated with sufficient spatial resolution in single FCC catalyst particle by using X-ray synchrotron techniques. The high resolution imaging technique enables the visualization of the pore structure of the different components of the catalyst.[291] Recently, using unusual probe molecules combined with microscopic X-ray techniques with three dimensional resolution, the detailed localization of Brönsted acidity and the different FCC catalyst particle domains and their correlation with deactivation (catalytic age) at single particle level have availed important insights into the future FCC catalyst formulation improvements.[292–295] For example, Buurmans et al.[292], by combining fluorescence microscopy with a staining method, (using thiophene and Nile Blue A) found that thiophene molecules were responsive to the Brönsted acid sites located in the zeolite component; the Nile Blue A, due to its larger size only stained the matrix component of the FCC catalyst, revealing the intra-particle heterogeneities (the differences in the position and size of zeolite domain) at the single particle level. The fluorescence intensity, which correlated with the Brönsted acidity showed a direct relationship with the catalytic activity that offered a possibility of determining the age of catalyst particles in the real FCC unit. A most recent study has revealed the possibility of visualizing the dealumination of a single zeolite domain in the real-life catalytic cracking catalyst. The method relies on mapping the loss in the tetrahedral Al atoms within the zeolite domain, with La as the zeolite marker. It was found that the loss of Al atoms from the zeolite lattices significantly correlated with the changes in the zeolite domain[296], which has made possible to monitor zeolite deactivation in a catalyst particle, where matrix and binder are key components. Some advanced characterization tools and the specific information derived for a catalyst at individual particle levels are summarized in Table 7.

6. Conclusions and future perspectives

In this review, we have revisited important developments in FCC process in recent years. Although the FCC process is an old and a very mature technology, it is still one of the cornerstones of the whole petrochemical industry and will continue to play essential roles in the modern industry with high significance. A number of changes have taken place in the FCC process technology. The feedstock range has been broadened to include tight oil as traditional FCC feedstock, and attempts have been made to use bio-oil either

Table 7. Deactivation and structural composition of FCC catalysts derived at single particle level.

Catalyst deactivation at a single FCC particle: observations	Characterization method	Ref.
Particle agglutination, pore structure	X-ray nanotomography	[8,297]
Pore structure, individual catalyst components	Micro-X-ray imaging	[291,298]
Catalytic activity, acid sites, sulfur location, individual catalyst components	Confocal fluorescence, dye staining	[140,292–294,299]
Metal contaminants, elemental and zeolite distribution, zeolite crystallinity and Si/Al ratio	X-ray micro-spectroscopies (μ-tomography, $\mu-$ XRF, $\mu-$ XRD)	[8,28,256,288,290,298]
Chemical states and distribution of iron	X-ray ptychography	[289]
Structural defects	Integrated Laser and Electron Microscopy (iLEM)	[298]
Dealumination, inter- and intra-particle heterogeneities	Scanning transmission X-ray microscopy (STXM), X-ray adsorption near edge spectroscopy (XANES)	[296]

as pure or blended with gas oil as FCC feed, although not yet commercialized; the new catalysts used for FCC are those of zeolite Y dispersed in amorphous silica/alumina and clay matrices. New zeolites and/or combined with the traditional zeolite Y have also been tested as the active catalyst component. The realization of the current FCC technology shift is fully accomplished by implementing operational changes in the processing conditions, catalyst design and/or reactors re-configuration.

The various contaminants in FCC process, including their origin and effects on the FCC catalysts and the detailed interaction mechanisms with the catalysts have been reviewed. Effects of metal poisons on FCC catalysts are widely studied and most of the research were conducted within the last three decades. Nonetheless, research in this particular area is still very active. The main findings are summarized as follows:

-It has been shown that vanadium is the most deleterious metal in petroleum feedstock to the FCC catalyst. It decreases the activity of FCC catalyst by destroying the crystalline structure of the zeolite via dealumination, leading to the collapse of catalyst structure and elimination of some acid sites where cracking reactions take place.

Nickel, also a recognized FCC catalyst poison, acts as a dehydrogenation catalyst, and consequently increases the formation of coke. Its effects on the structure of cracking catalyst and on the catalytic performance have not been investigated to the same extent as vanadium, and are merely limited to dehydrogenation reaction and coke production tendencies.

Iron severely reduces the accessibility of reactant molecules to the active sites in the catalyst by blocking the catalyst pores.

Sodium neutralizes the strong acid sites and inhibits framework aluminum hydrolysis at high concentrations. It seems that research on sodium effects has attracted much attention in recent years. However, it remains controversial on the most appropriate deactivation mechanism of the zeolite catalysts by sodium. In general, the effects of the FCC feedstock contaminants on the cracking catalyst include neutralization of the acidic sites, surface area degradation, dealumination of the framework aluminum, structure collapse and clogging of catalyst pores.

Clearly, greater attention should be given to organic nitrogen and sulfur contaminants in FCC feedstock due to their remarkable effects on the cracking catalyst as described in this review paper. Also, synergism resulting from the deposition onto the FCC catalyst of more than one metal poison can be harmful or beneficial depending on the specific deposited metals. The co-deposition of vanadium and sodium is synergistically deleterious, whereas the presence of vanadium and nickel concomitantly on a cracking catalyst affords mutual benefits to the catalyst catalytic and physiochemical properties, although most of these findings are limited to laboratory scale studies. It is important to comment that although many tests have been carried out using different FCC catalysts and/or feedstocks, discrepancies on the general behavior of the contaminants are rarely reported. In general, the metallic contaminants cause irreversible deactivation, whereas the non-metallic (coke) contamination is reversible.

In recent years, the use of advanced characterization tools that are able to provide spatial and temporal information similar to those prevalent in the commercial units have been exploited to study all stages of the lifecycle of a catalyst including deactivation and regeneration; this has deepened understanding of the deactivation mechanisms of FCC catalysts by contaminant metals. Most recent studies using a single FCC catalyst particle from the refineries have provided insights into the distribution and localization of the metal poisons in the catalyst particle, which could help the formulation of the next generation catalysts with optimized matrix and porosity to provide maximum resistance to metal poisoning.

A large proportion of previous studies have been focused on pure zeolites, which is far from the real catalyst used in FCC units. Therefore, the use of composite catalysts that comprise matrix and binder in addition to the active zeolite component are required for further studies, particularly in the case with presence of nickel. The interactions between the different components of the FCC catalysts particles deserve further studies to understand the roles of the individual components in cracking reactions. Theoretical studies on the mechanisms of FCC catalyst deactivation by contaminant metals are recommended to complement experimental results. This could afford comprehension of catalyst deactivation at molecular levels.

Acknowledgments

This work was financially supported by the National Key Research and Development Program of China (2017YFB030660), the Joint Funds of the National Natural Science Foundation of China and China National Petroleum Corporation (U1362202), Natural Science Foundation of China (21206195), the Fundamental Research Funds for the Central Universities (14CX02050A, 14CX02123A), Shandong Provincial Natural Science Foundation (ZR2012BM014), and the project sponsored by Scientific Research Foundation for Returned Overseas Chinese Scholars.

References

[1] Fluid Catalytic Cracking (FCC) Market Analysis, Market Size, Application Analysis, Regional Outlook, Competitive Strategies, and Forecasts, 2015 To 2022, Industry Reprot Summary, http://www.grandviewresearch.com/industry-analysis/fluid-catalytic-cracking-fcc-market

[2] Meyers, R. A.; Meyers, R. A. *Handbook of Petroleum Refining Processes*; McGraw-Hill: New York, 2004.

[3] Vogt, E.; Weckhuysen, B. Fluid Catalytic Cracking: Recent Developments on the Grand Old Lady of Zeolite Catalysis. *Chem Soc Rev*. 2015, *44*, 7342–7370. DOI: 10.1039/c5cs00376h.

[4] Marie, O.; Bazin, P.; Daturi, M. *Vibrational Spectroscopic Studies of Catalytic Processes on Oxide Surfaces, Spectroscopic Properties of Inorganic and Organometallic Compounds: Techniques, Materials and Applications*; The Royal Society of Chemistry, 2012; Vol.42, pp 34–103. DOI: 10.1039/9781849732833-00034.

[5] Sarrazin, P.; Baudouin, C.; Martino, G. Perspectives in Oil Refining. In *Handbook of Heterogeneous Catalysis*; Ertl, G., Weitkamp, H. K. J., Eds.; Wiley-VCH Verlag GmbH & Co. KGaA: Weinheim, Germany, 2008; pp 2677.

[6] Scherzer, J. Designing FCC Catalysts with High-Silica Y Zeolites. *Appl Catal*. 1991, *75*, 1–32. DOI: 10.1016/S0166-9834(00)83119-X.

[7] Hoffer, B. W.; Stockwell, D. M. Heavy Metal Passivator/Trap for FCC Processes. US Pat., 8632674 2014.

[8] Meirer, F.; Kalirai, S.; Morris, D.; Soparawalla, S.; Liu, Y.; Mesu, G.; Andrews, J. C.; Weckhuysen, B. M. Life and Death of a Single Catalytic Cracking Particle. *Science Advances*. 2015, *1*, e1400199. DOI: 10.1126/sciadv.1400199.

[9] Cao, X.; China's Choice of Gasoline Production Technology for the Future, Sinopec, 2012. http://www.pecj.or.jp/japanese/overseas/conference/pdf/conference10-01.pdf.

[10] Farshi, A.; Shaiyegh, F.; Burogerdi, S.; Dehgan, A. FCC Process Role in Propylene Demands. *Pet. Sci. Technol*. 2011, *29*, 875–885. DOI: 10.1080/10916460903451985.

[11] Mathieu, Y.; Corma, A.; Echard, M.; Bories, M. Single and Combined Effects of Bottom Cracking (BCA) and Propylene Booster (PBA) Separate Particles Additives Addition to a Fluid Catalytic Cracking (FCC) Catalyst on the FCC Product Distribution and Quality. *Appl Catal A Gen*. 2012, *439–440*, 57–73. DOI: 10.1016/j.apcata.2012.06.043.

[12] Wagner, K. *Improving FCC Economics with Light Olefins Additives*; Grace Davison Catalagram, 2011, No. 109, pp 34.

[13] Siddiqui, M. B.; Aitani, A.; Saeed, M.; Al-Khattaf, S. Enhancing the Production of Light Olefins by Catalytic Cracking of FCC Naphtha over Mesoporous ZSM-5 Catalyst. *Top. Catal*. 2010, *53*, 1387–1393. DOI: 10.1007/s11244-010-9598-1.

[14] Wallenstein, D.; Kanz, B.; Haas, A. Influence of Coke Deactivation and Vanadium and Nickel Contamination on the Performance of Low ZSM-5 Levels in FCC Catalysts. *Appl Catal A Gen*. 2000, *192*, 105–123. DOI: 10.1016/S0926-860X(99)00334-8.
[15] Akah, A.; Al-Ghrami, M. Maximizing Propylene Production via FCC Technology. *Appl Petrochem Res*. 2015, 1–16. DOI: 10.1007/s13203-015-0104-3.
[16] Liu, H.; Zhao, H.; Gao, X.; Ma, J. A Novel FCC Catalyst Synthesized via in Situ Overgrowth of NaY Zeolite on Kaolin Microspheres for Maximizing Propylene Yield. *Catal. Today*. 2007, *125*, 163–168. DOI: 10.1016/j.cattod.2007.05.005.
[17] Occelli, M. L. *Advances in Fluid Catalytic Cracking: Testing, Characterization, and Environmental Regulations*; CRC Press, 2010. https://www.crcpress.com/Advances-in-Fluid-Catalytic-Cracking-Testing-Characterization-and-Environmental/Occelli/p/book/9781138116351.
[18] Dean, C.; Naphtha Catalytic Cracking for Propylene Production: Investment in On-Purpose Propylene Production Technology Based on Naphtha-Based Feedstock Is Taking on Various Process Configurations, High Olefins FCC Technology Services, 2013. http://www.digitalrefining.com/article/1000787.
[19] Cerqueira, H. S.; Caeiro, G.; Costa, L.; Ramôa Ribeiro, F. Deactivation of FCC Catalysts. *J. Mol. Catal. A: Chem*. 2008, *292*, 1–13. DOI: 10.1016/j.molcata.2008.06.014.
[20] Sadeghbeigi, R. *Fluid Catalytic Cracking Handbook: An Expert Guide to the Practical Operation, Design, and Optimization of FCC Units*, 3rd ed.; Elsevier, 2012. https://www.elsevier.com/books/fluid-catalytic-cracking-handbook/sadeghbeigi/978-0-12-386965-4.
[21] Corma, A.; Sauvanaud, L. FCC Testing at Bench Scale: New Units, New Processes, New Feeds. *Catal. Today*. 2013, *218–219*, 107–114. DOI: 10.1016/j.cattod.2013.03.038.
[22] Harding, R. H.; Peters, A. W.; Nee, J. R. D. New Developments in FCC Catalyst Technology. *Appl Catal A Gen*. 2001, *221*, 389–396. DOI: 10.1016/S0926-860X(01)00814-6.
[23] Hudec, P.; FCC Catalyst-Key Element in Refinery Technology, 45th International Petroleum Conference in Bratislava, Slovakia. Retrieved Januray 2011, 21, 2013.
[24] Pinheiro, C. I. C.; Fernandes, J. L.; Domingues, L.; Chambel, A. J. S.; Graça, I.; Oliveira, N. M. C.; Cerqueira, H. S.; Ribeiro, F. R. Fluid Catalytic Cracking (FCC) Process Modeling, Simulation, and Control. *Ind. Eng. Chem. Res*. 2012, *51*, 1–29. DOI: 10.1021/ie200743c.
[25] Lloyd, L. *Catalytic Cracking Catalysts, Handbook of Industrial Catalysts*; Springer Science US, 2011; pp 169–210. DOI: 10.1007/978-0-387-49962-8_5.
[26] Bryden, K. J.; Weatherbee, G.; Habib, E. T., Jr. *Flexible Pilot Plant Technology for Evaluation of Unconventional Feedstocks and Processes*; Grace Davison catalagram, 2013, No. 113, pp 3-21.
[27] Ancheyta, J. *Modeling and Simulation of Catalytic Reactors for Petroleum Refining*; John Wiley & Sons, 2011; pp 1–52. DOI: 10.1002/9780470933565.
[28] Bare, S. R.; Charochak, M. E.; Kelly, S. D.; Lai, B.; Wang, J.; Chen-Wiegart, Y. C. K. Characterization of a Fluidized Catalytic Cracking Catalyst on Ensemble and Individual Particle Level by X-Ray Micro- and Nanotomography, Micro-X-Ray Fluorescence, and Micro-X-Ray Diffraction. *ChemCatChem*. 2014, *6*, 1427–1437. DOI: 10.1002/cctc.201490033.
[29] Vermeiren, W.; Gilson, J.-P. Impact of Zeolites on the Petroleum and Petrochemical Industry. *Top. Catal*. 2009, *52*, 1131–1161. DOI: 10.1007/s11244-009-9271-8.
[30] Perego, C.; Millini, R. Porous Materials in Catalysis: Challenges for Mesoporous Materials. *Chem Soc Rev*. 2013, *42*, 3956–3976. DOI: 10.1039/c2cs35244c.

[31] Buchanan, J. The Chemistry of Olefins Production by ZSM-5 Addition to Catalytic Cracking Units. *Catal. Today*. 2000, *55*, 207–212. DOI: 10.1016/S0920-5861(99)00248-5.
[32] Willis, M. J.; Folmar, K. W. Heavy Metals Trapping Co-Catalyst for FCC Processes. US Pat, 8,372,269 B2. 2013.
[33] Vierheilig, A. A.; Additives for Metal Contaminant Removal. US Pat., 2010/0025297 A1. 2010.
[34] Cheng, W.-C.; Kim, G.; Peters, A.; Zhao, X.; Rajagopalan, K.; Ziebarth, M.; Pereira, C. Environmental Fluid Catalytic Cracking Technology. *Catal Rev*. 1998, *40*, 39–79. DOI: 10.1080/01614949808007105.
[35] Chester, A. W. CO Combustion Promoters: Past and Present. *Stud Surf Sci Catal*. 2007, *166*, 67–77.
[36] Falco, M.; Morgado, E.; Amadeo, N.; Sedran, U. Accessibility in Alumina Matrices of FCC Catalysts. *Appl Catal A Gen*. 2006, *315*, 29–34. DOI: 10.1016/j.apcata.2006.08.028.
[37] Chen, W.; Han, D.; Sun, X.; Li, C. Studies on the Preliminary Cracking of Heavy Oils: Contributions of Various Factors. *Fuel*. 2013, *106*, 498–504. DOI: 10.1016/j.fuel.2012.12.090.
[38] Pinto, F. V.; Escobar, A. S.; de Oliveira, B. G.; Lam, Y. L.; Cerqueira, H. S.; Louis, B.; Tessonnier, J. P.; Su, D. S.; Pereira, M. M. The Effect of Alumina on FCC Catalyst in the Presence of Nickel and Vanadium. *Appl Catal A Gen*. 2010, *388*, 15–21. DOI: 10.1016/j.apcata.2010.07.055.
[39] Woltermann, G. M.; Magee, J. S.; Griffith, S. D. Commercial Preparation and Characterization of FCC Catalysts. In *Fluid Catalytic Cracking: Science and Technology, Studies in Surface Science and Catalysts*; Magee, J. S., Mitchell, M. M., Eds.; Elsevier, 1993; pp 105-144. DOI: 10.1016/S0167-2991(08)63827-6.
[40] Venuto, P. B.; Habib, T. Catalyst-Feedstock-Engineering Interactions in Fluid Catalytic Cracking. *Catal Rev*. 1978, *18*, 1–150. DOI: 10.1080/03602457808067529.
[41] Nee, J. R. D.; Harding, R. H.; Yaluris, G.; Cheng, W. C.; Zhao, X.; Dougan, T. J.; Riley, J. R. *Fluid Catalytic Cracking (FCC), Catalysts and Additives, Kirk-Othmer Encyclopedia of Chemical Technology*; John Wiley & Sons, Inc., 2004. DOI: 10.1002/0471238961.fluidnee.a01.
[42] Hargreaves, J.; Munnoch, A. A Survey of the Influence of Binders in Zeolite Catalysis. *Catal. Sci. Technol*. 2013, *3*, 1165–1171. DOI: 10.1039/c3cy20866d.
[43] Mitchell, B. R. Metal Contamination of Cracking Catalysts. 1. Synthetic Metals Deposition on Fresh Catalysts. *Ind. Eng. Chem. Res*. 1980, *19*, 209–213. DOI: 10.1021/i360074a015.
[44] Chiranjeevi, T.; Gokak, D.; Ravikumar, V.; Viswanathan, P. Development of New Deactivation Method for Simulation of Fluid Catalytic Cracking Equilibrium Catalyst. *J Chem Sci*. 2014, *126*, 353–360. DOI: 10.1007/s12039-014-0583-2.
[45] Wallenstein, D.; Harding, R.; Nee, J.; Boock, L. Recent Advances in the Deactivation of FCC Catalysts by Cyclic Propylene Steaming (CPS) in the Presence and Absence of Contaminant Metals. *Appl Catal A Gen*. 2000, *204*, 89–106. DOI: 10.1016/S0926-860X(00)00504-4.
[46] Gerritsen, L.; Wijngaards, H.; Verwoert, J.; O'Connor, P. Cyclic Deactivation: A Novel Technique to Simulate the Deactivation of FCC Catalyst in Commercial Units. *Catal. Today*. 1991, *11*, 61–72. DOI: 10.1016/0920-5861(91)87007-A.
[47] Lerner, B.; Deeba, M. Improved Methods for Testing and Assessing Deactivation from Vanadium Interaction with Fluid Catalytic Cracking Catalyst. In *Deactivation and Testing of Hydrocarbon-Processing Catalyst*, O'Connor, P., Takatsuka, T., Woolery, G. L., Eds.; ACS Symposium Series, 634, 1996; pp 296–311.

[48] Kayser, J. C.; Versatile Fluidized Bed Reactor. US Pat., 6069012 2000.
[49] Wallenstein, D.; Farmer, D.; Knoell, J.; Fougret, C.; Brandt, S. Progress in the Deactivation of Metals Contaminated FCC Catalysts by a Novel Catalyst Metallation Method. *Appl Catal A Gen*. 2013, *462*, 91–99. DOI: 10.1016/j.apcata.2013.02.002.
[50] Del Río, D.; Passamonti, F.; Sedran, U. Reliable Laboratory Reactor Data Analysis: Evaluation of Commercial FCC Catalysts in a Batch Fluidized Bed Reactor. *Chem. Eng. Commun*. 2015, *202*, 756–764. DOI: 10.1080/00986445.2013.871710.
[51] Young, G. W. Chapter 8 Realistic Assessment of FCC Catalyst Performance in the Laboratory. In *Studies in Surface Science and Catalysis*; John, S. M., Maurice, M. M., Eds.; Elsevier, 1993; pp 257–292. DOI: 10.1016/S0167-2991(08)63831-8.
[52] Corma, A.; Martínez, C.; Melo, F. V.; Sauvanaud, L.; Carriat, J. Y. A New Continuous Laboratory Reactor for the Study of Catalytic Cracking. *Appl Catal A Gen*. 2002, *232*, 247–263. DOI: 10.1016/S0926-860X(02)00110-2.
[53] Psarras, A.; Iliopoulou, E.; Nalbandian, L.; Lappas, A.; Pouwels, C. Study of the Accessibility Effect on the Irreversible Deactivation of FCC Catalysts from Contaminant Feed Metals. *Catal. Today*. 2007, *127*, 44–53. DOI: 10.1016/j.cattod.2007.05.021.
[54] Passamonti, F. J.; de la Puente, G.; Sedran, U. Laboratory Evaluation of FCC Commercial Catalysts: Analysis of Products of Industrial Importance. *Catal. Today*. 2008, *133*, 314–318. DOI: 10.1016/j.cattod.2007.12.123.
[55] Wallenstein, D.; Roberie, T.; Bruhin, T. Review on the Deactivation of FCC Catalysts by Cyclic Propylene Steaming. *Catal. Today*. 2007, *127*, 54–69. DOI: 10.1016/j.cattod.2007.05.023.
[56] Jiménez-García, G.; Aguilar-López, R.; Maya-Yescas, R. The Fluidized-Bed Catalytic Cracking Unit Building Its Future Environment. *Fuel*. 2011, *90*, 3531–3541. DOI: 10.1016/j.fuel.2011.03.045.
[57] Caeiro, G.; Costa, A. F.; Cerqueira, H. S.; Magnoux, P.; Lopes, J. M.; Matias, P.; Ribeiro, F. R. Nitrogen Poisoning Effect on the Catalytic Cracking of Gasoil. *Appl Catal A Gen*. 2007, *320*, 8–15. DOI: 10.1016/j.apcata.2006.11.031.
[58] Nagy, B.; Colombo, U. *Fundamental Aspects of Petroleum Geochemistry*; Elsevier, 1967. https://trove.nla.gov.au/work/21366160.
[59] Okunev, A.; Parkhomchuk, E. V. E.; Lysikov, A.; Parunin, P. D.; Semeikina, V.; Parmon, V. N. Catalytic Hydroprocessing of Heavy Oil Feedstocks. *Russ. Chem. Rev*. 2015, *84*, 981. DOI: 10.1070/RCR4486.
[60] Fletcher, R. P. *The History of Fluidized Catalytic Cracking: A History of Innovation: 1942-2008, Innovations in Industrial and Engineering Chemistry*; American Chemical Society, 2008; pp 189–249. DOI: 10.1021/bk-2009-1000.ch006.
[61] Wright, M. C.; Court, R. W.; Kafantaris, F.-C. A.; Spathopoulos, F.; Sephton, M. A. A New Rapid Method for Shale Oil and Shale Gas Assessment. *Fuel*. 2015, *153*, 231–239. DOI: 10.1016/j.fuel.2015.02.089.
[62] Furimsky, E. Properties of Tight Oils and Selection of Catalysts for Hydroprocessing. *Energy Fuel*. 2015, *29*, 2043–2058. DOI: 10.1021/acs.energyfuels.5b00338.
[63] Youngquist, W.; Shale oil–The Elusive Energy, Hubbert Centre Newsletter.
[64] Altun, N.; Hicyilmaz, C.; Hwang, J.-Y.; Bağci, A. S.; Kök, M. Oil Shales in the World and Turkey; Reserves, Current Situation and Future Prospects: A Review. *Oil Shale*. 2006, *23*, 211–227.
[65] Bryden, K. J.; Habib, E. T., Jr.; Topete, O. A. *Processing Shale Oils in FCC Challenges and Opportunities, Hydrocarbon Process*; Int. Ed., 2013. https://www.hydrocarbonprocessing.com/magazine/2013/september-2013/special-report-refining-developments/processing-shale-oils-in-fcc-challenges-and-opportunities.

[66] de Graaf, B.; Radcliffe, C.; Evans, M.; Diddams, P., *Processing Shale Oil in an FCC Unit: Catalyst and Profit Optimisation*; Johnson Matthey Process Technologies, 2015http://www.jmprotech.com/images-uploaded/files/Processing%20Shale%20Oil%20in%20an%20FCC%20Unit%20(2015).pdf.

[67] Zendehboudi, S.; Bahadori, A. *Shale Oil and Gas Handbook: Theory, Technologies, and Challenges*; Gulf Professional Publishing, 2016. https://www.elsevier.com/books/shale-oil-and-gas-handbook/zendehboudi/978-0-12-802100-2.

[68] Li, N.; Chen, C.; Wang, B.; Li, S.; Yang, C.; Chen, X. Retardation Effect of Nitrogen Compounds and Condensed Aromatics on Shale Oil Catalytic Cracking Processing and Their Characterization. *Appl Petrochem Res*. 2015, *5*, 285–295. DOI: 10.1007/s13203-015-0131-0.

[69] Brady, M. P.; Keiser, J. R.; Leonard, D. N.; Zacher, A. H.; Bryden, K. J.; Weatherbee, G. D. Corrosion of Stainless Steels in the Riser during Co-Processing of Bio-Oils in a Fluid Catalytic Cracking Pilot Plant. *Fuel Process. Technol*. 2017, *159*, 187–199. DOI: 10.1016/j.fuproc.2017.01.041.

[70] Rao, T. M.; Dupain, X.; Makkee, M. Fluid Catalytic Cracking: Processing Opportunities for Fischer–Tropsch Waxes and Vegetable Oils to Produce Transportation Fuels and Light Olefins. *Micropor Mesopor Mater*. 2012, *164*, 148–163. DOI: 10.1016/j.micromeso.2012.07.016.

[71] Dupain, X.; Costa, D. J.; Schaverien, C. J.; Makkee, M.; Moulijn, J. A. Cracking of a Rapeseed Vegetable Oil under Realistic FCC Conditions. *Appl Catal B*. 2007, *72*, 44–61.

[72] Dupain, X.; Krul, R. A.; Makkee, M.; Moulijn, J. A. Are Fischer–Tropsch Waxes Good Feedstocks for Fluid Catalytic Cracking Units? *Catal. Today*. 2005, *106*, 288–292. DOI: 10.1016/j.cattod.2005.07.148.

[73] Dupain, X.; Krul, R. A.; Schaverien, C. J.; Makkee, M.; Moulijn, J. A. Production of Clean Transportation Fuels and Lower Olefins from Fischer-Tropsch Synthesis Waxes under Fluid Catalytic Cracking Conditions: The Potential of Highly Paraffinic Feedstocks for FCC. *Appl Catal B Environ*. 2006, *63*, 277–295. DOI: 10.1016/j.apcatb.2005.10.012.

[74] Al-Sabawi, M.; Chen, J.; Ng, S. Fluid Catalytic Cracking of Biomass-Derived Oils and Their Blends with Petroleum Feedstocks: A Review. *Energy Fuel*. 2012, *26*, 5355–5372. DOI: 10.1021/ef3006417.

[75] de Rezende Pinho, A.; de Almeida, M. B.; Mendes, F. L.; Ximenes, V. L.; Casavechia, L. C. Co-Processing Raw Bio-Oil and Gasoil in an FCC Unit. *Fuel Process. Technol*. 2015, *131*, 159–166. DOI: 10.1016/j.fuproc.2014.11.008.

[76] Gueudré, L.; Chapon, F.; Mirodatos, C.; Schuurman, Y.; Venderbosch, R.; Jordan, E.; Wellach, S.; Gutierrez, R. M. Optimizing the Bio-Gasoline Quantity and Quality in Fluid Catalytic Cracking Co-Refining. *Fuel*. 2017, *192*, 60–70. DOI: 10.1016/j.fuel.2016.12.021.

[77] Fogassy, G.; Thegarid, N.; Toussaint, G.; van Veen, A. C.; Schuurman, Y.; Mirodatos, C. Biomass Derived Feedstock Co-Processing with Vacuum Gas Oil for Second-Generation Fuel Production in FCC Units. *Appl Catal B*. 2010, *96*, 476–485. DOI: 10.1016/j.apcatb.2010.03.008.

[78] Lindfors, C.; Paasikallio, V.; Kuoppala, E.; Reinikainen, M.; Oasmaa, A.; Solantausta, Y. Co-Processing of Dry Bio-Oil, Catalytic Pyrolysis Oil, and Hydrotreated Bio-Oil in a Micro Activity Test Unit. *Energy Fuel*. 2015, *29*, 3707–3714. DOI: 10.1021/acs.energyfuels.5b00339.

[79] Samolada, M.; Baldauf, W.; Vasalos, I. Production of a Bio-Gasoline by Upgrading Biomass Flash Pyrolysis Liquids via Hydrogen Processing and Catalytic Cracking. *Fuel*. 1998, *77*, 1667–1675. DOI: 10.1016/S0016-2361(98)00073-8.

[80] Vitolo, S.; Bresci, B.; Seggiani, M.; Gallo, M. Catalytic Upgrading of Pyrolytic Oils over HZSM-5 Zeolite: Behaviour of the Catalyst When Used in Repeated Upgrading–Regenerating Cycles. *Fuel*. 2001, *80*, 17–26. DOI: 10.1016/S0016-2361(00)00063-6.

[81] Vitolo, S.; Seggiani, M.; Frediani, P.; Ambrosini, G.; Politi, L. Catalytic Upgrading of Pyrolytic Oils to Fuel over Different Zeolites. *Fuel*. 1999, *78*, 1147–1159. DOI: 10.1016/S0016-2361(99)00045-9.

[82] de Miguel Mercader, F.; Groeneveld, M.; Kersten, S.; Way, N.; Schaverien, C.; Hogendoorn, J. Production of Advanced Biofuels: Co-Processing of Upgraded Pyrolysis Oil in Standard Refinery Units. *Appl Catal B*. 2010, *96*, 57–66. DOI: 10.1016/j.apcatb.2010.01.033.

[83] Nguyen, T.; Zabeti, M.; Lefferts, L.; Brem, G.; Seshan, K. Catalytic Upgrading of Biomass Pyrolysis Vapours Using Faujasite Zeolite Catalysts. *Biomass Bioenergy*. 2013, *48*, 100–110. DOI: 10.1016/j.biombioe.2012.10.024.

[84] Adjaye, J. D.; Bakhshi, N. Production of Hydrocarbons by Catalytic Upgrading of a Fast Pyrolysis Bio-Oil. Part I: Conversion over Various Catalysts. *Fuel Process. Technol*. 1995, *45*, 161–183. DOI: 10.1016/0378-3820(95)00034-5.

[85] Lappas, A.; Bezergianni, S.; Vasalos, I. Production of Biofuels via Co-Processing in Conventional Refining Processes. *Catal. Today*. 2009, *145*, 55–62. DOI: 10.1016/j.cattod.2008.07.001.

[86] Li, L.; Quan, K.; Xu, J.; Liu, F.; Liu, S.; Yu, S.; Xie, C.; Zhang, B.; Ge, X. Liquid Hydrocarbon Fuels from Catalytic Cracking of Rubber Seed Oil Using USY as Catalyst. *Fuel*. 2014, *123*, 189–193. DOI: 10.1016/j.fuel.2014.01.049.

[87] Watkins, B.; Olsen, C.; Sutovich, K.; Petti, N. New Opportunities for Co-Processing Renewable Feeds in Refinery Processes. Grace Davison Catalagram, 2008, No. 103, pp 1-13.

[88] Bielansky, P.; Weinert, A.; Schönberger, C.; Reichhold, A. Catalytic Conversion of Vegetable Oils in a Continuous FCC Pilot Plant. *Fuel Process. Technol*. 2011, *92*, 2305–2311. DOI: 10.1016/j.fuproc.2011.07.021.

[89] Melero, J. A.; Clavero, M. M.; Calleja, G.; García, A.; Miravalles, R.; Galindo, T. Production of Biofuels via the Catalytic Cracking of Mixtures of Crude Vegetable Oils and Nonedible Animal Fats with Vacuum Gas Oil. *Energy Fuel*. 2009, *24*, 707–717. DOI: 10.1021/ef900914e.

[90] Twaiq, F. A. A.; Mohamad, A. R.; Bhatia, S. Performance of Composite Catalysts in Palm Oil Cracking for the Production of Liquid Fuels and Chemicals. *Fuel Process. Technol*. 2004, *85*, 1283–1300. DOI: 10.1016/j.fuproc.2003.08.003.

[91] Taufiqurrahmi, N.; Mohamed, A. R.; Bhatia, S. Deactivation and Coke Combustion Studies of Nanocrystalline Zeolite Beta in Catalytic Cracking of Used Palm Oil. *Chem Eng J*. 2010, *163*, 413–421. DOI: 10.1016/j.cej.2010.07.049.

[92] Tamunaidu, P.; Bhatia, S. Catalytic Cracking of Palm Oil for the Production of Biofuels: Optimization Studies. *Bioresour. Technol*. 2007, *98*, 3593–3601. DOI: 10.1016/j.biortech.2006.11.028.

[93] Bielansky, P.; Reichhold, A.; Schönberger, C. Catalytic Cracking of Rapeseed Oil to High Octane Gasoline and Olefins. *Chem. Eng. Process*. 2010, *49*, 873–880. DOI: 10.1016/j.cep.2010.04.012.

[94] Ng, S. H.; Al-Sabawi, M.; Wang, J.; Ling, H.; Zheng, Y.; Wei, Q.; Ding, F.; Little, E. FCC Coprocessing Oil Sands Heavy Gas Oil and Canola Oil. 1. Yield Structure. *Fuel*. 2015, *156*, 163–176. DOI: 10.1016/j.fuel.2015.03.077.

[95] Emori, E. Y.; Hirashima, F. H.; Zandonai, C. H.; Ortiz-Bravo, C. A.; Fernandes-Machado, N. R. C.; Olsen-Scaliante, M. H. N. Catalytic Cracking of Soybean Oil Using ZSM5 Zeolite. *Catal. Today*. 2017, *279*, 168-173. DOI: 10.1016/j.cattod.2016.05.052.

[96] Li, H.; Shen, B.; Kabalu, J.; Nchare, M. Enhancing the Production of Biofuels from Cottonseed Oil by Fixed-Fluidized Bed Catalytic Cracking. *Renew Energ*. 2009, *34*, 1033–1039. DOI: 10.1016/j.renene.2008.08.004.

[97] He, Y.; Barnes, S. E.; Crunkleton, D. W.; Price, G. L. Comparison of Ginger Oil Conversion over MFI, BEA, and FAU. *Fuel*. 2012, *96*, 469–475. DOI: 10.1016/j.fuel.2012.01.033.

[98] Zheng, Q.; Huo, L.; Li, H.; Mi, S.; Li, X.; Zhu, X.; Deng, X.; Shen, B. Exploring Structural Features of USY Zeolite in the Catalytic Cracking of Jatropha Curcas L. Seed Oil Towards Higher Gasoline/Diesel Yield and Lower CO2 Emission. *Fuel*. 2017, *202*, 563–571. DOI: 10.1016/j.fuel.2017.04.073.

[99] Taufiqurrahmi, N.; Mohamed, A. R.; Bhatia, S. Production of Biofuel from Waste Cooking Palm Oil Using Nanocrystalline Zeolite as Catalyst: Process Optimization Studies. *Bioresour. Technol.* 2011, *102*, 10686–10694. DOI: 10.1016/j.biortech.2011.08.068.

[100] Vinh, T. Q.; Loan, N. T. T.; Yang, X.-Y.; Su, B.-L. Preparation of Bio-Fuels by Catalytic Cracking Reaction of Vegetable Oil Sludge. *Fuel*. 2011, *90*, 1069–1075. DOI: 10.1016/j.fuel.2010.10.060.

[101] Bielansky, P.; Weinert, A.; Schönberger, C.; Reichhold, A. Gasoline and Gaseous Hydrocarbons from Fatty Acids via Catalytic Cracking. *Biomass Convers Biorefin*. 2012, *2*, 53–61. DOI: 10.1007/s13399-011-0027-x.

[102] Ooi, Y.-S.; Zakaria, R.; Mohamed, A. R.; Bhatia, S. Catalytic Conversion of Palm Oil-Based Fatty Acid Mixture to Liquid Fuel. *Biomass Bioenergy*. 2004, *27*, 477–484. DOI: 10.1016/j.biombioe.2004.03.003.

[103] Ooi, Y.-S.; Zakaria, R.; Mohamed, A. R.; Bhatia, S. Hydrothermal Stability and Catalytic Activity of Mesoporous Aluminum-Containing SBA-15. *Catal. Commun*. 2004, *5*, 441–445. DOI: 10.1016/j.catcom.2004.05.011.

[104] Chen, D.; Tracy, N. I.; Crunkleton, D. W.; Price, G. L. Comparison of Canola Oil Conversion over MFI, BEA, and FAU. *Appl Catal A*. 2010, *384*, 206–212. DOI: 10.1016/j.apcata.2010.06.037.

[105] Zhao, X.; Wei, L.; Cheng, S.; Huang, Y.; Yu, Y.; Julson, J. Catalytic Cracking of Camelina Oil for Hydrocarbon Biofuel over ZSM-5-Zn Catalyst. *Fuel Process. Technol.* 2015, *139*, 117–126. DOI: 10.1016/j.fuproc.2015.07.033.

[106] Ooi, Y.-S.; Bhatia, S. Aluminum-Containing SBA-15 as Cracking Catalyst for the Production of Biofuel from Waste Used Palm Oil. *Micropor. Mesopor. Mater*. 2007, *102*, 310–317. DOI: 10.1016/j.micromeso.2006.12.044.

[107] Ooi, Y.-S.; Zakaria, R.; Mohamed, A. R.; Bhatia, S. Synthesis of Composite Material MCM-41/Beta and Its Catalytic Performance in Waste Used Palm Oil Cracking. *Appl. Catal. A*. 2004, *274*, 15–23. DOI: 10.1016/j.apcata.2004.05.011.

[108] Tian, H.; Li, C.; Yang, C.; Shan, H. Alternative Processing Technology for Converting Vegetable Oils and Animal Fats to Clean Fuels and Light Olefins. *Chin. J. Chem. Eng.* 2008, *16*, 394–400. DOI: 10.1016/S1004-9541(08)60095-6.

[109] Gómez, M.-E.; Vargas, C.; Lizcano, J. Petrochemical Promoters in Catalytic Cracking. *CTF Cienc. Tecnol. Futuro*. 2009, *3*, 143–158.

[110] Wang, G.; Xu, C.; Gao, J. Study of Cracking FCC Naphtha in a Secondary Riser of the FCC Unit for Maximum Propylene Production. *Fuel Process. Technol.* 2008, *89*, 864–873. DOI: 10.1016/j.fuproc.2008.02.007.

[111] Corma, A.; Melo, F. V.; Sauvanaud, L.; Ortega, F. Light Cracked Naphtha Processing: Controlling Chemistry for Maximum Propylene Production. *Catal. Today*. 2005, *107,108*, 699–706. DOI: 10.1016/j.cattod.2005.07.109.

[112] Verstraete, J.; Coupard, V.; Thomazeau, C.; Etienne, P. Study of Direct and Indirect Naphtha Recycling to a Resid FCC Unit for Maximum Propylene Production. *Catal. Today*. 2005, *106*, 62–71. DOI: 10.1016/j.cattod.2005.07.183.

[113] Chen, J. Q.; Bozzano, A.; Glover, B.; Fuglerud, T.; Kvisle, S. Recent Advancements in Ethylene and Propylene Production Using the UOP/Hydro MTO Process. *Catal. Today*. 2005, *106*, 103–107. DOI: 10.1016/j.cattod.2005.07.178.

[114] Chen, D.; Grønvold, A.; Moljord, K.; Holmen, A. Methanol Conversion to Light Olefins over SAPO-34: Reaction Network and Deactivation Kinetics. *Ind. Eng. Chem. Res*. 2007, *46*, 4116–4123. DOI: 10.1021/ie0610748.

[115] Bos, A. N. R.; Tromp, P. J. J.; Akse, H. N. Conversion of Methanol to Lower Olefins. Kinetic Modeling, Reactor Simulation, and Selection. *Ind. Eng. Chem. Res*. 1995, *34*, 3808–3816. DOI: 10.1021/ie00038a018.

[116] Pan, S.; Jiang, H.; Weng, H. Feeding Methanol in an FCC Unit. *Pet. Sci. Technol*. 2008, *26*, 170–180. DOI: 10.1080/10916460600805152.

[117] Avidan, A. A. Origin, Development and Scope of FCC Catalysis. *Stud. Surf. Sci. Catal*. 1993, *76*, 1–39.

[118] Castaneda, R.; Corma, A.; Fornes, V.; Martinez-Triguero, J.; Valencia, S. Direct Synthesis of A 9 × 10 Member Ring Zeolite (Al-Itq-13): A Highly Shape-Selective Catalyst for Catalytic Cracking. *J. Catal*. 2006, *238*, 79–87. DOI: 10.1016/j.jcat.2005.11.038.

[119] Corma, A.; Díaz-Cabañas, M. J.; Fornés, V. Synthesis, Characterization, and Catalytic Activity of a Large-Pore Tridirectional Zeolite, H-ITQ-7. *Angew. Chem. Int. Ed*. 2000, *39*, 2346–2349. DOI: 10.1002/1521-3773(20000703)39:13<2346::AID-ANIE2346>3.0.CO;2-B.

[120] Corma, A.; Martínez-Triguero, J. N.; Martínez, C. The Use of ITQ-7 as a FCC Zeolitic Additive. *J. Catal*. 2001, *197*, 151–159. DOI: 10.1006/jcat.2000.3065.

[121] Moliner, M.; Díaz-Cabañas, M.; Fornés, V.; Martínez, C.; Corma, A. Synthesis methodology, acidity and catalytic behaviour of the 18 × 10 member ring pores ITQ-33 zeolite. *Studies in Surface Science and Catalysis*, 2008, *174*, 155–160. DOI: 10.1016/S0167-2991(08)80167-X.

[122] Chen, Y.-M. Recent Advances in FCC Technology. *Powder Technol*. 2006, *163*, 2–8. DOI: 10.1016/j.powtec.2006.01.001.

[123] Letzsch, W. Fluid Catalytic Cracking (FCC). In: *Handbook of Petroleum Processing*, Jones, D. J. S., Pujadó, P., Eds.; Springer Netherlands, 2006; pp 239–286. DOI: 10.1007/1-4020-2820-2_6.

[124] Doyle, A.; Saavedra, A.; Tristão, M. L. B.; Aucelio, R. Q. Determination of S, Ca, Fe, Ni and V in Crude Oil by Energy Dispersive X-Ray Fluorescence Spectrometry Using Direct Sampling on Paper Substrate. *Fuel*. 2015, *162*, 39–46. DOI: 10.1016/j.fuel.2015.08.072.

[125] Jiménez-García, G.; de Lasa, H.; Quintana-Solórzano, R.; Maya-Yescas, R. Catalyst Activity Decay Due to Pore Blockage during Catalytic Cracking of Hydrocarbons. *Fuel*. 2013, *110*, 89–98. DOI: 10.1016/j.fuel.2012.10.082.

[126] Myrstad, T.; Seljestokken, B.; Engan, H.; Rytter, E. Effect of Nickel and Vanadium on Sulphur Reduction of FCC Naphtha. *Appl Catal A*. 2000, *192*, 299–305. DOI: 10.1016/S0926-860X(99)00405-6.

[127] Siddiqui, M.; Aitani, A. FCC Gasoline Sulfur Reduction by Additives: A Review. *Pet. Sci. Technol*. 2007, *25*, 299–313. DOI: 10.1081/LFT-200063072.

[128] Kumar, J.; Gota, K.; Modhera, B. Influence of Pyrrole Concentration on Cracking Activity of N-Hexane in a Performance FCC Catalyst and Additives. *APCBEE Procedia*. 2014, *9*, 159–164. DOI: 10.1016/j.apcbee.2014.01.028.

[129] Barth, J.-O.; Jentys, A.; Lercher, J. On the Nature of Nitrogen-Containing Carbonaceous Deposits on Coked Fluid Catalytic Cracking Catalysts. *Ind. Eng. Chem. Res*. 2004, *43*, 2368–2375. DOI: 10.1021/ie034163i.

[130] Li, Z. K.; Wang, G.; Shi, Q.; Xu, C.-M.; Gao, J.-S. Retardation Effect of Basic Nitrogen Compounds on Hydrocarbons Catalytic Cracking in Coker Gas Oil and Their Structural Identification. *Ind. Eng. Chem. Res*. 2011, *50*, 4123–4132. DOI: 10.1021/ie102117x.

[131] Zhao, X.; Peters, A.; Weatherbee, G. Nitrogen Chemistry and NO X Control in a Fluid Catalytic Cracking Regenerator. *Ind. Eng. Chem. Res*. 1997, *36*, 4535–4542. DOI: 10.1021/ie970130p.

[132] Babich, I.; Seshan, K.; Lefferts, L. Nature of Nitrogen Specie in Coke and Their Role in NO X Formation during FCC Catalyst Regeneration. *Appl. Catal. B*. 2005, *59*, 205–211. DOI: 10.1016/j.apcatb.2005.02.008.

[133] Fu, C. M.; Schaffer, A. M. Effect of Nitrogen Compounds on Cracking Catalysts. *Ind. Eng. Chem. Res*. 1985, *24*, 68–75. DOI: 10.1021/i300017a013.

[134] Li, Z.-K.; Gao, J.-S.; Wang, G.; Shi, Q.; Xu, C.-M. Influence of Nonbasic Nitrogen Compounds and Condensed Aromatics on Coker Gas Oil Catalytic Cracking and Their Characterization. *Ind. Eng. Chem. Res*. 2011, *50*, 9415–9424. DOI: 10.1021/ie2003973.

[135] Bobkova, T. V.; Doronin, V. P.; Potapenko, O. V.; Sorokina, T. P.; Ostrovskii, N. M. Poisoning Effect of Nitrogen Compounds on the Transformation of Model Hydrocarbons and Real Feed under Catalytic Cracking Conditions. *Catal. Ind.*. 2014, *6*, 218–222. DOI: 10.1134/S2070050414030040.

[136] Caeiro, G.; Magnoux, P.; Ayrault, P.; Lopes, J.; Ribeiro, F. R. Deactivating Effect of Coke and Basic Nitrogen Compounds during the Methylcyclohexane Transformation over H-MFI Zeolite. *Chem. Eng. J*. 2006, *120*, 43–54. DOI: 10.1016/j.cej.2006.03.036.

[137] Ho, T. C.; Katritzky, A. R.; Cato, S. J. Effect of Nitrogen Compounds on Cracking Catalysts. *Ind. Eng. Chem. Res*. 1992, *31*, 1589–1597. DOI: 10.1021/ie00007a002.

[138] Zhang, J. H.; Shan, H. H.; Yang, C. H.; Chen, X. B.; Li, C. Y. Catalytic Cracking of Coker Gas Oil at High Reaction Temperature and Catalyst to Oil Ratio. *Adv. Mater. Res*. 2013, *724*, 1112–1115.

[139] Leflaive, P.; Lemberton, J.; Perot, G.; Mirgain, C.; Carriat, J.; Colin, J. On the Origin of Sulfur Impurities in Fluid Catalytic Cracking gasoline—Reactivity of Thiophene Derivatives and of Their Possible Precursors under FCC Conditions. *Appl. Catal. A*. 2002, *227*, 201–215. DOI: 10.1016/S0926-860X(01)00936-X.

[140] Ruiz-Martínez, J.; Buurmans, I. L. C.; Knowles, W. V.; van der Beek, D.; Bergwerff, J. A.; Vogt, E. T. C.; Weckhuysen, B. M. Microspectroscopic Insight into the Deactivation Process of Individual Cracking Catalyst Particles with Basic Sulfur Components. *Appl. Catal. A Gen*. 2012, *419–420*, 84–94. DOI: 10.1016/j.apcata.2012.01.016.

[141] Hernández-Beltrán, F.; Quintana-Solórzano, R.; Sánchez-Valente, J.; Pedraza-Archila, F.; Figueras, F. Effect of Highly Reactive Sulfur Species on Sulfur Reduction in Cracking Gasoline. *Appl. Catal. B*. 2003, *42*, 145–154. DOI: 10.1016/S0926-3373(02)00237-0.

[142] Gil, B.; Mierzyńska, K.; Szczerbińska, M.; Datka, J. In Situ IR and Catalytic Studies of the Effect of Coke on Acid Properties of Steamed Zeolite Y. *Micropor. Mesopor. Mater.*. 2007, *99*, 328–333. DOI: 10.1016/j.micromeso.2006.09.025.

[143] Forzatti, P.; Lietti, L. Catalyst Deactivation. *Catal. Today*. 1999, *52*, 165–181. DOI: 10.1016/S0920-5861(99)00074-7.

[144] Jiménez-García, G.; Aguilar-López, R.; León-Becerril, E.; Maya-Yescas, R. Tracking Catalyst Activity during Fluidized-Bed Catalytic Cracking. *Ind. Eng. Chem. Res.* 2008, *48*, 1220–1227. DOI: 10.1021/ie800650y.

[145] Cheng, W.-C.; Juskelis, M.; Sua, W. Reducibility of Metals on Fluid Cracking Catalyst. *Appl. Catal. A*. 1993, *103*, 87–103. DOI: 10.1016/0926-860X(93)85176-P.

[146] Valla, J.; Lappas, A.; Vasalos, I.; Kuehler, C.; Gudde, N. Feed and Process Effects on the in Situ Reduction of Sulfur in FCC Gasoline. *Appl. Catal. A*. 2004, *276*, 75–87. DOI: 10.1016/j.apcata.2004.07.042.

[147] Brunet, S.; Mey, D.; Pérot, G.; Bouchy, C.; Diehl, F. On the Hydrodesulfurization of FCC Gasoline: A Review. *Appl. Catal. A*. 2005, *278*, 143–172. DOI: 10.1016/j.apcata.2004.10.012.

[148] Gilbert, W. R. Formation of Thiophenic Species in FCC Gasoline from H2S Generating Sulfur Sources in FCC Conditions. *Fuel*. 2014, *121*, 65–71. DOI: 10.1016/j.fuel.2013.12.033.

[149] Lappas, A.; Valla, J.; Vasalos, I.; Kuehler, C.; Francis, J.; O'Connor, P.; Gudde, N. The Effect of Catalyst Properties on the in Situ Reduction of Sulfur in FCC Gasoline. *Appl. Catal. A*. 2004, *262*, 31–41. DOI: 10.1016/j.apcata.2003.11.014.

[150] Valla, J.; Mouriki, E.; Lappas, A.; Vasalos, I. The Effect of Heavy Aromatic Sulfur Compounds on Sulfur in Cracked Naphtha. *Catal. Today*. 2007, *127*, 92–98. DOI: 10.1016/j.cattod.2007.05.017.

[151] Wolf, E.; Alfani, F. Catalysts Deactivation by Coking. *Cat. Rev. Sci. Eng.*. 1982, *24*, 329–371. DOI: 10.1080/03602458208079657.

[152] Snape, C.; McGhee, B.; Andresen, J.; Hughes, R.; Koon, C.; Hutchings, G. Characterisation of Coke from FCC Refinery Catalysts by Quantitative Solid State 13 C NMR. *Appl. Catal. A*. 1995, *129*, 125–132. DOI: 10.1016/0926-860X(95)00104-2.

[153] Menon, P. Coke on Catalysts-Harmful, Harmless, Invisible and Beneficial Types. *J. Mol. Catal.* 1990, *59*, 207–220. DOI: 10.1016/0304-5102(90)85053-K.

[154] Doolin, P. K.; Hoffman, J. F.; Mitchell, M. M. Role of Metal Contaminants in the Production of Carbon Dioxide during the Regeneration of Cracking Catalysts. *Appl Catal.* 1991, *71*, 233–246. DOI: 10.1016/0166-9834(91)85082-7.

[155] Den Hollander, M.; Makkee, M.; Moulijn, J. Coke Formation in Fluid Catalytic Cracking Studied with the Microriser. *Catal. Today*. 1998, *46*, 27–35. DOI: 10.1016/S0920-5861(98)00348-4.

[156] Mann, R. Catalyst Deactivation by Coke Deposition: Approaches Based on Interactions of Coke Laydown with Pore Structure. *Catal. Today*. 1997, *37*, 331–349. DOI: 10.1016/S0920-5861(97)00023-0.

[157] He, S.; Sun, C.; Yang, X.; Wang, B.; Dai, X.; Bai, Z. Characterization of Coke Deposited on Spent Catalysts for Long-Chain-Paraffin Dehydrogenation. *Chem. Eng. J.* 2010, *163*, 389–394. DOI: 10.1016/j.cej.2010.07.024.

[158] Occelli, M. L.; Olivier, J. P.; Auroux, A. The Location and Effects of Coke Deposition in Fluid Cracking Catalysts during Gas Oil Cracking at Microactivity Test Conditions. *J. Catal.* 2002, *209*, 385–393. DOI: 10.1006/jcat.2002.3639.

[159] Wang, G.; Li, Z. K.; Liu, Y.-D.; Gao, J. S.; Xu, C. M.; Lan, X. Y.; Ning, G. Q.; Liang, Y. M. FCC-catalyst Coking: Sources and Estimation of Their Contribution during Coker Gas Oil Cracking Process. *Ind. Eng. Chem. Res.* 2012, *51*, 2247–2256. DOI: 10.1021/ie2012328.

[160] Praserthdam, P.; Mongkhonsi, T.; Kunatippapong, S.; Jaikaew, B.; Lim, N. Determination of Coke Deposition on Metal Active Sites of Propane Dehydrogenation Catalysts. *Stud. Surf. Sci. Catal.* 1997, *111*, 153–158.

[161] Afonso, J. C.; Schmal, M.; Fréty, R. The Chemistry of Coke Deposits Formed on a Pt• Sn Catalyst during Dehydrogenation of N-Alkanes to Mono-Olefins. *Fuel Process. Technol.* 1994, *41*, 13–25. DOI: 10.1016/0378-3820(94)90056-6.

[162] Radovic, L. R. *Chemistry & Physics of Carbon*; CRC Press, 2004. https://www.taylorfrancis.com/books/9780824740887.

[163] Callejas, M. A.; Martínez, M. T.; Blasco, T.; Sastre, E. Coke Characterisation in Aged Residue Hydrotreating Catalysts by Solid-State 13C-NMR Spectroscopy and Temperature-Programmed Oxidation. *Appl Catal A.* 2001, *218*, 181–188. DOI: 10.1016/S0926-860X(01)00640-8.

[164] Snape, C. E.; McGhee, B. J.; Martin, S. C.; Andresen, J. M. Structural Characterisation of Catalytic Coke by Solid-State 13C-NMR Spectroscopy. *Catal. Today.* 1997, *37*, 285–293. DOI: 10.1016/S0920-5861(97)00021-7.

[165] Mance, D.; van der Zwan, J.; Velthoen, M. E.; Meirer, F.; Weckhuysen, B. M.; Baldus, M.; Vogt, E. T. A DNP-supported Solid-State NMR Study of Carbon Species in Fluid Catalytic Cracking Catalysts. *Chem. Commun.* 2017, *53*, 3933–3936. DOI: 10.1039/C7CC00849J.

[166] Corella, J. On the Modeling of the Kinetics of the Selective Deactivation of Catalysts. Application to the Fluidized Catalytic Cracking Process. *Ind. Eng. Chem. Res.* 2004, *43*, 4080–4086. DOI: 10.1021/ie040033d.

[167] Cerqueira, H. S.; Ayrault, P.; Datka, J.; Magnoux, P.; Guisnet, M. m-Xylene Transformation over a USHY Zeolite at 523 and 723 K: Influence of Coke Deposits on Activity, Acidity, and Porosity. *J. Catal.* 2000, *196*, 149–157. DOI: 10.1006/jcat.2000.3012.

[168] Cerqueira, H. S.; Ayrault, P.; Datka, J.; Guisnet, M. Influence of Coke on the Acid Properties of a USHY Zeolite. *Micropor. Mesopor. Mater.* 2000, *38*, 197–205. DOI: 10.1016/S1387-1811(99)00304-2.

[169] Richard, F. W.; Wu-Cheng, C.; Gwan, K.; Robert, H. H. *Vanadium Mobility in Fluid Catalytic Cracking In: Deactivation and Testing of Hydrocarbon-Processing Catalysts*; American Chemical Society, 1996; pp 283–295. DOI: 10.1021/bk-1996-0634.ch021.

[170] Rawlence, D.; Gosling, K. Irreversible Deactivation of Fcc Catalysts. *Catal. Today.* 1991, *11*, 47–59. DOI: 10.1016/0920-5861(91)87006-9.

[171] Escobar, A. S.; Pereira, M. M.; Cerqueira, H. S. Effect of Iron and Calcium over USY Coke Formation. *Appl Catal A.* 2008, *339*, 61–67. DOI: 10.1016/j.apcata.2008.01.008.

[172] Pereira, J. S. F.; Moraes, D. P.; Antes, F. G.; Diehl, L. O.; Santos, M. F. P.; Guimarães, R. C. L.; Fonseca, T. C. O.; Dressler, V. L.; Flores, É. M. M. Determination of Metals and Metalloids in Light and Heavy Crude Oil by ICP-MS after Digestion by Microwave-Induced Combustion. *Microchem. J.* 2010, *96*, 4–11. DOI: 10.1016/j.microc.2009.12.016.

[173] Duyck, C.; Miekeley, N.; Porto Da Silveira, C. L.; Aucélio, R. Q.; Campos, R. C.; Grinberg, P.; Brandão, G. P. The Determination of Trace Elements in Crude Oil and Its Heavy Fractions by Atomic Spectrometry. *Spectrochim. Acta B.* 2007, *62*, 939–951. DOI: 10.1016/j.sab.2007.04.013.

[174] Duyck, C.; Miekeley, N.; Da Silveira, C. L. P.; Szatmari, P. Trace Element Determination in Crude Oil and Its Fractions by Inductively Coupled Plasma Mass Spectrometry Using Ultrasonic Nebulization of Toluene Solutions. *Spectrochim. Acta B.* 2002, *57*, 1979–1990. DOI: 10.1016/S0584-8547(02)00171-4.

[175] Sánchez, R.; Todolí, J. L.; Lienemann, C.-P.; Mermet, J.-M. Determination of Trace Elements in Petroleum Products by Inductively Coupled Plasma Techniques: A Critical Review. *Spectrochim. Acta B.* 2013, *88*, 104–126. DOI: 10.1016/j.sab.2013.06.005.

[176] de Souza, R. M.; Meliande, A. L.; Da Silveira, C. L.; Aucélio, R. Q. Determination of Mo, Zn, Cd, Ti, Ni, V, Fe, Mn, Cr and Co in Crude Oil Using Inductively Coupled Plasma Optical Emission Spectrometry and Sample Introduction as Detergentless Microemulsions. *Microchem. J.* 2006, *82*, 137–141. DOI: 10.1016/j.microc.2006.01.005.

[177] Olsen, S. D.; Westerlund, S.; Visser, R. G. Analysis of Metals in Condensates and Naphtha by Inductively Coupled Plasma Mass Spectrometry. *Analyst*. 1997, *122*, 1229–1234. DOI: 10.1039/a704017b.

[178] Botto, R. I. Applications of Ultrasonic Nebulization in the Analysis of Petroleum and Petrochemicals by Inductively Coupled Plasma Atomic Emission Spectrometry. *J. Anal. At. Spectrom*. 1993, *8*, 51–57. DOI: 10.1039/ja9930800051.

[179] Bettinelli, M.; Spezia, S.; Baroni, U.; Bizzarri, G. Determination of Trace Elements in Fuel Oils by Inductively Coupled Plasma Mass Spectrometry after Acid Mineralization of the Sample in a Microwave Oven. *J. Anal. At. Spectrom*. 1995, *10*, 555–560. DOI: 10.1039/ja9951000555.

[180] Bettinelli, M.; Tittarelli, P. Evaluation and Validation of Instrumental Procedures for the Determination of Nickel and Vanadium in Fuel Oils. *J. Anal. At. Spectrom*. 1994, *9*, 805–812. DOI: 10.1039/ja9940900805.

[181] Wondimu, T.; Goessler, W.; Irgolic, K. Microwave Digestion of "Residual Fuel oil"(NIST SRM 1634b) for the Determination of Trace Elements by Inductively Coupled Plasma-Mass Spectrometry. *Fresenius. J. Anal. Chem*. 2000, *367*, 35–42.

[182] Denoyer, E. R.; Siegel, L. A. Determination of Sulfur, Nickel and Vanadium in Fuel and Residual Oils by X-Ray Fluorescence Spectrometry. *Anal. Chim. Acta*. 1987, *192*, 361–366. DOI: 10.1016/S0003-2670(00)85725-6.

[183] Iwasaki, K.; Tanaka, K. Preconcentration and X-Ray Fluorescence. *Anal. Chim. Acta*. 1982, *136*, 293–299. DOI: 10.1016/S0003-2670(01)95389-9.

[184] Lord, C. J. Determination of Trace Metals in Crude Oil by Inductively Coupled Plasma Mass Spectrometry with Microemulsion Sample Introduction. *Anal. Chem*. 1991, *63*, 1594–1599. DOI: 10.1021/ac00015a018.

[185] Murillo, M.; Chirinos, J. Use of Emulsion Systems for the Determination of Sulfur, Nickel and Vanadium in Heavy Crude Oil Samples by Inductively Coupled Plasma Atomic Emission Spectrometry. *J. Anal. At. Spectrom*. 1994, *9*, 237–240. DOI: 10.1039/ja9940900237.

[186] Turunen, M.; Peräniemi, S.; Ahlgrén, M.; Westerholm, H. Determination of Trace Elements in Heavy Oil Samples by Graphite Furnace and Cold Vapour Atomic Absorption Spectrometry after Acid Digestion. *Anal. Chim. Acta*. 1995, *311*, 85–91. DOI: 10.1016/0003-2670(95)00166-W.

[187] Stratiev, D.; Shishkova, I.; Dinkov, R.; Nikolova, R.; Mitkova, M.; Stanulov, K.; Sharpe, R.; Russell, C.; Obryvalina, A.; Telyashev, R. Reactivity and Stability of Vacuum Residual Oils in Their Thermal Conversion. *Fuel*. 2014, *123*, 133–142. DOI: 10.1016/j.fuel.2014.01.043.

[188] Reynolds, J. G. Nickel in Petroleum Refining. *Pet. Sci. Technol*. 2001, *19*, 979–1007. DOI: 10.1081/LFT-100106915.

[189] Jones, D. S. S. An Introduction to Crude Oil and Its Processing. In *Handbook of Petroleum Processing*; David, S. J. J., Pujadó, P. P., Eds.; Springer, 2008; pp 1–45. DOI: 10.1007/1-4020-2820-2_1.

[190] Yaluris, G.; Cheng, W.-C.; Peters, M.; McDowell, L.; Hunt, L. Mechanism of Fluid Cracking Catalysts Deactivation by Fe. *Stud. Surf. Sci. Catal*. 2004, *149*, 139–163.

[191] Bayraktar, O. *Effect of Pretreatment on the Performance of Metal Contaminated Commercial FCC Catalyst*; Ph.D. Dissertation submitted to the College of Engineering and Mineral Resources, West Virginia University, 2001.

[192] Zrinscak, F. S.; Karsner, G. G. Catalytic Cracking of Metal-Contaminated Oils. US Pat., 4162213 1979.
[193] Du, X.; Zhang, H.; Cao, G.; Wang, L.; Zhang, C.; Gao, X. Effects of La2O3, CeO2 and LaPO4 Introduction on Vanadium Tolerance of USY Zeolites. *Micropor. Mesopor. Mater.* 2015, *206*, 17–22. DOI: 10.1016/j.micromeso.2014.12.010.
[194] Escobar, A. S.; Pereira, M. M.; Pimenta, R. D. M.; Lau, L. Y.; Cerqueira, H. S. Interaction between Ni and V with USHY and Rare Earth HY Zeolite during Hydrothermal Deactivation. *Appl. Catal. A.* 2005, *286*, 196–201. DOI: 10.1016/j.apcata.2005.03.002.
[195] Etim, U. J.; Xu, B.; Ullah, R.; Yan, Z. Effect of Vanadium Contamination on the Framework and Micropore Structure of Ultra Stable Y-Zeolite. *J. Colloid Interface Sci.* 2016, *463*, 188–198. DOI: 10.1016/j.jcis.2015.10.049.
[196] Wormsbecher, R. F.; Peters, A. W.; Maselli, J. M. Vanadium Poisoning of Cracking Catalysts: Mechanism of Poisoning and Design of Vanadium Tolerant Catalyst System. *J. Catal.* 1986, *100*, 130–137. DOI: 10.1016/0021-9517(86)90078-3.
[197] Wang, H.; Wang, F.; Wu, W. Effect of Vanadium Poisoning and Vanadium Passivation on the Structure and Properties of FCC Catalysts. In *Abstracts of Papers of the American Chemical Society*, 2000; Vol. 220, pp U394–U394. https://web.anl.gov/PCS/acsfuel/preprint%20archive/Files/45_3_WASHINGTON%20DC_08-00_0623.pdf.
[198] Torrealba, M.; Goldwasser, M. R.; Perot, G.; Guisnet, M. Influence of Vanadium on the Physicochemical and Catalytic Properties of USHY Zeolite and FCC Catalyst. *Appl. Catal. A.* 1992, *90*, 35–49. DOI: 10.1016/0926-860X(92)80246-9.
[199] Chester, A. W. Studies on the Metal Poisoning and Metal Resistance of Zeolitic Cracking Catalysts. *Ind. Eng. Chem. Res.* 1987, *26*, 863–869. DOI: 10.1021/ie00065a001.
[200] Greenwood, N. N.; Earnshaw, A. *Chemistry of the Elements*; Elsevier, 2012. https://books.google.com/books?isbn=0080501095.
[201] Altomare, C. A.; Koermer, G. S.; Martins, E.; Schubert, P. F.; Suib, S. L.; Willis, W. S. Vanadium Interactions with Treated Silica Aluminas. *Appl. Catal.* 1988, *45*, 291–306. DOI: 10.1016/S0166-9834(00)83035-3.
[202] Andersson, S. L. T.; Lundin, S. T.; Järås, S.; Ottersedt, J.-E. An ESCA Study of Metal Deposition on Cracking Catalysts. *Appl. Catal.* 1984, *9*, 317–325. DOI: 10.1016/0166-9834(84)80003-2.
[203] Occelli, M. L. Vanadium-Zeolite Interactions in Fluidized Cracking Catalysts. *Catal. Rev.* 1991, *33*, 241–280. DOI: 10.1080/01614949108020301.
[204] Sajkowski, D.; Roth, S.; Iton, L.; Meyers, B.; Marshall, C.; Fleisch, T.; Delgass, W. X-Ray Absorption Study of Vanadium on Regenerated Catalytic-Cracking Catalysts. *Appl. Catal.* 1989, *51*, 255–262. DOI: 10.1016/S0166-9834(00)80210-9.
[205] Trujillo, C. A.; Uribe, U. N.; Knops-Gerrits, -P.-P.; Jacobs, P. A. The Mechanism of Zeolite Y Destruction by Steam in the Presence of Vanadium. *J. Catal.* 1997, *168*, 1–15. DOI: 10.1006/jcat.1997.1550.
[206] Tangstad, E.; Myrstad, T.; Myhrvold, E.; Dahl, I.; Stöcker, M.; Andersen, A. Passivation of Vanadium in an Equilibrium FCC Catalyst at Short Contact-Times. *Appl. Catal. A Gen.* 2006, *313*, 35–40. DOI: 10.1016/j.apcata.2006.07.001.
[207] Yujian, L.; Jun, L.; Huiping, T.; Han, Z. Effects of Vanadium Oxidation Number on Light Olefins Selectivity of FCC Catalyst. *China Petrol Process Petrochem. Technol.* 2011, *13*, 1–8.
[208] Long, J.; Zhu, Y.; Liu, Y.; Da, Z.; Zhou, H. Effects of Vanadium Oxidation Number on Desulfurization Performance of FCC Catalyst. *Appl. Catal. A Gen.* 2005, *282*, 295–301. DOI: 10.1016/j.apcata.2004.12.039.

[209] Yujian, L.; Jun, L.; Han, Z.; Yuxia, Z.; Zhijian, D. Molecular Simulation Study on Interaction of Thiophene Sulfides with Transition Metals. *China Petrol Process Petrochem. Technol*. 4, 2003.
[210] Tangstad, E.; Myrstad, T.; Spjelkavik, A.; Stöcker, M. Vanadium Species and Their Effect on the Catalytic Behavior of an FCC Catalyst. *Appl. Catal. A Gen*. 2006, *299*, 243–249. DOI: 10.1016/j.apcata.2005.10.058.
[211] Yang, S.-J.; Chen, Y.-W.; Li, C. Vanadium-Nickel Interaction in REY Zeolite. *Appl. Catal. A*. 1994, *117*, 109–123. DOI: 10.1016/0926-860X(94)85092-5.
[212] Pimenta, R. D. M.; Pereira, M. M.; Do Nascimento, U.; Gorne, J.; Bernadete, E.; Lau, L. Y. Effect of Vanadium Contamination on H-ZSM-5 Zeolite Deactivation. *Catal. Today*. 2008, *133*, 805–808. DOI: 10.1016/j.cattod.2007.12.098.
[213] Cristiano-Torres, D. V.; Osorio-Pérez, Y.; Palomeque-Forero, L. A.; Sandoval-Díaz, L. E.; Trujillo, C. A. The Action of Vanadium over Y Zeolite in Oxidant and Dry Atmosphere. *Appl. Catal. A*. 2008, *346*, 104–111. DOI: 10.1016/j.apcata.2008.05.006.
[214] Sandoval-Diaz, L. E.; Martinez-Gil, J. M.; Trujillo, C. A. The Combined Effect of Sodium and Vanadium Contamination upon the Catalytic Performance of USY Zeolite in the Cracking of N-Butane: Evidence of Path-Dependent Behavior in Constable-Cremer Plots. *J. Catal*. 2012, *294*, 89–98. DOI: 10.1016/j.jcat.2012.07.009.
[215] Ray, G.; Meyers, B.; Marshall, C. 29 Si and 27 Al Nmr Study of Steamed Faujasites—Evidence for Non-Framework Tetrahedrally Bound Aluminium. *Zeolites*. 1987, *7*, 307–310. DOI: 10.1016/0144-2449(87)90032-7.
[216] Lappas, A.; Nalbandian, L.; Iatridis, D.; Voutetakis, S.; Vasalos, I. Effect of Metals Poisoning on FCC Products Yields: Studies in an FCC Short Contact Time Pilot Plant Unit. *Catal. Today*. 2001, *65*, 233–240. DOI: 10.1016/S0920-5861(00)00588-5.
[217] Myrstad, T. Effect of Vanadium on Octane Numbers in FCC-naphtha. *Appl. Catal. A*. 1997, *155*, 87–98. DOI: 10.1016/S0926-860X(96)00403-6.
[218] Pine, L. A. Vanadium-Catalyzed Destruction of USY Zeolites. *J. Catal*. 1990, *125*, 514–524. DOI: 10.1016/0021-9517(90)90323-C.
[219] Du, X.; Li, X.; Zhang, H.; Gao, X. Kinetics Study and Analysis of Zeolite Y Destruction. *Chin. J. Catal*. 2016, *37*, 316–323. DOI: 10.1016/S1872-2067(15)60975-5.
[220] Anderson, M. W.; Occelli, M. L.; Suib, S. L. Tin Passivation of Vanadium in Metal-Contaminated Fluid-Cracking Catalysts: Electron Paramagnetic Resonance Studies. *J. Catal*. 1990, *122*, 374–383. DOI: 10.1016/0021-9517(90)90291-Q.
[221] Sanchez, J.; Hager, J. EDP Congress 1993. Proceedings from the Symposium of the TMS Annual Meeting of the Minerals, Metals & Materials Society: Warrendale, PA, 1993; pp 655.
[222] Pompe, R.; Järóas, S.; Vannerberg, N.-G. On the Interaction of Vanadium and Nickel Compounds with Cracking Catalyst. *Appl. Catal*. 1984, *13*, 171–179. DOI: 10.1016/S0166-9834(00)83335-7.
[223] Busca, G.; Riani, P.; Garbarino, G.; Ziemacki, G.; Gambino, L.; Montanari, E.; Millini, R. The State of Nickel in Spent Fluid Catalytic Cracking Catalysts. *Appl. Catal. A*. 2014, *486*, 176–186. DOI: 10.1016/j.apcata.2014.08.011.
[224] Petti, T. F.; Tomczak, D.; Pereira, C. J.; Cheng, W.-C. Investigation of Nickel Species on Commercial FCC Equilibrium Catalysts-Implications on Catalyst Performance and Laboratory Evaluation. *Appl. Catal. A*. 1998, *169*, 95–109. DOI: 10.1016/S0926-860X(97)00373-6.

[225] Cadet, V.; Raatz, F.; Lynch, J.; Marcilly, C. Nickel Contamination of Fluidised Cracking Catalysts: A Model Study. *Appl. Catal.* 1991, *68*, 263–275. DOI: 10.1016/S0166-9834(00)84107-X.

[226] Stöcker, M.; Tangstad, E.; Aas, N.; Myrstad, T. Quantitative Determination of Ni and V in FCC Catalysts Monitored by ESR Spectroscopy. *Catal. Lett*. 2000, *69*, 223–229. DOI: 10.1023/A:1019094611940.

[227] Long-Xiang, T.; Feng-Mei, Z.; Dong-Fan, L.; Lu-Bin, Z. Characteristics of the Poisoning Effect of Nickel Deposited on USY Zeolite. *Appl. Catal. A*. 1992, *91*, 67–80. DOI: 10.1016/0926-860X(92)85066-K.

[228] Occelli, M.; Psaras, D.; Suib, S. Luminescence as a Probe of Metal Poisoning Effects on a High-Activity Fluid Cracking Catalyst (FCC). *J. Catal*. 1985, *96*, 363–370. DOI: 10.1016/0021-9517(85)90306-9.

[229] Bartholomew, C. H.; Pannell, R. B. The Stoichiometry of Hydrogen and Carbon Monoxide Chemisorption on Alumina- and Silica-Supported Nickel. *J. Catal*. 1980, *65*, 390–401. DOI: 10.1016/0021-9517(80)90316-4.

[230] Tatterson, D. F.; Mieville, R. L. Nickel/Vanadium Interactions on Cracking Catalyst. *Ind. Eng. Chem. Res*. 1988, *27*, 1595–1599. DOI: 10.1021/ie00081a007.

[231] Corma, A.; Grande, M. S.; Iglesias, M.; Del Pino, C.; Rojas, R. M. Nickel Passivation on Fluidised Cracking Catalysts with Different Antimony Complexes. *Appl. Catal. A*. 1992, *85*, 61–71. DOI: 10.1016/0926-860X(92)80129-Z.

[232] Nielsen, R. H.; Doolin, P. K. Chapter 10 Metals Passivation. In *Studies in Surface Science and Catalysis*; John, S. M., Maurice, M. M., Eds.; Elsevier, 1993; pp 339–384. DOI: 10.1016/S0167-2991(08)63833-1.

[233] Bayraktar, O.; Kugler, E. L. Visualization of the Equilibrium FCC Catalyst Surface by AFM and SEM–EDS. *Catal. Lett*. 2003, *90*, 155–160. DOI: 10.1023/B:CATL.0000004110.98820.d9.

[234] Rainer, D. R.; Rautiainen, E.; Nelissen, B.; Imhof, P.; Vadovic, C. Simulating Iron-Induced FCC Accessibility Losses in Lab-Scale Deactivation. In *Studies in Surface Science and Catalysis*; Occelli, M., Ed.; Elsevier, 2004; pp 165–176. DOI: 10.1016/S0167-2991(04)80761-4.

[235] Mathieu, Y.; Corma, A.; Echard, M.; Bories, M. Single and Combined Fluidized Catalytic Cracking (FCC) Catalyst Deactivation by Iron and Calcium Metal–Organic Contaminants. *Appl. Catal. A*. 2014, *469*, 451–465. DOI: 10.1016/j.apcata.2013.10.007.

[236] Liu, Z.; Zhang, Z.; Liu, P.; Zhai, J.; Yang, C. Iron Contamination Mechanism and Reaction Performance Research on FCC Catalyst. *J. Nanotechnol*. 2015, 2015. DOI: 10.1155/2015/273859.

[237] Tangstad, E.; Andersen, A.; Myhrvold, E. M.; Myrstad, T. Catalytic Behaviour of Nickel and Iron Metal Contaminants of an FCC Catalyst after Oxidative and Reductive Thermal Treatments. *Appl. Catal. A*. 2008, *346*, 194–199. DOI: 10.1016/j.apcata.2008.05.022.

[238] Yuxia, Z.; Quansheng, D.; Wei, L.; Liwen, T.; Jun, L. Studies of Iron Effects on FCC Catalysts. *Stud. Surf. Sci. Catal*. 2007, *166*, 201–212.

[239] Rainer, D. R.; Rautiainen, E.; Imhof, P. Novel Lab-Scale Deactivation Method for FCC Catalyst: Inducing Realistic Accessibility Responses to Iron Poisoning. *Appl. Catal. A*. 2003, *249*, 69–80. DOI: 10.1016/S0926-860X(03)00203-5.

[240] Whitcombe, J. M.; Agranovski, I. E.; Braddock, R. D. Identification of Metal Contaminants on FCC Catalyst. *Part. Part. Syst. Charact*. 2005, *22*, 268–275. DOI: 10.1002/ppsc.v22:4.

[241] Tian, H.; Huang, C.; Fan, Z. Metals on a Novel USY Zeolite after Hydrothermal Aging. *Stud. Surf. Sci. Catal.* 2001, *139*, 351–358.
[242] Kumar, C. P.; Mandal, S.; Ravichandran, G.; Dinda, S.; Gohel, A. V.; Yadav, A.; Das, A. K. Development of a FCC Catalyst/Additive Combination with High Tolerance to Calcium Contamination from Lower Cost Feedstock. Calcium containing feedstock processing. 2016, http://www.digitalrefining.com/article/1001268.
[243] Hagiwara, K.; Ebihara, T.; Urasato, N.; Ozawa, S.; Nakata, S. Effect of Vanadium on USY Zeolite Destruction in the Presence of Sodium Ions and Steam—Studies by Solid-State NMR. *Appl. Catal. A*. 2003, *249*, 213–228. DOI: 10.1016/S0926-860X(03)00289-8.
[244] Sandoval-Diaz, L. E.; Palomeque-Forero, L. A.; Trujillo, C. A. Towards Understanding Sodium Effect on USY Zeolite. *Appl. Catal. A*. 2011, *393*, 171–177. DOI: 10.1016/j.apcata.2010.11.038.
[245] Fritz, P. O.; Lunsford, J. H. The Effect of Sodium Poisoning on Dealuminated Y-Type Zeolites. *J. Catal.* 1989, *118*, 85–98. DOI: 10.1016/0021-9517(89)90303-5.
[246] Tangstad, E.; Myhrvold, E.; Myrstad, T. A Study on the Effect of Sodium Chloride Deposition on an FCC Catalyst in A Cyclic Deactivation Unit. *Appl. Catal. A*. 2000, *193*, 113–122. DOI: 10.1016/S0926-860X(99)00414-7.
[247] Tangstad, E.; Bendiksen, M.; Myrstad, T. Effect of Sodium Deposition of FCC Catalysts Deactivation. *Appl. Catal. A*. 1997, *150*, 85–99. DOI: 10.1016/S0926-860X(96)00284-0.
[248] Xu, M.; Liu, X.; Madon, R. J. Pathways for Y Zeolite Destruction: The Role of Sodium and Vanadium. *J. Catal.* 2002, *207*, 237–246. DOI: 10.1006/jcat.2002.3517.
[249] Sandoval-Díaz, L.-E.; Ruíz-Cardona, Y.-S.; Trujillo, C.-A. Amorphization of USY Zeolite Induced by Sodium Chloride and High Temperature Steaming. *Micropor. Mesopor. Mater.* 2016, *224*, 168–175. DOI: 10.1016/j.micromeso.2015.11.021.
[250] Liu, Z.; Dadyburjor, D. B. Activity, Selectivity, and Deactivation of High-Sodium HY Zeolite. *J. Catal.* 1992, *134*, 583–593. DOI: 10.1016/0021-9517(92)90344-H.
[251] Siegel, J.; Olsen, C. Feed Contaminants in Hydroprocessing Units. Upgrading the Bottom of the Barrel, Grace Davison Catalagram, 2008.
[252] Escobar, A. S.; Pinto, F. V.; Cerqueira, H. S.; Pereira, M. M. Role of Nickel and Vanadium over USY and RE-USY Coke Formation. *Appl. Catal. A*. 2006, *315*, 68–73. DOI: 10.1016/j.apcata.2006.09.004.
[253] Etim, U.; Xu, B.; Bai, P.; Ullah, R.; Subhan, F.; Yan, Z. Role of Nickel on Vanadium Poisoned FCC Catalyst: A Study of Physiochemical Properties. *J. Energy Chem.* 2016, *25*, 667–676. DOI: 10.1016/j.jechem.2016.04.001.
[254] Jaras, S. Rapid Methods of Determining the Metals Resistance of Cracking Catalysts. *Appl. Catal.* 1982, *2*, 207–218. DOI: 10.1016/0166-9834(82)80068-7.
[255] Yang, S.-J.; Chen, Y.-W.; Chiuping, L. The Interaction of Vanadium and Nickel in USY Zeolite. *Zeolites.* 1995, *15*, 77–82. DOI: 10.1016/0144-2449(94)00010-P.
[256] Kalirai, S.; Boesenberg, U.; Falkenberg, G.; Meirer, F.; Weckhuysen, B. M. X-Ray Fluorescence Tomography of Aged Fluid-Catalytic-Cracking Catalyst Particles Reveals Insight into Metal Deposition Processes. *Chem. Cat. Chem.* 2015, *7*, 3674–3682. DOI: 10.1002/cctc.201500710.
[257] Jiang, H.; Livi, K. J.; Kundu, S.; Cheng, W.-C. Characterization of Iron Contamination on Equilibrium Fluid Catalytic Cracking Catalyst Particles. *J. Catal.* 2018, *361*, 126–134. DOI: 10.1016/j.jcat.2018.02.025.
[258] Etim, U.; Wu, P.; Bai, P.; Xing, W.; Ullah, R.; Subhan, F.; Yan, Z. Location and Surface Species of Fluid Catalytic Cracking Catalyst Contaminants: Implications for Alleviating Catalyst Deactivation. *Energy Fuel.* 2016, *30*, 10371–10382. DOI: 10.1021/acs.energyfuels.6b02505.

[259] Silverman, L. D.; Winkler, S.; Tiethof, J. A.; Witoshkin, A. Matrix Effects in Catalytic Cracking. Silverman, L. D., Winkler, S., Tiethof, J. A., Witoshkin, A. eds NPRA Annual Meeting. National Petroleum Refiners Association annual meeting, Los Angeles 1986, 1–38.
[260] Ali, M. F.; Abbas, S. A Review of Methods for the Demetallization of Residual Fuel Oils. *Fuel Process. Technol.* 2006, *87*, 573–584. DOI: 10.1016/j.fuproc.2006.03.001.
[261] Tatterson, D. F.; Ford, W. D. Fluid Catalytic Cracking of Heavy Petroleum Fractions. US Pat. 4,298,459 1981.
[262] George, D.; Myers, D.; Hettinger, W. P.; Kovach, S. M.; Zandona, O. J. Steam Reforming of Carbo-Metallic Oils. US Pat., 4432863 1984.
[263] Boock, L. T.; Petti, T. F. Catalyst Design for Resid Cracking Operation: Benefits of Metal Tolerant Technologies. *Stud. Surf. Sci. Catal.* 2001, *134*, 201–208.
[264] Forester, D. R.; Passivation of FCC Catalysts. US Pat., 5064524 1991.
[265] Dreiling, M.; Schaffer, A. Interaction of Antimony with Reduced Supported Nickel Catalysts. *J. Catal.* 1979, *56*, 130–133. DOI: 10.1016/0021-9517(79)90097-6.
[266] Corma, A.; Grande, M.; Iglesias, M.; Del Pino, C.; Rojas, R. Nickel Passivation on Fluidised Cracking Catalysts with Different Antimony Complexes. *Appl. Catal. A.* 1992, *85*, 61–71. DOI: 10.1016/0926-860X(92)80129-Z.
[267] Corma, A.; Mocholi, F. New Silica-Alumina-Magnesia FCC Active Matrix and Its Possibilities as a Basic Nitrogen Passivating Compound. *Appl. Catal. A.* 1992, *84*, 31–46. DOI: 10.1016/0926-860X(92)80337-C.
[268] Stockwell, D. M.; FCC Additive for Partial and Full Burn NOx Control. US Pat., 7678735 2010.
[269] Gallezot, P.; Bourgogne, M. Hydrothermal Aging of Cracking Catalysts: V. Vanadium Passivation by Rare-Earth Compounds Soluble in the Feedstock. *J. Catal.* 1992, *134*, 469–478. DOI: 10.1016/0021-9517(92)90335-F.
[270] Baugis, G. L.; Brito, H. F.; de Oliveira, W.; de Castro, F. R.; Sousa-Aguiar, E. F. The Luminescent Behavior of the Steamed EuY Zeolite Incorporated with Vanadium and Rare Earth Passivators. *Micropor. Mesopor. Mater.* 2001, *49*, 179–187. DOI: 10.1016/S1387-1811(01)00416-4.
[271] Wormsbecher, R.; Cheng, W.; Wallenstein, D. Role of the Rare Earth Elements in Fluid Catalytic Cracking. *Grace Davison Catalagram*2010, No. 108, pp 19-26.
[272] Kumar, R.; Catalytic Cracking Catalysts and Additives. US Pat., 5304299 1994. DOI: 10.3168/jds.S0022-0302(94)77044-2.
[273] Deitz, P. S.; Suarez, W.; Kumar, R.; Wormsbecher, R. F. Rare Earth Carbonate Compositions for Metals Tolerance in Cracking Catalysts. US Pat., 12/936009 2009.
[274] Occelli, M. L.; Kennedy, J. V. Process for Cracking High Metals Content Feedstocks. US Pat., 4944865 1990. DOI: 10.1099/00221287-136-2-327.
[275] Etim, U. J.; Bai, P.; Ullah, R.; Subhan, F.; Yan, Z. Vanadium Contamination of FCC Catalyst: Understanding the Destruction and Passivation Mechanisms. *Appl. Catal. A.* 2018, *555*, 108–117. DOI: 10.1016/j.apcata.2018.02.011.
[276] Pan, H.; Wu, X.; Tang, A. The Design of Vanadium Trapping System for FCC Catalysts. *Chin. J. Chem. Eng.* 1996, *4*, 120–124.
[277] Groenenboom, C. J.; Barium Titanium Oxide-Containing Fluidizable Cracking Catalyst Composition. US Pat., 4791085 1988. DOI: 10.3168/jds.S0022-0302(88)79586-7.
[278] Mitchell, B. R.; Vogel, R. F. Vanadium Passivation in a Hydrocarbon Catalytic Cracking Process. US Pat., 4451355 1984.
[279] Mitchell, B. R.; Vogel, R. F. Vanadium Passivation in a Hydrocarbon Catalytic Cracking Process. US Pat., 4520120 1985.

[280] Jeon, H. J.; Park, S. K.; Woo, S. I. Evaluation of Vanadium Traps Occluded in Resid Fluidized Catalytic Cracking (RFCC) Catalyst for High Gasoline Yield. *Appl. Catal. A*. 2006, *306*, 1–7. DOI: 10.1016/j.apcata.2006.02.048.

[281] Beck, H. W.; Carruthers, J. D.; Cornelius, E. B.; Hettinger, W. P.; Kovach, S. M.; Palmer, J. L.; Zandona, O. J. Immobilization of Vanadia Deposited on Catalytic Materials during Carbo-Metallic Oil Conversion. US Pat., 4432890 1984.

[282] Trujillo, C. A.; Uribe, U. N.; Aguiar, L. A. O. Vanadium Traps for Catalyst for Catalytic Cracking. US Pat., 6159887 2000.

[283] Catana, G.; Grünert, W.; Van Der Voort, P.; Vansant, E. F.; Schoonheydt, R. A.; Weckhuysen, B. M. AlO X Coating of Ultrastable Zeolite Y: A Possible Method for Vanadium Passivation of FCC Catalysts. *J. Phys. Chem. B*. 2000, *104*, 9195–9202. DOI: 10.1021/jp001021i.

[284] Karthikeyani, A. V.; Sarkar, B.; Chidambaram, V.; Swamy, B.; Kasliwal, P. K.; Mishra, G. S.; Kuvettu, M. P. Process for Enhancing Nickel Tolerance of Heavy Hydrocarbon Cracking Catalysts. US Pat., 20140235429 2014.

[285] Madon, R.; Harris, D. H.; Xu, M.; Stockwell, D.; Lerner, B.; Dodwell, G. W. FCC Catalysts for Feeds Containing Nickel and Vanadium. US Pat., 6716338 2004.

[286] Etim, U. J.; Xu, B.; Zhang, Z.; Zhong, Z.; Bai, P.; Qiao, K.; Yan, Z. Improved Catalytic Cracking Performance of USY in the Presence of Metal Contaminants by Post-Synthesis Modification. *Fuel*. 2016, *178*, 243–252. DOI: 10.1016/j.fuel.2016.03.060.

[287] Zhongdong, Z.; Zhaoyong, L.; Zifeng, Y.; Xionghou, G.; Haitao, Z.; Zhifeng, W. Application of New Heavy Metals Resistant Porous Binder Material Used in Fluid Catalytic Cracking Reaction. *China Petrol Process Petrochem. Technol*. 2014, *1*, 007.

[288] Ruiz-Martínez, J.; Beale, A. M.; Deka, U.; O'Brien, M. G.; Quinn, P. D.; Mosselmans, J. F. W.; Weckhuysen, B. M. Correlating Metal Poisoning with Zeolite Deactivation in an Individual Catalyst Particle by Chemical and Phase-Sensitive X-Ray Microscopy. *Angew. Chem. Int. Ed*. 2013, *52*, 5983–5987. DOI: 10.1002/anie.201210030.

[289] Wise, A. M.; Weker, J. N.; Kalirai, S.; Farmand, M.; Shapiro, D. A.; Meirer, F.; Weckhuysen, B. M. Nanoscale Chemical Imaging of an Individual Catalyst Particle with Soft X-Ray Ptychography. *ACS Catal*. 2016, *6*, 2178–2181. DOI: 10.1021/acscatal.6b00221.

[290] Meirer, F.; Morris, D. T.; Kalirai, S.; Liu, Y.; Andrews, J. C.; Weckhuysen, B. M. Mapping Metals Incorporation of a Whole Single Catalyst Particle Using Element Specific X-Ray Nanotomography. *J. Am. Chem. Soc*. 2015, *137*, 102–105. DOI: 10.1021/ja511503d.

[291] Da Silva, J. C.; Mader, K.; Holler, M.; Haberthür, D.; Diaz, A.; Guizar-Sicairos, M.; Cheng, W. C.; Shu, Y.; Raabe, J.; Menzel, A. Assessment of the 3 D Pore Structure and Individual Components of Preshaped Catalyst Bodies by X-Ray Imaging. *Chem. Cat. Chem*. 2015, *7*, 413–416. DOI: 10.1002/cctc.201402925.

[292] Buurmans, I. L. C.; Ruiz-Martínez, J.; Knowles, W. V.; van der, B.; Bergwerff, J. A.; VogtEelco, T. C.; Weckhuysen, B. M. Catalytic Activity in Individual Cracking Catalyst Particles Imaged Throughout Different Life Stages by Selective Staining. *Nat. Chem*. 2011, *3*, 862–867. DOI: 10.1038/nchem.1148.

[293] Buurmans, I. L. C.; Ruiz-Martínez, J.; Van Leeuwen, S. L.; Van Der Beek, D.; Bergwerff, J. A.; Knowles, W. V.; Vogt, E. T. C.; Weckhuysen, B. M. Staining of Fluid-Catalytic-Cracking Catalysts: Localising Brønsted Acidity within a Single Catalyst Particle. *Chem. Eur. J*. 2012, *18*, 1094–1101. DOI: 10.1002/chem.201102949.

[294] Buurmans, I. L. C.; Soulimani, F.; Ruiz-Martínez, J.; van der Bij, H. E.; Weckhuysen, B. M. Structure and Acidity of Individual Fluid Catalytic Cracking

Catalyst Particles Studied by Synchrotron-Based Infrared Micro-Spectroscopy. *Micropor. Mesopor. Mater.* 2013, *166*, 86–92. DOI: 10.1016/j.micromeso.2012.08.007.

[295] Buurmans, I. L.; Weckhuysen, B. M. Heterogeneities of Individual Catalyst Particles in Space and Time as Monitored by Spectroscopy. *Nat. Chem.* 2012, *4*, 873–886. DOI: 10.1038/nchem.1478.

[296] Kalirai, S.; Paalanen, P. P.; Wang, J.; Meirer, F.; Weckhuysen, B. M. Visualizing Dealumination of a Single Zeolite Domain in a Real-Life Catalytic Cracking Particle. *Angew. Chem.* 2016, *55*, 11134-11138.

[297] Meirer, F.; Kalirai, S.; Weker, J. N.; Liu, Y.; Andrews, J.; Weckhuysen, B. Agglutination of Single Catalyst Particles during Fluid Catalytic Cracking as Observed by X-Ray Nanotomography. *Chem. Commun.* 2015, *51*, 8097–8100. DOI: 10.1039/C5CC00401B.

[298] Karreman, M. A.; Buurmans, I. L.; Agronskaia, A. V.; Geus, J. W.; Gerritsen, H. C.; Weckhuysen, B. M. Probing the Different Life Stages of a Fluid Catalytic Cracking Particle with Integrated Laser and Electron Microscopy. *Chem. Eur. J.* 2013, *19*, 3846–3859. DOI: 10.1002/chem.201203491.

[299] Ristanović, Z.; Kerssens, M. M.; Kubarev, A. V.; Hendriks, F. C.; Dedecker, P.; Hofkens, J.; Roeffaers, M. B.; Weckhuysen, B. M. High-Resolution Single-Molecule Fluorescence Imaging of Zeolite Aggregates within Real-Life Fluid Catalytic Cracking Particles. *Angew. Chem. Int. Ed.* 2015, *54*, 1836–1840. DOI: 10.1002/anie.201410236.